

Institut für Agrartechnik in den Tropen und Subtropen

Universität Hohenheim

Prof. Dr.-Ing. Dr. h.c. W. Mühlbauer

**Development and Optimisation of a Low-Temperature
Drying Schedule for *Eucalyptus grandis* (Hill) ex Maiden
in a Solar-Assisted Timber Dryer**

Dissertation

zur Erlangung des Grades eines Doktors

der Agrarwissenschaften (Dr.sc.agr.)

vorgelegt

der Fakultät Agrarwissenschaften

von

Konrad Bauer

Heidelberg, Baden-Württemberg

Hohenheim, 2003

Die vorliegende Arbeit wurde am 03. Juli 2003 von der Fakultät Agrarwissenschaften der Universität Hohenheim als „Dissertation zur Erlangung des Grades eines Doktors der Agrarwissenschaften“ angenommen.

Tag der mündlichen Prüfung: 30. September 2003

Dekan: Prof. Dr. K. Stahr

Hauptberichter: Prof. Dr.-Ing. Dr. h.c. W. Mühlbauer

Mitberichter: Prof. Dr.-Ing. Dr. h.c. H. D. Kutzbach

Mündliche Prüfung: Prof. Dr.-Ing. Dr. h.c. W. Mühlbauer

Prof. Dr.-Ing. Dr. h.c. H. D. Kutzbach

Prof. Dr. R. Böcker

D 100

Copyright 2003

im Selbstverlag

Konrad Bauer

Bezugsquellen: Universität Hohenheim

Institut für Agrartechnik in den Tropen und Subtropen

Garbenstraße 9

70 599 Stuttgart

Alle Rechte, auch die der Übersetzung und des Nachdrucks, sowie jede Art der photomechanischen Wiedergabe, auch auszugsweise, bleiben vorbehalten.

All rights reserved, including the right to reproduce this book or portions thereof in any form whatever.

VORWORT

Die vorliegende Arbeit entstand während meiner Tätigkeit als wissenschaftlicher Mitarbeiter am Institut für Agrartechnik in den Tropen und Subtropen der Universität Hohenheim im Rahmen eines vom Ministerium für Bildung, Wissenschaft, Forschung und Technologie (BMBF), sowie vom brasilianischen Forstunternehmen CAF Santa Bárbara Ltda. geförderten deutsch-brasilianischen Forschungsprojekts. Den Projektträgern danke ich für die Bereitstellung der finanziellen Mittel zur Durchführung der umfangreichen Forschungsaktivitäten.

Mein besonderer Dank gilt meinem Doktorvater Herrn Prof. Dr.-Ing. Dr. h.c. W. Mühlbauer, nicht nur für die wissenschaftliche Betreuung, sondern auch für das entgegengebrachte Vertrauen, die hervorragenden Arbeitsbedingungen und die intensive Mitwirkung bei der schriftlichen Darstellung. Herrn Prof. Dr.-Ing. Dr. h.c. H. D. Kutzbach danke ich für die spontane Bereitschaft zur Übernahme des Mitberichts. Ein ganz besonderer Dank gilt meinem Betreuer Herrn Dr.sc.agr. M. Bux für die uneingeschränkte Unterstützung, das unermüdliche Engagement, den anerkennenden Zuspruch während schwieriger Projektphasen und das ausgezeichnete Arbeitsklima. Er hat maßgeblich zum Gelingen der Arbeit beigetragen.

Ein besonderer Dank gilt auch den Mitarbeitern der CAF Santa Bárbara Ltda. für ihre Hilfsbereitschaft, Gastfreundschaft und für das Vertrauen, das Sie in meine Arbeit gesetzt haben. Besonders seien hierbei Herr A. Pimenta und Herr V. Lopes für ihre engagierte Unterstützung während der umfassenden Forschungsarbeiten erwähnt. Danken möchte ich auch der Firma THERMO-SYSTEM Industrie- und Trocknungstechnik GmbH für die ausgezeichnete Zusammenarbeit während den Entwicklungs- und Montagearbeiten.

Zu besonderem Dank verpflichtet bin ich auch all meinen Kollegen, deren Hilfsbereitschaft und Unterstützung für eine gute und angenehme Arbeitsatmosphäre gesorgt haben. Hier seien auch die Mitarbeiter des Zeichenbüros, des Sekretariats, der Messtechnik und der Werkstatt erwähnt.

Zuletzt möchte ich noch meinen Eltern, meinen Geschwistern, meiner Frau Irilda sowie all jenen einen Dank aussprechen, die mir durch ihr Verständnis, ihre Geduld, ihre Freundschaft und Unterstützung auch in schweren Zeiten den nötigen Rückhalt gegeben haben.

Hohenheim, Mai 2003

Konrad Bauer

1	INTRODUCTION	13
2	FUNDAMENTALS OF SAWNWOOD DRYING.....	19
2.1	Drying Relevant Wood Characteristics.....	19
2.1.1	Anatomical Structure	19
2.1.2	Density	21
2.1.3	Moisture Content	22
2.1.4	Shrinkage and Anisotropy	26
2.1.5	Growth Stress.....	28
2.2	Drying Behaviour of Sawnwood.....	30
2.2.1	Influence of Drying Air Conditions on the Drying Rate	30
2.2.1.1	Temperature.....	31
2.2.1.2	Relative Humidity.....	32
2.2.1.3	Air Velocity	33
2.2.2	Influence of the Drying Process on the Sawnwood Quality.....	35
2.2.2.1	Wood Moisture Content	35
2.2.2.2	Casehardening	36
2.2.2.3	Deformation.....	38
2.2.2.4	Fissures	39
2.2.2.5	Cell Collapse.....	40
2.2.2.6	Discoloration	41
2.2.3	Specific Drying Demands of <i>Eucalyptus grandis</i>	42
3	SAWNWOOD DRYING TECHNOLOGIES	44
3.1	Ambient Air Drying	46
3.2	Solar Dryer	47
3.3	Low Temperature Dryer.....	50
3.4	Medium Temperature Dryer.....	51
3.5	High Temperature Dryer	54
4	OPERATING PERFORMANCE OF THE SOLAR-ASSISTED TIMBER DRYER	57
4.1	Material and Methods.....	57
4.1.1	Design of the Solar-Assisted Timber Dryer	57
4.1.2	Functional Principle of the Drying Process	60
4.1.3	Control of the Drying Conditions	61
4.1.4	Data Acquisition	63
4.1.5	Methods of Calculation.....	64
4.1.5.1	Heat Transfer at the Air Bubble Foil	64
4.1.5.2	Condensation of Moisture at the Air Bubble Foil	66
4.1.5.3	Efficiency of the Solar Collector	67
4.1.5.4	Electrical Energy Demand.....	72
4.2	Results	74

4.2.1	Operating Behaviour of the Solar Collector	74
4.2.2	Operating Behaviour of the Supplementary Heater.....	79
4.2.3	Operating Behaviour of the Humidifying System	79
4.2.4	Operating Behaviour of the Axial Flow Fans.....	80
4.2.5	Operating Behaviour of the Whole Dryer.....	83
4.3	Evaluation of the Results.....	87
5	SOLAR-ASSISTED DRYING OF EUCALYPTWOOD IN BRAZIL.....	88
5.1	Material and Methods.....	88
5.1.1	Location and Climate.....	88
5.1.2	Raw Material.....	89
5.1.3	Test Conditions	90
5.1.3.1	Solar-Assisted Dryer.....	90
5.1.3.2	Ambient Air.....	92
5.1.4	Timber Quality.....	92
5.1.4.1	Sample Strategy	92
5.1.4.2	Wood Moisture Content	93
5.1.4.3	Casehardening	95
5.1.4.4	Warp	96
5.1.4.5	Fissuring	97
5.1.4.6	Cell Collapse.....	97
5.1.4.7	Discolorations.....	97
5.1.4.8	Quality Classification of the Sawnwood	97
5.1.5	Energy Balance	98
5.1.6	Data Acquisition	99
5.1.7	Methods of Calculation.....	100
5.1.7.1	Energy Flow	100
5.1.7.2	Statistics.....	101
5.2	Results.....	105
5.2.1	Drying Performance.....	105
5.2.1.1	Gradient of the Drying Conditions Along the Timber Stack.....	105
5.2.1.2	Daily Temperature Oscillations.....	107
5.2.1.3	Drying Air Velocity.....	110
5.2.1.4	Wood Temperature	111
5.2.1.5	Wood Moisture Content	112
5.2.1.6	Drying Time	114
5.2.1.7	Drying Schedules.....	116
5.2.2	Timber Quality.....	121
5.2.2.1	Wood Moisture Content	121
5.2.2.2	Casehardening	125
5.2.2.3	Warp	126
5.2.2.4	Fissures	129
5.2.2.5	Cell Collapse.....	130

5.2.2.6	Discolorations	130
5.2.2.7	Quality Classification	131
5.2.3	Energy Balance	133
5.3	Evaluation of the Results.....	136
6	ECONOMIC EVALUATION OF THE SOLAR DRYER.....	138
6.1	Material and Methods.....	138
6.1.1	Investment Costs	138
6.1.2	Drying Costs	139
6.1.3	Methods of Calculation.....	139
6.2	Results	140
6.2.1	Investment Costs	140
6.2.2	Drying Costs	141
6.2.2.1	Fixed Costs	141
6.2.2.2	Variable Costs.....	142
6.2.3	General Cost Comparison	143
6.2.4	Sensitivity Analysis for Important Cost Factors.....	145
6.2.4.1	Investment Costs.....	145
6.2.4.2	Interest Rate	145
6.2.4.3	Energy Costs.....	146
6.2.5	Payback Period	147
6.3	Evaluation of the Results.....	147
7	SUMMARY	149
8	ZUSAMMENFASSUNG	152
9	REFERENCES	155
10	APPENDIX	175

Notation

A	m ² , ha	Area
AN	Euro	Annuity
AF	-	Anisotropy factor
A ₀	Euro	Total investment costs
B	-	Factor B
DF	-	Degree of freedom
E	-	Equation of time
FSP	%	Fibre saturation point
F	-	Level of significance
G	kW/m ²	Global radiation
G ₀ *	kW/m ²	Extraterrestrial radiation
G ₀	kW/m ²	Solar constant
I	A	Amperage
K	-	Equilibrium coefficient
N	-	Number of measurements
Nu	-	Nusselt number
P	W	Electrical power
Pr	-	Prandtl's number
P _C	-	Delivery rate
Q̇	kW	Energy flow
S	Euro	Salvage value
RF	Euro	Return flow
Re	-	Reynolds number
S	%	Volumetric shrinkage
SQ	-	Sum of the square deviations
S _{crit}	m	Critical point
T	-	Rank sum
T	K	Temperature
TA	n	Amortisation
U	W/m ² ·K	Heat transfer coefficient

Notation

U	V	Voltage
V	-	Matched pair rank sum
V	m ³	Volume
\dot{V}	m ³ /s	Volume flow
W	-	Molecular weight
c _p	kJ/kg · K	Specific heat capacity
d	mm	Thickness
h	W/m ² · K	Convection heat transfer coefficient
i	%	Interest rate
k _c	-	Hourly clearness index
l	m	Overflowed length
m	g, kg	Mass
m	-	Groups of treatment
\dot{m}	kg/s	Mass flow
n	a	Depreciation period
n	-	Day of the year
n	-	Number of repetitions
p	Pa, bar	Pressure
q	-	Interest coefficient
r	kJ/kg	Evaporation enthalpy
s ²	-	Variance
t	h	Time
u	-	Approximation value
v	m/s	Velocity
x	%	Moisture content
Δ	-	Difference
θ	°	Angle of incidence
φ	°	Geographical latitude
α	-	Error of the first kind
α	-	Absorption coefficient
α _D	-	Drying coefficient
β	°	Inclination, slope

Notation

β	%	Shrinkage
γ	$^{\circ}$	Surface azimuth angle
δ	$^{\circ}$	Declination
ε	-	Emission coefficient
η	-	Efficiency
ϑ	$^{\circ}\text{C}$	Temperature
λ	$\text{W}/\text{m}\cdot\text{K}$	Thermal conductivity
ν	m^2/s	Kinematic viscosity
ρ	kg/m^3	Density
σ	$\text{W}/\text{m}^2\cdot\text{K}^4$	Radiation coefficient
τ	-	Transmission coefficient
φ	%	Relative humidity
φ	$^{\circ}$	Geographical longitude
φ	$^{\circ}$	Phase difference
ω	$^{\circ}$	Hour angle

Indices

A	Air	b	between
Ab	Absorber	bea	beam
Ae	Air exchange	con	condensation
C	Collector	dew	dew point
Conv	Convection	dry	dry, drying
Eva	Evaporation	diff	diffuse
F	Air bubble foil	eq	equilibrium
Fa	Fans	e	external
Fl	Flow pipe	e	within
He	Heater	f	final
Hu	Humidifier	glob	global
L	Loss	i	internal
Loc	Local	in	initial
Rad	Radiation	min	minimum
Re	Return pipe	max	maximum
S	Saturated	opt	optical
Sky	Sky	r	radial
Stan	Standard	rec	received
V	Vapour	s	solar radiation
W	Water	set	set
Wi	Wind	st	stored
		t	tangential
		th	thermal
		use	useable
		wet	wet

1 INTRODUCTION

Wood is the most important regrowing raw material in the world due to its wide range of applications. This makes the global timber industry, with an average annual growth rate of approximately 2 %, one of the most important sectors of the world economy [1; 2]. Wood is used as an energy source, as raw material for paper processing and as construction material in the building and furniture industry [3]. For these purposes approximately 3.7 billion m³ of natural and replanted forests are felled world-wide every year. Furthermore, the wood demand still increases due to a rising world population and an ongoing industrialisation in different countries [4]. The annual sawnwood consumption, for example, is expected to increase from 456 million m³ in 1990 to 745 million m³ in 2010 [5]. This fast growing demand for the different wood products results in an overexploitation of the still existing natural tropical forests in many countries of the world. Currently, the area of the tropical forests diminishes irretrievably at about 180 000 ha per year world-wide [5; 6]. This area is often not reforested which results in erosion and even desertification not to mention the immense loss of biodiversity. In addition, both natural and planted forests are necessary for the reduction of the carbon dioxide concentration in the atmosphere. This means that the present overexploitation of the existing forests has to be replaced by a sustainable forest management. This insight resulted in an increasing political pressure on a national and international level to protect the remaining tropical forests [5; 6].

One of the most threatened natural forests in the world is the Brazilian tropical rainforest with an extension of approximately 400 million ha. The current annual wood consumption of the Brazilian timber industry is approximately 190 million m³ and increases at a rate of about 3 % whereby 25 % are used for the production of sawnwood [7]. Almost 4 million employees work directly in the wood industry or in related sectors. Thereby, 30 000 companies contribute to 30 billion US\$ or 4 % of the Brazilian gross national product. Only the large Brazilian wood companies invested about 2 billion US\$ between 1996 and 2001 for expansion and modernisation purposes [7; 8]. However, more severe political and legal restrictions on the cutting of the tropical rainforest and an increasing distance between the forests and the sawmills respectively the manufacturing industries caused an enormous rise in prices for tropical sawnwood in the last few years [9].

An economical and sustainable alternative to the often illegally cut tropical wood species can be seen in fast growing eucalypt species [10; 11]. Originally coming from Australia, Tasmania, Papua New Guinea and parts of Indonesia and the Philippines, eucalypts have been planted throughout the world in more than 100 countries due to their outstanding rapid growth and their genetic variability which enables them to adapt to many different climates and soils [12-14]. Eucalypts were first introduced to Brazil in 1904. The suitable climate, the favourable soil characteristics and the availability of huge planting areas in this country resulted in an extensive reforestation with different eucalypt species during the last few decades. Brazil has, with 20 m³/ha and year, one of the highest average growth rates for eucalypts world-wide. Besides this, record growth rates of up to 110 m³/ha and year were measured on test areas. Today, Brazil possesses about 3 million hectares respectively 27 % of all reforested eucalypt plantations world-wide, which makes it the worlds largest producer of eucalypt wood [8; 12-16].

Considering ecological aspects during cultivation, eucalypt timber provides an interesting alternative to sawnwood from the tropical rainforests [12; 17]. Meanwhile, several Brazilian forest companies with extensive eucalypt plantations operate big sawmills for eucalypts. Only the three largest sawmills produce about 13 000 m³ of eucalypt sawnwood per month. The demand in Brazil for eucalypt products like sawnwood and flooring expands so rapidly that over-supplying seems to be unlikely for the next 10 years. Besides this, the Brazilian government has announced plans to boost furniture exports from 400 million US\$ per year to 2.5 billion US\$ by the year 2002 [10].

More than 720 different eucalypt species are described, with about 250 of them being used in the wood working industry. Within this range of species, the wood density varies from 450 to over 1000 kg/m³ and the colour reaches from light brown to deep red. This shows, that the different eucalypt species differ extremely with regard to their anatomical and physiological structure [13; 14; 18]. The most common eucalypt species grown in Brazilian plantations are *Eucalyptus grandis*, *Eucalyptus saligna* and *Eucalyptus cloeziana*. Special attention is currently paid to *E.grandis* due to its characteristic similarity to mahogany, a common tropical wood species in the Brazilian furniture industry [19]. But until now, these fast growing species were almost exclusively used for the production of cellulose, firewood and charcoal. However, the charcoal producing companies did search for alternatives for their existing eucalypt plantations due to falling prizes for hard coal during the

last years. But also the cellulose industry discovered the great potential and possibilities linked with the production of sawnwood from the available eucalypt forests. However, the existing plantations were managed for the needs of these industries which means that the available raw material is extremely inhomogeneous and prone to deformations, fissuring and cell collapse during sawing and drying. Even in countries like South-Africa and Australia, where plantations of selected eucalypt varieties are managed for sawnwood production since many years and suitable but costly production procedures are available, eucalypt is seen as a very sensitive and problematic wood species compared to other hardwoods [18; 20]. Since economically feasible technologies for an appropriate eucalypt processing are not available, the demand for hardwood in the Brazilian furniture industry is still supplied mainly by native wood from the Mata Atlantica and the Amazonian forest [7; 19].

Green eucalypt wood has a moisture content between 60 and 100 % d.b.¹ which has to be reduced to moisture contents between 8 and 12 % d.b. before it can be manufactured to high quality products in the furniture industry. This low moisture content is not only required for a higher resistance against pests and to improve the mechanical properties but also for a high deformation resistance of the final product. Since wood is a hygroscopic material, it adapts its moisture content to the surrounding air conditions. A changing wood moisture content results in swelling respectively shrinking and consequently in deformations. In this respect especially eucalypt wood is extremely prone to deformations due to a high anisotropy factor, a high wood density variation within the log and a severe spiral growth [21; 22]. Furthermore, the fast growing eucalypts are often characterised by high growth stresses which result in checking during felling and forced drying. Eucalypts are also highly susceptible to cell collapse when using an inadequate drying process [18; 20]. These unfavourable wood properties can only partially be equalised by an adequate sawing and drying technique. This means that suitable processing of the eucalypt wood is essential for the production of high quality products for national and international markets [23]. There is a clear agreement in the literature that a suitable drying process for sensitive eucalypt wood is a slow drying process. However, quite different opinions can be found about the adequate temperature and humidity level of the drying air and the required drying time. Furthermore, investigations are mainly available for South-African or Australian eucalypt

¹ The wood moisture content x is generally calculated on dry basis d.b. and not on wet basis w.b. as common in agriculture; $x = (m_{wet} - m_{dry}) / m_{dry} \cdot 100$ and is expressed in percent.

varieties which vary significantly from Brazilian varieties in terms of their genetic predisposition and growth conditions [18; 20; 24-27]. This is why the Brazilian timber industry considers the search for a suitable and economical drying process for eucalypt hardwoods the main challenge for the next years. A drying process that prevents quality losses and allows the production of eucalypt wood with a stable average moisture content and an uniform moisture distribution in both the single board and in the whole timber load [16; 28].

The available drying technologies, however, are either not suitable or too expensive for an economical production of sawnwood from eucalypts. Ambient air drying is more and more substituted by artificial drying due to long drying times, insufficient high final moisture contents, the lack of climate control, insufficient wood quality and high losses [29]. By the use of artificial drying methods, the drying rate can be increased, the timber can be dried to the desired moisture content and the timber quality can be improved. However, common high temperature dryers are designed for elevated drying air temperatures and high drying air velocities which results in a high specific thermal and electrical energy consumption. Furthermore, most of the reliable wood dryers still have to be imported. To prevent heat losses, the cover of the dryer is normally well insulated due to high drying and comparatively low ambient air temperatures in moderate climates. This high insulation increases investment costs but is not necessary for low temperature drying in warm climates. In addition, high import taxes increase the required investments costs. On the other side, the dryers available in Brazil are often of low reliability and show an even higher electrical energy consumption due to the use of low efficient fans. The investment costs and the energy demand of these high temperature dryers increases the drying costs and makes low-temperature-drying, as required for sensitive eucalypts, uneconomical [23; 30-32]. To solve this problem, various research projects were carried out to investigate the utilisation of solar energy as an economic energy source for timber drying. Several types of solar drying plants have been developed and tested, but until now, none of them could substitute high temperature dryers in a larger scale. This was mainly due to their low drying capacities, the high specific investment costs, the low reliability and especially due to a lacking control of the drying climate which is fundamental for the production of high quality timber [33-36].

It can be concluded that the high costs for artificial timber drying can only be diminished significantly by reducing the investment and/or the energy costs. Therefore, Bux developed

in the framework of a close cooperation with the Institute of Agricultural Engineering in the Tropics and Subtropics of the University of Hohenheim (ATS), the German company THERMO-SYSTEM Industrie- & Trocknungstechnik Ltd (THS), Alfdorf, and the Brazilian forest company CAF Santa Barbara Ltda (CAF) a patented solar-assisted dryer for sawnwood [37-39]. A simple greenhouse design consisting of an aluminium structure with a transparent cover made of highly UV-stabilised polyethylene air bubble foil was used to keep the investment cost low. The transparent cover of the solar dryer allowed the utilisation of the freely available solar energy as heat source without additional costs for a solar collector. During night and adverse weather conditions, when there was not sufficient solar energy, additional heat was supplied by a biomass furnace. Highly efficient axial flow fans, adapted to the typically low pressure drop along the dryer, were installed to reduce the electrical energy demand. The condition of the drying air was controlled by means of a humidifying system, an automatic air flap and a microcomputer [38; 39].

In the framework of this research work, the first solar-assisted timber dryer of this type was installed in the Brazilian Federal State of Minas Gerais for the drying of sensitive eucalypt hardwood. First studies were conducted in a solar dryer with one drying chamber to analyse its general suitability for the drying of sawnwood at an industrial scale. Then, further drying experiments were conducted in a commercially operated solar drying plant with an annual drying capacity of approximately 10 000 m³ of eucalypt timber.

Because the Brazilian variety of *Eucalyptus grandis* was never used for the production of sawnwood, technical drying experience was not available. Furthermore, known high temperature drying regimes for South-African and Australian eucalypt species, requiring a high relative humidity of the drying air and a constant temperature level, could not be used in the solar dryer. This is mainly due to the lower thermal insulation of the cover of the solar dryer which causes a higher dependence of the drying temperature on the ambient air temperature. This means that the drying air temperature has to be adjusted to the required relative humidity level of the drying air and the existing ambient air temperature to avoid condensation of moisture at the cover. Therefore, the temperature of the dryer had to follow the varying day and night temperatures within certain limits. In addition, the thermal energy gain from solar radiation as a fluctuating energy source is not predictable for a specific drying period. The dryer was heated by solar energy at good weather conditions. However, to keep the drying air temperature at the required level at cloudy and adverse

weather or during night, the dryer had to be heated additionally by a biomass furnace. For this reasons, the control of the drying air conditions in the solar dryer was significantly more complicated than in a high temperature dryer. Therefore, the operating behaviour of the solar dryer had to be analysed and the interaction of its single components had to be adjusted and optimised to enable a reliable drying process for high quality drying.

For both reasons, the sensitive eucalypt variety and the drying behaviour of the solar dryer, a totally new type of drying regime had to be elaborated. This drying regime had to consider the system immanent properties of the solar dryer, the specific drying requirements for sensitive eucalypt hardwood and the existing subtropical climate conditions. Therefore, various drying experiments with varying drying air conditions were executed and compared with each other. Thereby, main attention was given to the energy consumption, the drying time and the quality of the dried timber. However, due to missing international standards for the quality evaluation of sawnwood, an evaluation method and a classification system was adapted and standardised from an European pre-norm to the specific needs of eucalypts [40; 41].

The drying quality, the drying time and the energy consumption was then compared to the still widely distributed ambient air drying of eucalypt woods and to high temperature drying. Furthermore, the economic efficiency of the solar dryer was compared to common high temperature dryers. For this purpose, the drying costs of one cubic meter of sawn eucalypt wood was used as reference value. Then, the influence of the most important cost parameters like the investment costs, the current interest rate and the energy costs on the drying costs was investigated by a sensitivity analysis. The required amortisation time was calculated depending on the sales price for the dried timber.

2 FUNDAMENTALS OF SAWNWOOD DRYING

The drying behaviour of sawnwood depends on the one hand on its biological and physical properties and on the other hand on the conditions of the drying air. This means that a technical drying process has to be adapted to the specific characteristics of each wood species. The following chapters give a general review about the drying relevant wood characteristics, the influence of the drying air on the drying rate and the effects of drying on the wood quality, hereby placing special emphasis on the studied hardwood species *Eucalyptus grandis*.

2.1 Drying Relevant Wood Characteristics

The quality of wood, used for industrial sawnwood production, is defined primarily by its specific biological and physical properties. These specific wood characteristics are not only determined by the wood species but also by the variety and origin of the species, the growing conditions, the applied forest management and the position inside the log. This means that both the ambient influence and the genetic predisposition define a specific wood characteristic like wood density, spirality or growth stress. Thereby, each wood characteristic has either a positive, an indifferent or a negative influence on a specific production step like sawing or drying [21; 29; 42; 43].

The following chapters describe the general anatomical wood structure and give an overview about those wood properties that highly influence the drying behaviour of sawnwood.

2.1.1 Anatomical Structure

Wood tissue is defined biologically as a secondary xylem that is produced by plants during the secondary radial growth. Secondary radial growth means the increment of the circumference of plant organs that have finished longitudinal growth and is caused by the cambium. Cambium is a lateral meristem that consists of living wood cells that are capable to subdivide. This radial growth is characteristic for all wooden plants. In regions with distinct seasonal climates, the periodical activity of the cambium produces annual respectively growth rings. For example, wood cells with thin cell walls and big cell lumina are built in springtime while wood cells with thick cell walls and small cell lumina are built in au-

tumn. Therefore, the growth rings can be subdivided in earlywood and latewood. Furthermore, a log can be divided in sapwood and heartwood. Sapwood is the outer region of the log where mineral solutions are transported and manufactured food is stored. The region in which the cells do no longer fulfil these functions is called heartwood [44; 45], **Figure 1**.

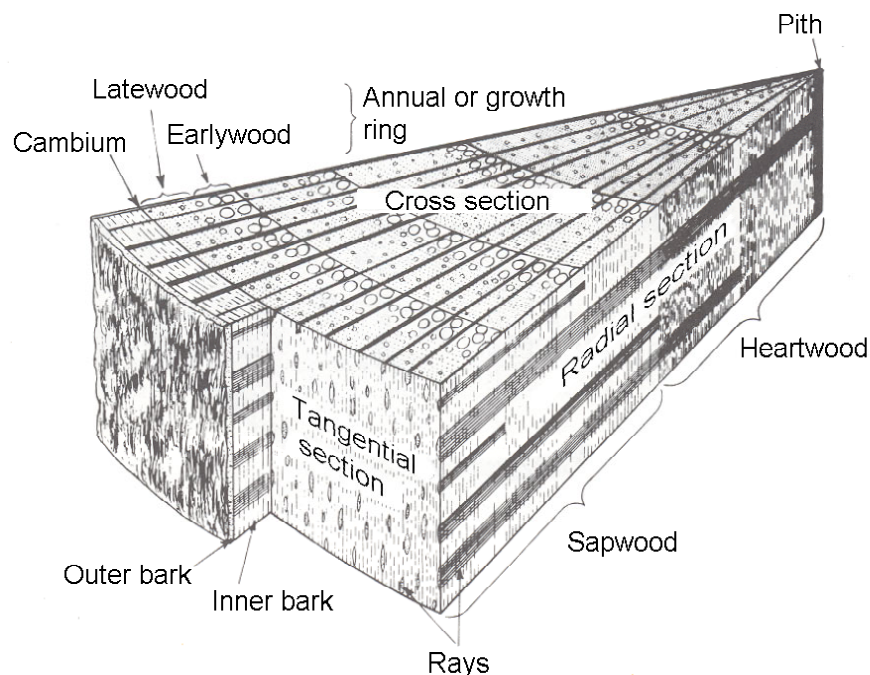


Figure 1: Principal structural features of a hardwood tree [45].

All wooden plants are divided in gymnosperms and dicotyledones. Coniferous trees are the most important group of gymnosperms and deciduous trees are the main group of dicotyledones that are used in the wood working industry for sawnwood production. Coniferous and deciduous trees have a quite different anatomical structure. With regard to evolution, coniferous trees are older and have a more primitive and porous structure than deciduous trees which facilitates the movement of the wood moisture during drying, **Figure 2**. The higher evolved deciduous trees have a higher number of different cell types and contain wood vessel elements. This characteristic is missing in coniferous trees. Due to the distribution of these vessels, the deciduous trees are divided furthermore in ring-porous trees like eucalypts and diffuse-porous trees like beech [44; 46].

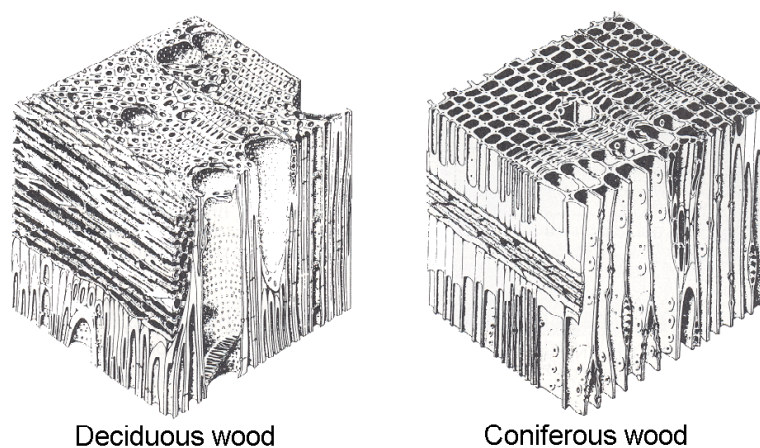


Figure 2: Deciduous wood with a dense and highly differentiated wood structure. Coniferous wood with a porous and primitive structure.

2.1.2 Density

Next to the biological differentiation of wood in coniferous and deciduous wood, the classification in soft- and hardwood is more important for the wood industry. This is due to the fact that most mechanical wood properties are defined by its hardness and therefore primarily by its density. Normally, deciduous wood is indicated as hardwood and coniferous wood as softwood due to their anatomical structure. But there exists also soft deciduous wood like Balsa wood and hard coniferous wood like Western Hemlock wood. However, the wood density is not only influenced by the species but also by its origin, the growing location, the age of the tree and the location inside the stem. This means that large density variations can be found among trees of the same species and growing area. Therefore, average wood densities are cited to define the hardness of a certain species, **Table 1**. More important than the average wood density for sawnwood quality, however, is the density variation inside an individual tree [47; 48]. While wood gets harder and more durable with increasing density, drying gets more difficult and energy intensive [49].

Different average wood densities are cited for *Eucalyptus grandis*. Young trees are given with 380 kg/m^3 while older trees have average densities between 510 and 570 kg/m^3 . The density increases rapidly with increasing distance from the pith, especially in the zone of juvenile wood. The radial increase, however, becomes less pronounced with increasing height. High density gradients from the pith to the bark from 120 kg/m^3 in young trees and 200 kg/m^3 in older trees are cited. Extreme variations of 400 kg/m^3 are also found. Low

wood densities of 290 kg/m³ can be found in the pith while densities up to 630 kg/m³ exist in the sapwood. Variations in density along the stem are less consistent than those in radial direction [27; 42; 50-56].

Table 1: Classification of wood according to its hardness respectively density in kg/m³ [49; 57].

	Hardness	Wood species	Wood density		
			Min.	Average	Max.
Softwood	Very soft	<i>Ochroma lagopus</i> (Balsa wood)	50	130	410
	Soft	<i>Picea abies</i> (Spruce)	300	430	640
		<i>Pinus sylvestris</i> (Pine)	300	490	860
Hardwood	Medium hard	<i>Eucalyptus grandis</i>	290	450	630
		<i>Juglans nigra</i> (Walnut)	450	640	750
	Hard	<i>Fagus sylvatica</i> (Beech)	490	680	880
		<i>Eucalyptus globulus</i>	660	700	790
	Very hard	<i>Robinia pseudoacacia</i> (Robinia)	540	740	870
	Hard as bone	<i>Guajacum officinale</i> (Guaiac resin)	950	1200	1300

2.1.3 Moisture Content

The water distribution in trees depends on both the wood species and the environmental conditions. The moisture can either be distributed equally in the whole log or significant moisture gradients can exist in radial or longitudinal direction. In *Eucalyptus grandis* for example a high moisture content of 170 % d.b. can be found in the sapwood in contrast to a low moisture content in the heartwood of 50 % d.b.. Next to the moisture differences in a single log, there can also exist significant differences of moisture content and distribution in different logs of the same wood species at the same growing conditions [27; 58-61].

Water is needed primarily in trees for the transportation of nutrients and minerals. Therefore, wood fibres contain water in their cell walls and cavities. The water in the cavities is

called “free” water due to low binding forces. The water in the cell walls is called “bound” water due to the strong bonds caused by chemical and physical binding forces. At a wood moisture content between 0 and 6 % d.b., water is bound by a chemical-sorptive manner, between 6 and 15 % d.b. by different types of adsorption forces and between 15 and about 30 % d.b. by capillary condensation. The range in which the cell walls of the wood fibres are saturated and free water is available is called the fibre saturation point (FSP). The numerical value of the fibre saturation point depends not only on the wood species but also on the wood temperature and can therefore range between 22 and 35 % d.b.. However, average values are given for softwood species with 26 % d.b. and for hardwood species with 27 % d.b. [30; 57; 62; 63].

Wood is a hygroscopic material due to cellulose macromolecules in its tissue that have a big attraction for water. Therefore, the moisture content of sawnwood adapts with time to the surrounding air conditions. The resulting moisture content is called the “equilibrium wood moisture content” and depends mainly on the temperature and the relative humidity of the ambient air [49]. This correlation is well described by the Keylwerth-diagram which is based on extensive measurements of European sitka spruce (*Picea sitchensis*) [29], **Figure 3**. The diagram shows that the equilibrium wood moisture content decreases significantly with decreasing relative humidity of the surrounding air whereas the influence of the temperature is less significant. However, the equilibrium moisture content of other wood species can differ significantly from the described values in the Keylwerth-diagram. But this fact is normally neglected in drying praxis due to missing data on most wood species [29; 64]. It should also be observed that wood has a sorption hysteresis which means that the desorption- and adsorption isotherms do not align. This can result in varying equilibrium wood moisture contents.

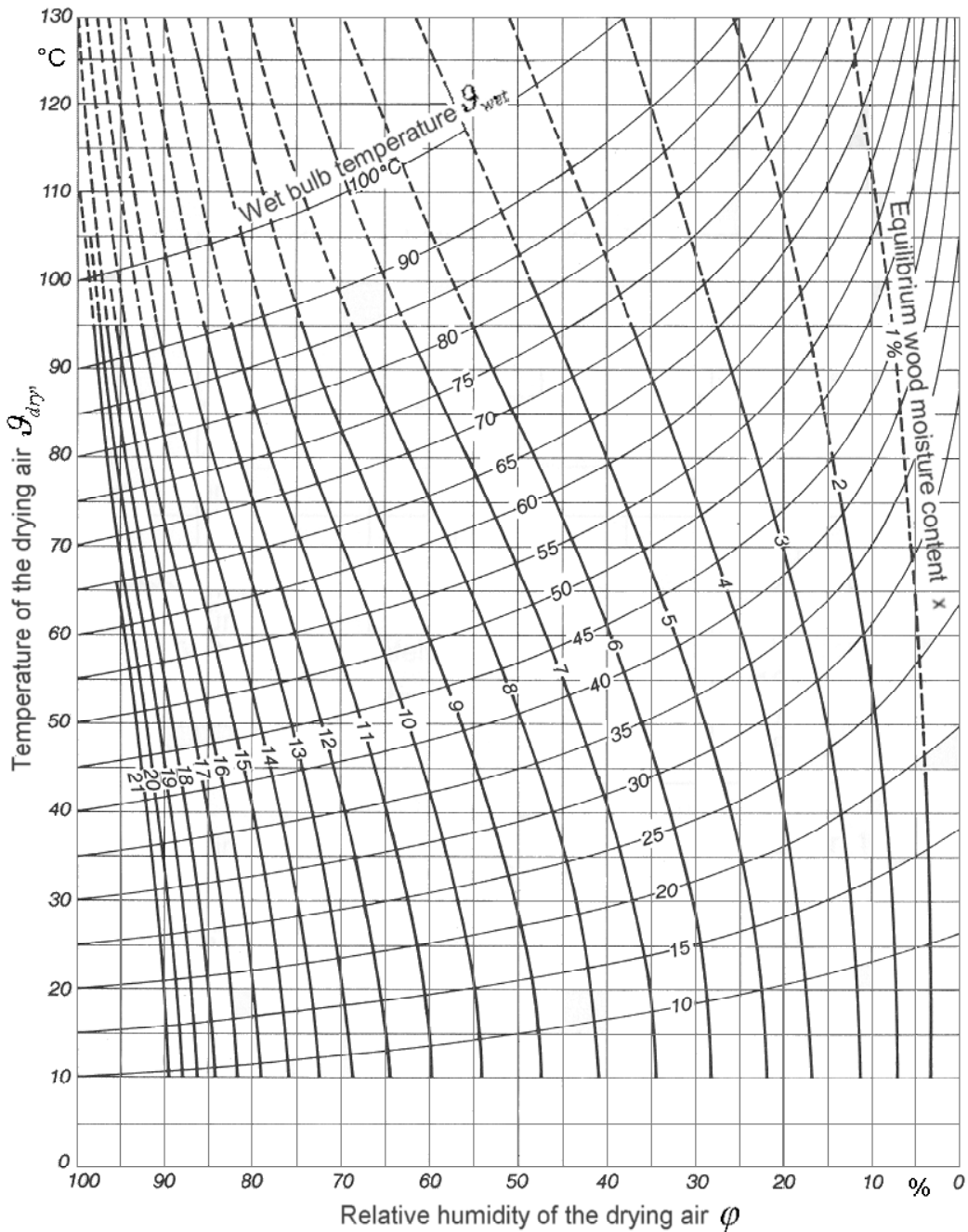


Figure 3: Equilibrium wood moisture content in % d.b., modified according to Keylwerth [29].

Simpson mathematically described the correlation between surrounding air conditions and the wood moisture content [65]. The presented formula is based on sorption theory and measured data. Thus, equilibrium wood moisture content values x_{eq} can be predicted on the basis of the drying air temperature θ and the relative humidity of the drying air ϕ by:

$$x_{\text{eq}} = \left(\frac{K_1 \cdot K_2 \cdot \frac{\varphi}{100}}{1 + K_1 \cdot K_2 \cdot \frac{\varphi}{100}} + \frac{K_2 \cdot \frac{\varphi}{100}}{1 - K_2 \cdot \frac{\varphi}{100}} \right) \cdot \frac{1800}{W} \quad (1).$$

The equilibrium constant K_1 is the equilibrium between the hydrated water and the dissolved water:

$$K_1 = 4,737027 + 0,0477346 \cdot \vartheta - 0,0005012 \cdot \vartheta^2 \quad (2),$$

while the equilibrium constant K_2 is the equilibrium between the dissolved water and the water vapour of the surrounding air:

$$K_2 = 0,706 + 0,001698 \cdot \vartheta - 0,000005556 \cdot \vartheta^2 \quad (3),$$

and W is the molecular weight of the polymer:

$$W = 211,7 - 0,62365 \cdot \vartheta - 0,01853 \cdot \vartheta^2 \quad (4).$$

A comparison between the mathematical model by Simpson and the Keylwerth-diagram shows that the values of the equilibrium wood moisture contents are very similar at low temperature and humidity levels of the surrounding air, **Figure 4**. The difference of the equilibrium wood moisture content between these two methods at a relative humidity of about 20 % is almost zero at a surrounding air temperature of 20 °C and still less than 1 % at a high temperature of 80 °C. At a relative humidity of 90 % this difference is still relatively small with about 2 % at a temperature of 20 °C while it is almost 10 % at a high temperature of 80 °C. Assuming that the extensive measurements of the Keylwerth-diagram are more representative for the real conditions than the calculation method by Simpson, this comparison shows that the mathematical determination of the equilibrium wood moisture content is only reliable at ambient air conditions but is not transferable to conditions in a wood dryer at high temperatures and a high relative humidity.

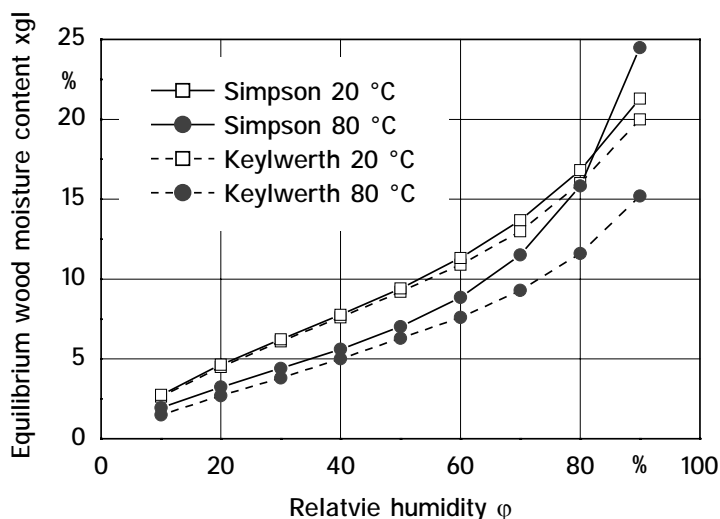


Figure 4: Comparison of the equilibrium wood moisture content x_{gl} of the Keylwerth-diagram and the mathematical model by Simpson.

2.1.4 Shrinkage and Anisotropy

During drying of green wood, the freely available water evaporates easily, primarily due to low binding forces. This has no influence on the wood dimensions. However, as soon as the moisture content falls below the fibre saturation point, the more strongly bound water evaporates from the cell walls. Thus, the drying velocity decelerates and the wood changes its size with changing moisture content, **Figure 5**. A decreasing moisture content causes shrinkage with a defined factor. This factor depends on the wood species and is called β -value. In contrast to this, the factor for swelling is called α -value.

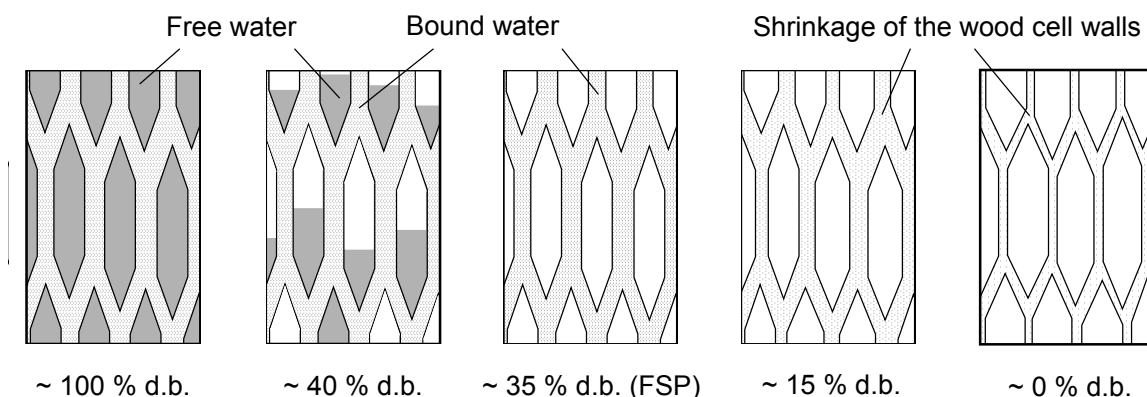


Figure 5: Shrinkage of the wood tissue depending on the moisture content [57].

The grade of total volumetric shrinkage is proportional to the wood moisture content and the wood density, whereby denser wood shrinks more than lighter wood. Therefore, an

inhomogeneous density distribution in wood causes differential shrinkage and therefore deformations [27]. The volumetric shrinkage S in % from green to oven dry can be estimated, on the average, by the wood density ρ and the fibre saturation point FSP by the relationship [22; 57]:

$$S = \rho \cdot FSP \quad (5).$$

with the unity of the wood density ρ being g/cm^3 and the fibre saturation point being given at 26 % d.b. for softwood and 27 % d.b. for hardwood (see chapter 2.1.3). However, the estimated shrinkage can differ significantly with wood species as prone to collapse as eucalypts. Low volumetric shrinkage is found in stable wood like mahogany with 8.6 %, **Table 2**. Average values can be found in softwood like pine and spruce while high values exist in beech and *Eucalyptus grandis* with almost 19 %. Extreme high values of almost 27 % can be found in certain other eucalypt species [22; 57; 66-70].

Wood shrinkage differs in radial, tangential and longitudinal direction following its inhomogeneous anatomical structure [27; 60; 61]. This typical characteristic is called anisotropy and is responsible for inevitable deformations during drying. **Figure 6** shows these natural deformations of sawnwood resulting from different shrinkage in tangential and radial direction.

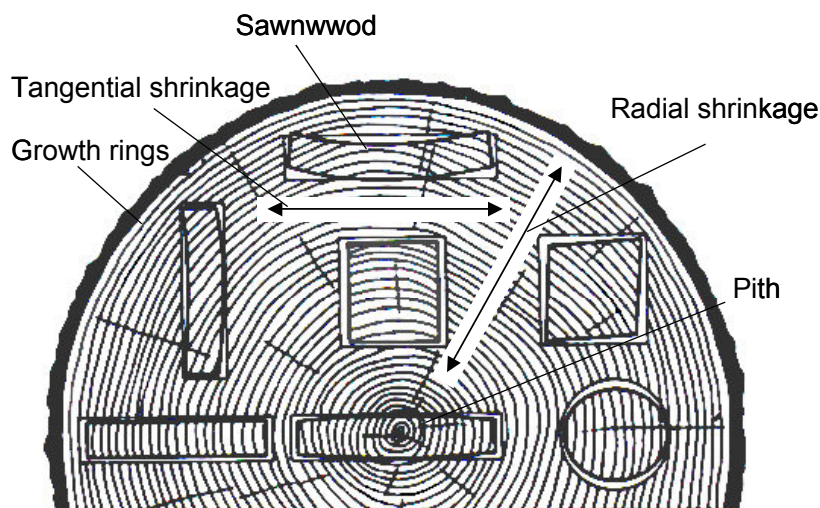


Figure 6: Deformation of wood through natural shrinkage depending on the location in a log [30].

The anisotropy can be quantified by the anisotropy factor AF by:

$$AF = \beta_t / \beta_r \quad (6),$$

with β_t is the tangential and β_r is the radial shrinkage. The tangential shrinkage β_t with approximately 4 to 17 % is significantly higher than the radial shrinkage β_r with values between 3 and 7 %, Table 2. The shrinkage in longitudinal direction is normally less than 0.5 % and therefore has no influence on the wood quality. Total volumetric shrinkage is uniform if the anisotropy factor is equal 1. The higher the anisotropy factor, the stronger are the drying defects. Wood with an anisotropy factor between 1.2 and 1.5 like Mahogany is evaluated as very stable. Factors between 1.6 and 1.9 as found in softwood like pine and spruce are still normal while timber with values higher than 2 like beech and most eucalypt species (AF of *Eucalyptus grandis* = 2.2) is seen as problematic wood [22; 30; 71].

Table 2: Tangential, radial and volumetric shrinkage in percent and the anisotropy factor AF for different wood species [22; 49; 72].

Wood species	Tangential	Radial	Volumetric	AF
<i>Swietenia macrophylla</i> (Mahogany)	4.5	3.2	8.6	1.4
<i>Pinus sylvestris</i> (Pine)	7.8	4.5	12.1	1.7
<i>Picea abies</i> (Spruce)	7.4	3.8	11.9	1.9
<i>Quercus spec.</i> (Oak)	9.0	4.5	12.2	2.0
<i>Fagus sylvatica</i> (Beech)	11.9	5.4	17.9	2.2
<i>Eucalyptus grandis</i>	11.6	5.5	18.8	2.2
<i>Eucalyptus regnans</i>	17.0	6.8	26.7	2.5

2.1.5 Growth Stress

Growth stress exists already in green logs and is developed by the trees for their structural needs. Therefore, growth stress has to be distinguished from stress caused by the drying process [73; 74].

Growth stress develops in the xylem and distributes in the stem in longitudinal, radial and tangential directions. During the growing process of the log, the added wood layers (growth rings) are shortened in longitudinal direction due to the lignification of the wood cell walls. At this irreversible process, the secondary cell walls of the wood fibres swell due to the polymerisation of the lignin which causes the microfibrils to shorten or extend. During this process tensile stress develops in the sapwood and compressive stress in the pith [74; 75], **Figure 7**. Tensile stress in the sapwood is independent from log diameter while compressive stress in the pith increases with increasing diameter. When the compressive stress exceeds a certain limit value the wood tissue collapses which leads to the so called “brittleheart” [74].

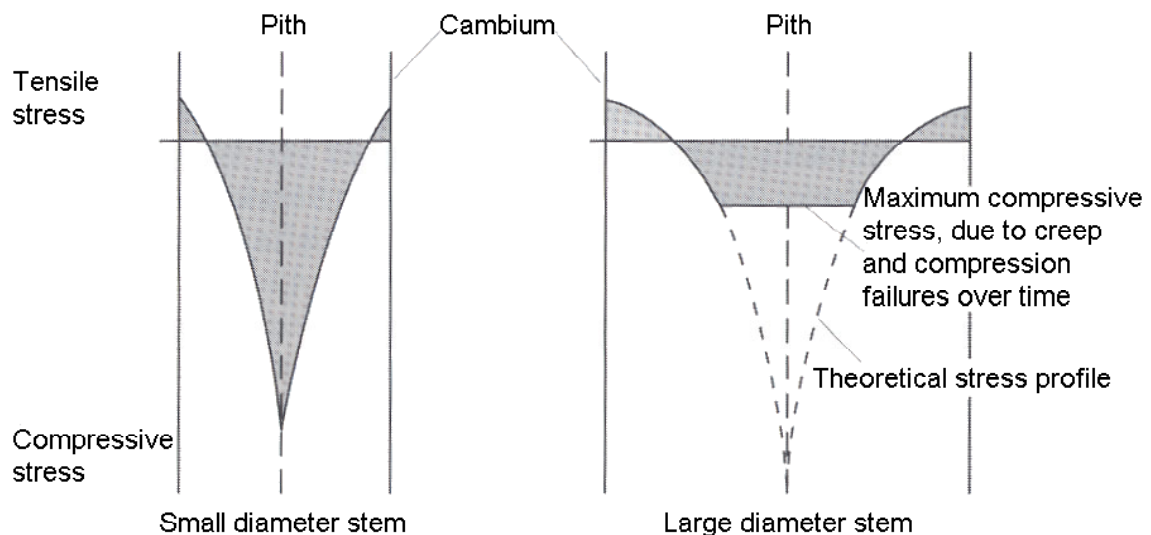


Figure 7: Longitudinal growth stresses across a log [73; 76].

Existing longitudinal growth stresses can cause extensive degrade through severe end splitting already during felling, crosscutting and conversion of trees. During sawing and drying, warping and splitting of boards can often be found. Even at very mild drying conditions heart cracks appear due to shrinkage of the end surface [74; 75; 77-79].

Growth stress can vary enormously between different species or subgroups. But also within the same wood species or even between single stems of the same species and the same growing conditions. Growth stress depends strongly on environmental conditions (e.g. forest management), diameter, age and especially genetic specification of the single

tree. However, tension stress in the sapwood is not correlated significantly to environmental conditions and for that reason a strong genetic control of end splitting is postulated. Growth stress is directly linked to the structure of the wood fibres. Logs with high growth stresses have a high density gradient from the sapwood to the pith, thick cell walls and long fibre cells. At that the fibre cells of logs of different origin differ significantly in length, width, diameter and wall thickness [51; 78].

Splitting of boards during sawing as a consequence of high growth stresses is more severe in fast growing species like *Eucalyptus grandis* and young trees with a smaller diameter compared with older and thicker logs of the same species. This is due to the larger stress gradient between sapwood and heartwood. Because wood close to the pith has a high tendency to split, this part of the log is usually cut off by a suitable sawing technique and is used for low quality products. However, young trees of *Eucalyptus grandis* (< 10 to 12 years) do not have a sufficient log diameter for these sawing techniques to be implemented [18; 51; 61; 79; 80].

2.2 Drying Behaviour of Sawnwood

Sawnwood has to be dried to a low final moisture content of 8 to 12 % d.b. for various reasons. Primarily, wood is a hygroscopic material that changes its dimensions with a changing moisture content. Therefore, only when the moisture content of the manufactured wood is adapted to the surrounding air, the shrinkage of the final wood product can be kept at an acceptable level and quality problems can be prevented. In addition, dry wood has better mechanical properties than green wood. This facilitates its mechanical processing and increases the firmness of joints with screws and nails and the durability of gluing and painting. Also the resistance against mould and insects increases with a decreasing wood moisture content [81; 82].

2.2.1 Influence of Drying Air Conditions on the Drying Rate

The drying rate of timber is influenced by both the wood characteristics and the conditions of the drying air. The complex wood structure with its typical porous distribution and cell wall structure influences the moisture movement of water vapour, liquid water and bound water (see chapter 2.1.1). The state of the drying air can be defined sufficiently by the tem-

perature, the relative humidity and the air velocity. A variation of these parameters has a significant influence on the drying rate [46; 83].

2.2.1.1 Temperature

Drying wood is, like any other drying process, significantly influenced by the temperature level. The correlation between the temperature of the drying air and the drying rate is shown in **Figure 8**.

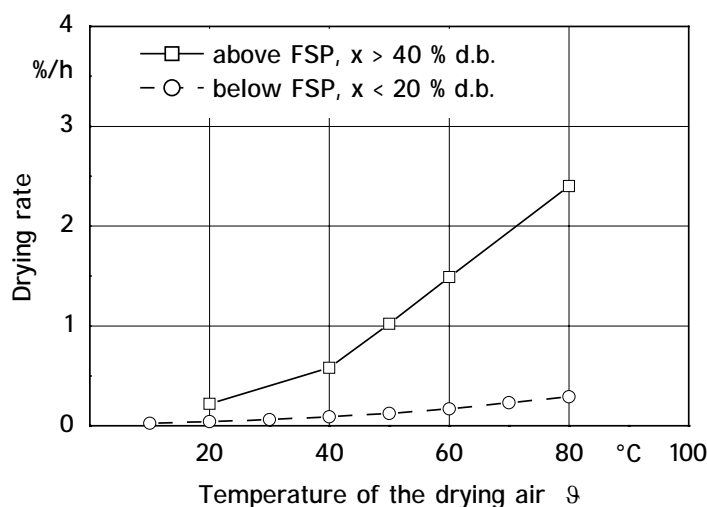


Figure 8: Effect of the drying air temperature on the drying rate of 52 mm thick sapwood from Scots pine (*Pinus sylvestris*) at a relative humidity of the drying air of 70 % and an air velocity of 1.3 m/s at a wood moisture content above (> 40 % d.b.) and below (< 20 % d.b.) the fibre saturation point (FSP ~ 26 % d.b.) [85].

According to this temperature dependence, wood drying is classified in „low-temperature-drying“ at temperatures between 15 and 45 °C, „normal-temperature-drying“ at temperatures between 45 and 90 °C and „high-temperature-drying“ at temperatures between 90 and 130 °C. Normally, low-temperature-drying results in good drying quality but also in relatively long drying times. Due to high investment and operation costs of high temperature dryers, this method is almost only used for the pre-drying of sensitive hardwoods like eucalypts to a wood moisture content of approximately 20 % d.b.. High-temperature-drying has negative influences on the wood characteristics and for that reason it is used only in special cases like in the drying of coniferous softwoods. Hardwoods are generally not suitable for this drying method due to strong discolorations. However, high drying

temperatures can cause plastification of the wood which can protect it from warping during drying thus leading to a better wood quality. While low-temperature-drying and high-temperature-drying are used only in some special cases, the normal-temperature-drying is by far the most common method of artificial drying [84].

A higher drying air temperature causes a raised wood temperature which increases the vapour pressure inside the wood. This causes a higher diffusion coefficient which facilitates the moisture transport. A relieved moisture transport leads to a flatter moisture gradient inside the board and thus an increased drying rate. The average wood temperature depends on the surface temperature due to thermal conduction from the surface to the core. Thereby, the heat conductivity λ of wood between 0.13 and 0.16 W/K·m allows a relatively slow but permanent temperature equalisation. Humid wood evaporates sufficient water during the drying process to cool down the board surface. However, the moisture movement to the wood surface decreases with decreasing wood moisture content, which results in an increasing board surface temperature. Therefore, during the drying process the wood temperature gradually reaches the drying air temperature. Generally, the importance of the drying temperature increases with board thickness, since the moisture transport to the surface becomes the limiting factor for the speed of the drying process [46; 86; 87].

2.2.1.2 Relative Humidity

While the temperature is important for the moisture transport in wood, the relative humidity of the drying air φ is decisive for the evaporation velocity of the moisture from the board surface. Decreasing the relative humidity of the drying air increases its water absorption capacity, which increases the evaporation of the wood moisture. This leads to an intensification of the drying rate. On the other hand, increasing the relative humidity decelerates the drying rate. Therefore, the drying rate of sawnwood is mainly determined by the relative humidity level of the drying air above fibre saturation point. Below fibre saturation point, the influence of the drying air humidity is less due to a high temperature dependence of the water transport inside the wood [46; 49], **Figure 9**.

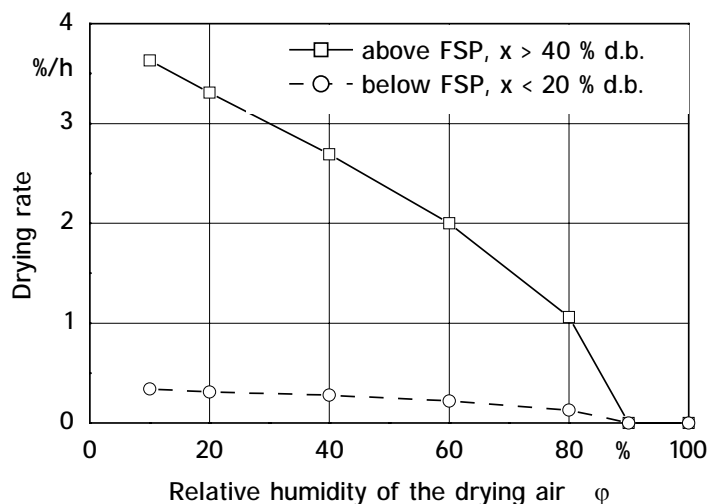


Figure 9: Effect of the relative humidity of the drying air on the drying rate of 52 mm thick sapwood from Scots pine (*Pinus sylvestris*) at an air temperature of 60 °C and an air velocity of 1.3 m/s at a wood moisture content above (> 40 % d.b.) and below (< 20 % d.b.) the fibre saturation point (FSP ~ 26 % d.b.) [62; 85].

2.2.1.3 Air Velocity

Next to the temperature and the relative humidity of the drying air, the air velocity between the wood layers has a significant influence on the drying rate [88]. At that, the air velocity is necessary for both the heat transfer from the drying air to the wood and the moisture transfer from the wood to the drying air – a humid wood surface presumed.

The flow of air can be turbulent or laminar, which depends on the Reynolds number that is deduced from the air velocity, the cinematic air viscosity and the characteristic length respectively the overflowed distance. A laminar flow of air builds a thicker boundary layer on the wood surface than a turbulent flow of air which decelerates the drying process by reducing the heat and moisture transfer. Because the Reynolds number depends also on the characteristic length, it is not possible to give an exact air velocity where the flow of air changes from laminar to turbulent. Besides this, the specific arrangement of the timber and the board surface has a small but noticeable influence [89]. This complexity explains why many investigations about the influence of the air velocity postulate different minimum air flow velocities between 1.3 and 2.5 m/s to prevent a laminar air flow under normal wood drying conditions [90-92].

A high drying air velocity can increase the drying rate at moisture contents above fibre saturation point significantly for fast drying wood species **Figure 10**. During the process, the wood moisture evaporates directly at the wood surface as long as sufficient free water is delivered through the pores from lower wood layers. In the 1980's the suggested limit of air velocity was 8 m/s while today it is given at 3 to 5 m/s for normal high-temperature-drying. Only for very humid wood or for high-temperature-drying above 80 °C higher velocities are recommended. With decreasing wood moisture content the influence of the air velocity decreases due to a decreasing water transfer per time. Thereby, the evaporation layer recedes inside the wood which increases the diffusion distance of the water vapour [29; 46; 58; 90; 92; 93].

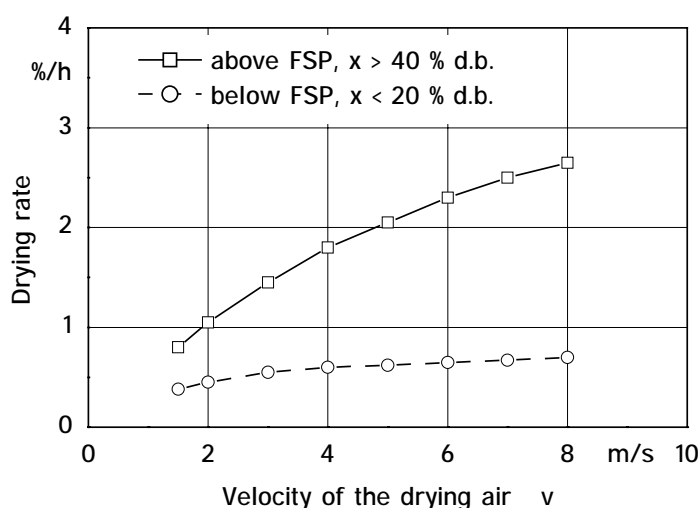


Figure 10: Effect of the drying air velocity on the drying rate of mixed sugar maple sapwood and heartwood (*Acer saccharum*) at an air temperature of 54 °C and a relative humidity of the drying air of 76 % at a wood moisture content above (> 40 % d.b.) and below (< 20 % d.b.) the fibre saturation point (FSP ~ 27 % d.b.) [94].

In order to insure that the final wood moisture content along the inside of the drying chamber is uniform, the flow of air has to be uniform at all locations of the wood stack. When the drying air passes through the timber load, the temperature decreases due to the evaporation of the wood moisture and the relative humidity increases due to the decreased temperature and the evaporated moisture. This means that the higher the evaporation rate, normally at the beginning of the drying process, the higher the air velocity has to be, in order to prevent a moisture gradient in the wood stack. A high air velocity respectively volume flow can only be provided by a high fan capacity, which increases the investment

cost and the energy demand due to an increasing pressure drop in the dryer. The high fan capacity however is only needed at the beginning of the drying process and is normally oversized for the longer part of the drying process below fibre saturation point. Therefore, the fan speed respectively the air velocity is often controlled by a frequency converter. Thus, the air velocity can be adapted to the specific drying conditions, different electricity tariffs, wood species and wood moisture gradients, which reduces the electrical energy consumption. Today high temperature dryers are generally manufactured for air velocities between 1.8 and 3.0 m/s [29; 46; 58; 89-91; 95].

2.2.2 Influence of the Drying Process on the Sawnwood Quality

An adapted drying process can improve significantly the value of the dried sawnwood. On the other hand, improper drying conditions can devalue timber entirely. Therefore, the supervision of the drying quality is of prime importance in wood production. Quality parameters influenced by drying are: the average wood moisture content, the moisture distribution in the wood, casehardening, special types of checks, cell collapse, drying induced discolorations and specific types of warp [41]. Quality parameters that are influenced by the growth conditions, the inhomogeneous structure respectively anisotropy of the wood and the biological properties of the wood species are assigned to the natural wood quality and cannot be influenced by the drying process. For example, wood deformations can result from an inhomogeneous wood density or from spiral growth. These quality losses depend on the raw material and cannot be prevented neither in ambient air drying nor in technical drying. Natural wood defects and drying defects can often not be separated when dried wood is evaluated. National and international accepted directives and norms for the quality evaluation of the technical drying process and the wood quality are still missing. Therefore, the drying quality is still often determined by a subjective evaluation [96]. However, the most important quality criteria for sawnwood are well known and will be explained in the following chapters.

2.2.2.1 Wood Moisture Content

To prevent deformations through shrinkage, timber has to be dried to the required equilibrium wood moisture content. For this purpose, a low moisture variation is required in both the single board and the whole timber load. The equilibrium wood moisture content de-

depends on both the final geographical location and the final type of utilisation. Equilibrium wood moisture contents between 14 and 16 % d.b. are given for ambient air conditions in Central Europe while values between 10 and 21 % d.b. are cited for the different climatic regions of Brazil. High values between 18 and 21 % are found in the tropical Amazonas region, values between 15 and 17 % are given for the colder and rainy South and values between 10 and 14 % are cited for the dry regions in the Northeast and Southwest [97-99]. Compared to this, very similar equilibrium wood moisture contents for the different final applications are cited in Brazil and Central Europe, **Table 3**. This is primarily due to the fact that the surrounding air at the location of utilisation has a higher influence on the equilibrium wood moisture content than the local climate.

Table 3: Equilibrium wood moisture content x_{eq} in % d.b. for different applications under Central European and Brazilian climate conditions [29; 81].

Wood utilisation	Equilibrium wood moisture content	
	Central Europe	Brazil
Construction wood at ambient air	16 – 25	12 – 18
Outdoor windows and doors	12 – 15	12 – 16
Furniture with heating	6 – 12	6 – 10
Furniture without heating	-	12 – 16
Casing for radio and television, parquet	6 – 8	5 – 8
Particle boards, musical instruments	5 – 7	5 – 8

2.2.2.2 Casehardening

A moisture gradient develops between the surface and the core layers of a single board during every drying process. This moisture gradient is necessary to transport the water from the inner layers to the surface. According to the development of the moisture gradient inside the board, tension stresses develop in the surface layers as the moisture content falls below the fibre saturation point and the wood begins to shrink. Compression stresses develop in the board's centre where the wood moisture content is still above the FSP. The

consequence from a high drying stress is called casehardening. This term is generally used for wood that is characterised by overly expanded outer layers, **Figure 11**.

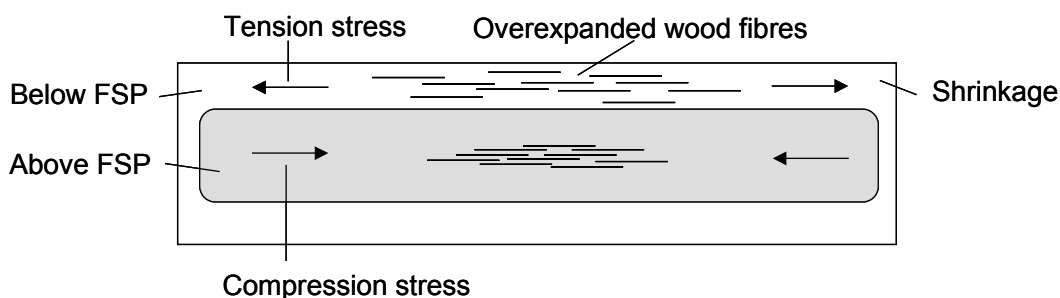


Figure 11: Model for the formation of casehardening.

Casehardening can result in surface and internal checking or permanent deformations of the board. While certain tensions during the drying process are inevitable due to the moisture gradients, the timber should be free of tension at the end. Therefore, drying stresses and moisture gradients between the board’s surface and the core can be relieved through conditioning treatments during or at the end of the drying process. Existing casehardening in the wood can be determined by the slicing or fork tests [29; 40; 41; 100; 101], **Figure 12**.

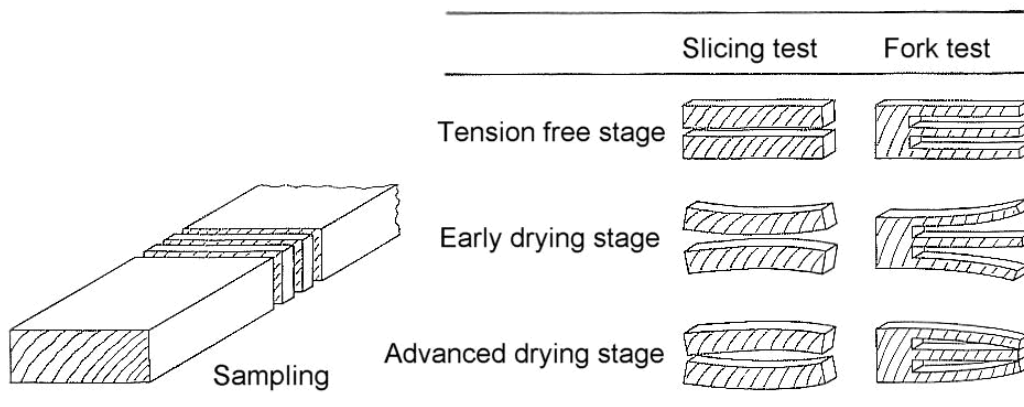


Figure 12: Fork and slicing test for the control of casehardening after drying [30].

2.2.2.3 Deformation

Deformation respectively warp results from differential shrinkage of the wood dimensions during the drying process. Warp of sawnwood due to wood anisotropy is to a certain level a natural process and is not a drying defect (see chapter 2.1.4, Figure 6). For example, thin boards from the outer layers of big logs are less prone to deformation than thick boards or beams from small logs. Twist, a very strong degree of warp, occurs when wood anisotropy exists together with spiral growth. Extreme spiral growth can be found in many tropical wood species and especially eucalypts. Thus, especially boards cut from juvenile trees, having annual rings with a small radius, twist more during the drying process than boards cut from larger trees having a large ring radius. In general, every type of warp is more severe in juvenile than in mature wood and very often cannot be prevented even at very mild drying conditions [27; 50; 67; 102; 103]. Spiral growth can be detected by a turning bark and at the board by undulating wood fibres [27; 29; 30; 71]. However, the inevitable deformations are increased by improper drying e.g. by unequal drying temperature distribution or too severe drying conditions. On the other hand there are various methods of reducing warp, like putting weights on the top of the timber stacks during drying, sawing timber with enough oversize to machine out warp after drying, modifying the drying regime or straightening warped lumber after drying [104]. **Figure 13** shows the most common types of warp. They are characterised as bow, cup, crook and twist. Thereby cup, crook and twist are more important while bow is often neglected in quality evaluation of sawnwood due to an easy equilibration of this defect by jointing various boards.

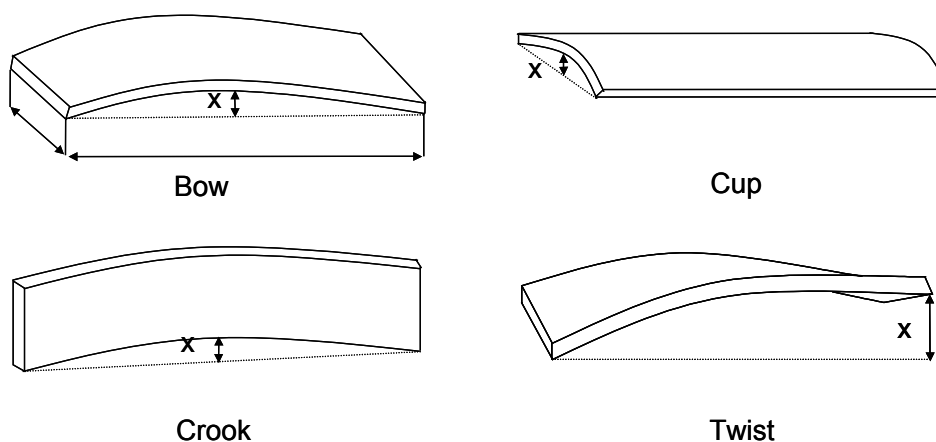


Figure 13: Different types of wood deformation respectively warp of sawnwood.

2.2.2.4 Fissures

Fissures are separated into checks and splits, whereby splits extend over the whole board thickness while checks do not. Despite occurring during drying, it has to be noted that not all fissures are caused by inadequate drying conditions. Both drying checks and splits are separated into those which are caused by an inadequate drying process and those which develop due to the presence of wood specific properties like growth stress. Wood specific checkings are pith checking, checking due to interlocked grain, ring shake and fissuring due to growth stress. These types of checking will not be explained in detail due to its missing significance for the quality of the drying process. The three types of fissures resulting from inaccurate drying conditions are specified below. However, a strict separation from wood specific checking is often not possible. All types of checks are observed with *Eucalyptus grandis* at severe drying conditions but can be prevented by an adapted drying process [26; 29; 40; 105].

- **Surface checks**

Surface checks are deep checks on the wood surface. They develop during the initial stages of the drying process when the timber surface is drying too fast and steep moisture gradients develop as a consequence. Surface checks which do not extend beyond 2 mm in depth have to be accepted because the rough sawn timber surfaces have to be planed anyway and such surface checks will be removed by the planing process [29; 40].

- **End checks and splits**

End checks and splits occur as a result of fast drying at the end of a board due to a facilitated moisture movement along the fibres. End fissures can be reduced by correctly stacking the boards, coating the end of the boards with vapour tight paint and an adequate drying process [29; 40].

- **Internal checks**

Internal checking, which is also known as honeycombing, occurs towards the end of the drying process by casehardening. Honeycombing results as a consequence of harsh drying

conditions at the beginning of the drying process when tension stresses in the wood surface lead to severe plastic deformations. During later stages of the drying process the stress pattern reverses and compression stress develops in the surface and tension stress in the core. As soon as the tension stresses exceed the strength of the timber internal checking occurs. Internal checking is often associated with timber affected by collapse, although here checking occurs at moisture contents above fibre saturation [40].

2.2.2.5 Cell Collapse

Cell collapse of wood occurs during the drying process at wood moisture contents above the fibre saturation point. It results in a large abnormal shrinkage due to the deformation respectively physical collapse of the wood fibre lumina, **Figure 14**. It must be distinguished between collapse shrinkage and normal shrinkage with the latter occurring below fibre saturation point as soon as the cell walls shrink. Cell collapse is considered as one of the worst kinds of damage caused by an inadequate drying process.

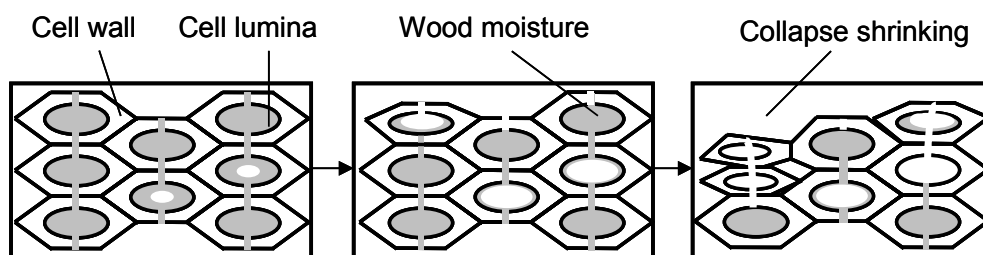


Figure 14: Formation of cell collapse in sawnwood over time.

Collapse is especially found when semi-hard deciduous wood species like eucalypts are dried at inadequately severe drying conditions. Therefore, all eucalypt species are highly susceptible to collapse. High degrade due to collapse is cited for rapid artificial drying of *Eucalyptus grandis*. In these species collapse is more frequent in wood tissues with higher moisture contents and lower densities i.e. collapse is stronger in heartwood than in sapwood and stronger in earlywood than in latewood. This higher shrinkage in the earlywood leads to the characteristic “washboarded” appearance of collapsed wood. While normal shrinkage is positively correlated with its density (see 2.2.2.3) collapse susceptible material has often a negative relationship between shrinkage and basic density. This is explained by the fact that the thickness of the cell wall is critical in resisting liquid-tension forces during the drying process. Thereby, water evaporates rapidly on the wood surface during sharp

drying conditions, which causes high levels of capillary tension forces. The weaker wood cell walls cannot resist the developing pressure drop, which leads to cell collapse. This explains why wood cells with thin cell walls respectively wood of lower density collapses more easily thus causing higher shrinkage [29; 106-108]. It is known that collapse is the result of the interaction between the liquid water content of wood and its anatomical structure. A number of biological and physical factors are known to cause collapse like the transpiration effects, surface tension of water, hydrostatic tension in the fibre lumina, drying stresses caused by steep moisture gradients and the wood anatomy, however, their interaction is still not well understood [27; 29; 47; 107-112].

The intensity of cell collapse increases with higher drying temperatures. An increasing temperature reduces the strength of the wood tissue by changing the chemical bonds of the hemicelluloses and the lignin in the wood cell walls. Therefore, collapse prone wood species have to be dried at low temperatures, whereby the minimum temperature varies depending on the different wood species, until the wood moisture content falls below the fibre saturation point. For some species a drying temperature threshold is defined. It was shown that collapse can be avoided by drying at temperatures below this value while even a slight temperature increase above the temperature threshold increased collapse significantly. Other drying parameters like the relative humidity of the drying air or the size of the boards are of less importance compared to the temperature [87; 107; 111; 113].

Collapse shrinkage is often associated with the formation of internal checks. Internal checking can often be found in boards, which show minimal visible external collapse, while boards which do show washboarding may not be internally checked. Collapse shrinkage can be partially recovered by reconditioning the wood with steam, but collapse induced internal checking is a permanent form of degrade [87; 107; 111].

2.2.2.6 Discoloration

Discolorations are changes of the natural wood colour. Most discolorations occur during the drying process but they are not always caused by the drying conditions. The reasons of discolorations are manifold and various. The most common discolorations are either caused at slow drying conditions by the activity of micro-organisms (blue stain or superficial mould) and biochemical enzyme reactions of the wood or at high temperatures by

physiological and chemical reactions of the wood tissue. In addition, discolorations can be caused by inadequate stacking laths i.e. wet and dirty stickers or stickers of an inadequate wood species [29; 40]. The natural wood colour of *Eucalyptus grandis* varies from greyish–white in young trees and the sapwood of older trees to all shades of pink to dark red in large logs. Thereby, the heartwood is mostly red and sapwood lighter-coloured. Discolorations in eucalypts occur normally only on the outer surface by the exposure to weather conditions and are never described as a serious problem during the drying process [10; 77].

2.2.3 Specific Drying Demands of *Eucalyptus grandis*

The drying of *Eucalyptus grandis* is generally a difficult task due to its specific wood properties which facilitate the development of various forms of degrade while especially young eucalypt trees show an excessive shrinkage and check formation [114]. But also the large variability between individual trees, next to the general biological properties of eucalypt, results in inefficient artificial drying. This is due to the fact that the drying regime has to be adapted to the most degrade prone material. This explains why *E.grandis* is one of the most sensitive woods and why it has to be dried under very mild drying conditions [1; 20; 24-27; 47; 105].

Usually, continuously varying drying regime with constantly raising drying air temperature and decreasing relative humidity of the drying air are used for high temperature drying of eucalypts. These schedules can reduce the drying time compared to former stepped schedules up to one third for the drying of eucalypt hardwood [115-117]. The drying process is normally separated into a drying period before and after the fibre saturation point due to the specific distribution of the wood moisture (see chapter 2.1.3). During the drying process the wood moisture is removed slowly but continuously over the whole drying time to avoid drying stress in the wood. Above fibre saturation point very soft drying conditions are needed to prevent collapse. The drying temperature has to be kept low at the beginning of the process with a maximum of about 40 °C and the relative humidity has to be kept high between 75 and 85 %. While the wood moisture content decreases during the drying process, the drying rate also decreases due to a lower diffusion coefficient. Therefore the temperature is increased continuously up to 50 °C and the relative humidity is decreased to 45 and 70 % depending on the board thickness. Below fibre saturation point the drying process is accelerated by increasing the temperature continuously to a maximum between

55 and 70 °C, with most studies stating an assumption for a maximum temperature tolerance of 65 °C for eucalypt wood. The relative humidity is also decreased to 25 and 45 % [13; 20; 24; 25; 50; 100; 114-116; 118; 119].

To reduce the extensive drying times resulting from mild drying conditions and to prevent drying degrade during the drying process, different kinds of reconditioning treatments like re-humidifying cycles are discussed in literature. Different types of degrade like fissuring, warp and collapse will increase through drying stress caused by an over-dried wood surface. To prevent this, the wood surface is moistured by increasing the relative humidity of the drying air for a certain time period during defined time intervals. This can be done with saturated steam at atmospheric pressure or with high humidity treatments > 90 % at low temperatures which has the advantage that hereby the wood absorbs less water [43; 115; 116; 120; 121]. During the re-humidification treatment only the outer layer of the wood surface is moistured to reduce the high drying stress while the moisture gradient inside the wood still remains constant. This means that the moisture transport from the centre of the board goes on during humidification and the drying process of the outer layers proceeds when the wood surface dries again. This method allows an acceleration of the drying process without a negative influence on the wood quality. Next to the reconditioning phases during the drying process different types of pre-treatments like pre-freezing or boiling respectively preheating in hot water prior to the drying process in order to accelerate the drying rate by diminishing the drying degrade are described in literature. However, these methods are very costly and in praxis almost never applied [113; 119; 122-126].

A melioration of the wood quality is also expected due to intermittent respectively cyclic drying which is naturally found in solar dryers. But this method was proposed as being an adequate technique also in high temperature dryers due to an observed high quality of timber dried in solar dryers. The combination of drying during the day and relaxation at night was seen to be effective in relieving the induced drying stress [127].

3 SAWNWOOD DRYING TECHNOLOGIES

The wood industry differentiates between the drying of construction timber, sawnwood, veneer wood, splints and wood chips, while the drying of sawnwood has the highest commercial relevance. In addition to ambient air drying, various artificial drying technologies were developed for sawnwood to increase timber quality and to reduce drying time. The different types of timber dryers can be classified by the maximum allowable drying air temperature, **Table 4**. Every drying method uses specific thermal energy sources for heating and a typical mode of drying air movement. The drying air can either be moved at fresh air mode or partially respectively completely re-circulated for the reduction of the thermal energy consumption.

Table 4: Thermal energy source and mode of drying air movement for the different drying methods for sawnwood.

Drying Method	Energy Source	Mode of Air Movement
Ambient air drying	solar radiation, wind	natural convection, fresh air mode
Solar dryers	solar radiation	forced ventilation with partial recirculation
Low temperature dryers	gas, oil, biomass	forced ventilation with partial recirculation
Medium temperature dryers	gas, oil, electricity, biomass	forced ventilation with recirculation
High temperature dryers	gas, oil, electricity, biomass	forced ventilation with partial recirculation

Figure 15 shows the classification of the most common drying technologies for sawnwood. Rarely used drying methods like high frequency or microwave drying were ignored. It has to be observed, that the temperature level during a drying process depends rather on the wood species and board thickness than on the type of dryer. For example, high and normal temperature dryers are run at low temperatures during the drying of sensitive wood species to prevent losses in quality.

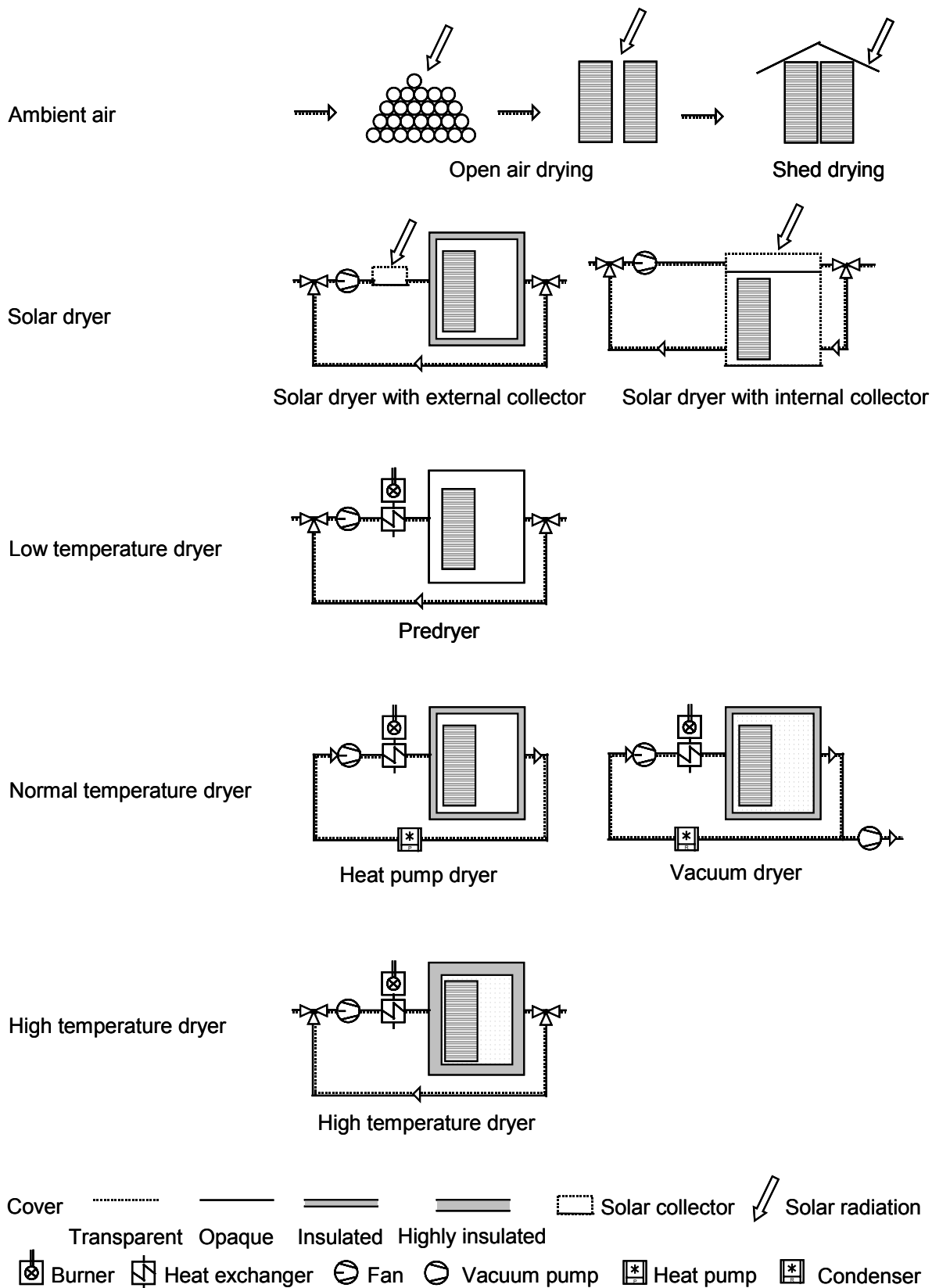


Figure 15: Classification of the most common drying technologies for timber according to the maximum allowable drying temperature.

3.1 Ambient Air Drying

Drying with ambient air is the simplest and oldest form of wood drying. All types of wood, i.e. logs, firewood and sawnwood are dried. Ambient air drying is a weather dependent process, which is influenced by local climatic conditions. The energy source for the evaporation of the wood moisture are environmental energies like solar energy and wind. The drying temperature depends on the ambient air temperature and is therefore relatively low. The drying air is moved by natural convection with fresh air.

The sawnwood is stacked uniformly either outdoor or in open sheds. Exposure to intense solar radiation and wind accelerates the drying rate but causes also drying defects like casehardening, checks and warp. On the other side, a high protection against weather influences decelerates the drying rate but prevents also an adequate air exchange which facilitates the attack of fungi and insects. This shows that a control of the drying conditions is almost not possible at ambient air drying. Therefore, high decreases in value between 5 and 30 % are found at ambient air drying. Besides this, the low wood moisture contents of 8 to 12 %, required in the furniture industry, cannot be reached with ambient air drying in most regions of the world. For example, under moderate climate minimum final wood moisture contents of 15 % d.b. can be reached while under tropical climate minimal moisture contents between 18 and 20 % d.b. are possible. Therefore, ambient air drying is only sufficient for predrying when high quality wood has to be produced. Furthermore, the drying times at ambient air are very long and vary between a few months up to several years depending on wood species, board thickness and microclimatic conditions [29; 30; 84; 128; 129].

The drying costs for ambient air drying of sawnwood are low due to low energy and investment costs. However, costs arise from long drying times through fixed capital and big stocking places [84; 129]. Due to the simplicity and low drying costs, ambient air drying of sawnwood is still the dominating drying method world-wide for all wood species including eucalypts.

3.2 Solar Dryer

The suitability of solar energy as a thermal energy source for wood drying was already studied at the beginning of the last century [130]. Up until now, over 30 different types of solar dryers were developed and investigated under different climatic conditions all over the world [131; 132]. However, most of them were installed for experimental purposes and only very few are sporadically applied at industrial scale [34]. A classification system for the different dryer designs is not yet available. Therefore, various terms like “dryers with separate collector“, “greenhouse type dryers”, “semi-greenhouse type dryers”, “high temperature dryers with additional solar heating”, “solar drying tunnels” are used in the literature. However, this variety can be classified basically in two categories - the external and the internal collector type solar dryer.

External Collector Type Solar Dryer

External collector type solar dryers are characterised by the separation of the solar collector from the drying chamber. Thereby, either solar water or solar air heaters are used. Using water as transport medium for the thermal energy facilitates the storage of the heat energy during adverse weather conditions. However, solar water heaters require a water to air heat exchanger which makes them technically complex and expensive. Therefore, most solar dryers are equipped with simple solar air heaters [34; 133].

The size of the external solar collector can vary independently from the size of the drying chamber. This facilitates the adaptation of the collector area to the desired wood capacity, drying air temperature and drying rate. The drying chamber of the solar dryer has to be insulated to reduce heat losses at its surface. The drying air is recirculated inside the dryer by axial flow fans and is substituted partially by fresh air either manually or automatically. If solar energy is used exclusively as thermal energy source, the drying process has to be run at low temperatures. If high temperature dryers (see chapter 3.5) are equipped with a solar collector, solar energy is used to reduce the consumption of expensive fossil fuels like gas or oil. However, the higher the drying air temperature the lower is the share of solar energy of the total thermal energy [35; 134], **Figure 16**.

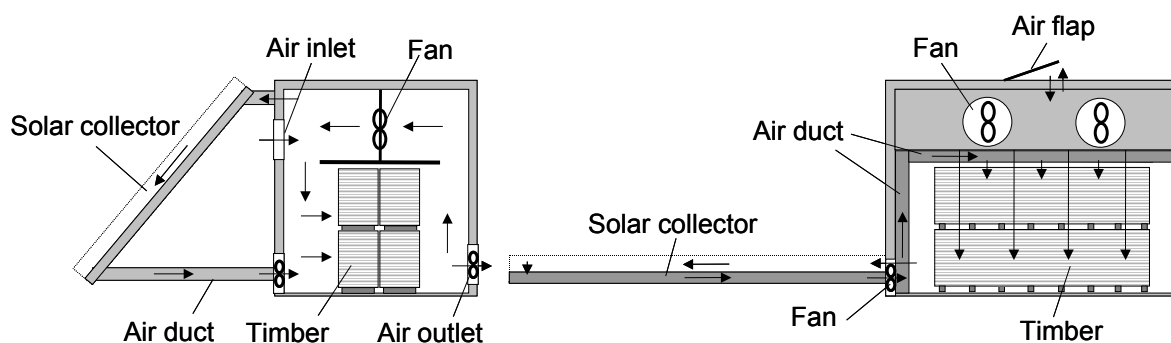


Figure 16: Examples of external collector type solar dryers [131; 135].

The thermal energy demand can be reduced in this type of solar dryer up to between 30 and 60 % compared to a high temperature dryer, depending on the drying regime and timber volume [136-142].

Different opinions exist concerning the economical advantages of an external collector type solar dryer compared to a high temperature dryer. Applied technologies are often complicated which causes high investment costs. At the same time, cost savings through energy saving are relatively low resulting in long payback periods [35].

Therefore, external collector type solar dryers were mostly installed for experimental purposes in industrialised countries under moderate climates for the drying of sensitive hardwoods at low temperatures and were only sporadically applied in tropical countries. However, small external collector type solar dryers with a wood capacity up to 20 m³ were even patented and commercialised [34; 135; 143-153].

Internal Collector Type Solar Dryer

The internal collector type solar dryer (greenhouse type solar dryer) is defined by an integration of the solar collector in the drying chamber. The structure of this solar dryer is kept simple for cost reduction. The wood capacity of these solar dryers varies from less than 0.5 up to 200 m³ [154-156]. Depending on the construction, the roof, the sun exposed walls or the whole dryer is covered with a transparent material, **Figure 17**. Due to the importance of the cover for the performance of the dryer, different materials were tested, like single or double glass and different types of plastic materials like polycarbonate, polyvinyl chloride, polyvinyl fluoride and polyethylene [132; 155; 157-159]. The transparent parts of the dryer

serve as solar collector. Non transparent parts are insulated well. However, due to the transparent construction, the internal collector type solar dryer has a relatively low thermal insulation. During night and unfavourable weather conditions, the solar collector serves as a cooling unit which causes severe problems for the control of the drying climate. Therefore, a higher insulation of the drying chamber, a heat storage unit or control unit for the air movement were tested [143]. Different possibilities of heat storage like black concrete blocks reduce the drying time significantly. But high construction and electrical energy costs for loading and unloading of the storage unit makes this additional installation un-economic [130; 143; 160-164].

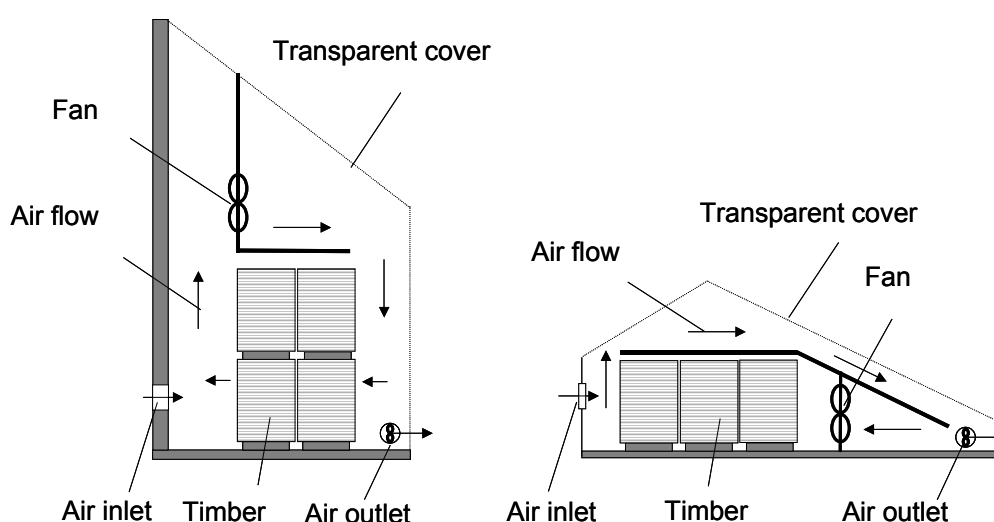


Figure 17: Examples of internal collector type solar dryers [131; 165].

The drying conditions inside of an internal collector type solar dryer are influenced significantly by the local climatic situation, which can cause severe drying defects in sensitive sawnwood [166]. This dependence can be reduced by a supplementary heating and humidification system and an automatic control of the drying climate [159; 167]. Manual control is not sufficient due to the fact that the climatic conditions like solar radiation and ambient air temperature change continuously. However, most solar dryers are not or only manually controlled [23; 33; 155; 166-173].

Depending on the situation, the internal collector type solar dryer has about 50 to 200 % longer drying times than a high temperature dryer [157; 174]. On the other side, timber dries about 60 % faster in a solar dryer than at ambient air. The final wood moisture content is lower and moisture distribution is more uniform, which makes solar drying signifi-

cantly more efficient than ambient air drying [143; 159; 165; 175-177]. Furthermore, solar dried timber has normally an equal or even better quality with less drying defects than ambient air and high temperature dried timber [157; 162-164; 166; 176; 177]. It is assumed that cooling down the stack of wood during the night allows the timber to relax and thus increases the drying quality. Therefore, solar drying is sometimes preferred for sensitive timbers, which are notoriously difficult to dry at high temperatures [155].

If the drying schedule and the structure of the solar dryer is adapted to the local climate, entire solar drying or partial solar drying combined with high temperature drying can be more economic than entire high temperature drying even under moderate climate. Cost reductions of up to 40 % for solar timber drying compared to high temperature drying can be observed under tropical and subtropical conditions [132; 157; 174; 176-178].

In contrast to external collector type solar dryers internal collector type solar dryers are run successfully in tropical and subtropical countries due to elevated ambient air temperatures and a high solar radiation. The efficiency of this type of solar dryer decreases with increasing distance from the equator and with increasing precipitation [157]. However, these dryers can be found with a high insulated cover, a heat storage or additional heating system even at higher latitudes [34; 36; 130; 141; 154; 157; 165; 166; 169; 170; 174-186]. But until now, only few internal collector type solar dryers with wood capacities up to a maximum of 200 m³ were commercialised for the drying of sensitive hardwoods like eucalypts [155; 187-193].

3.3 Low Temperature Dryer

Predryer

Predryers are large timber dryers with wood capacities between 400 and 1 000 m³ or even more. They have a very simple structure with low insulation in order to reduce the investment costs. Compared to high temperature dryers, they possess some quite distinctive features like multiple parallel drying lines, single fan systems for all drying lines, smaller heating surfaces and heat exchangers between the drying lines [16; 194], **Figure 15**.

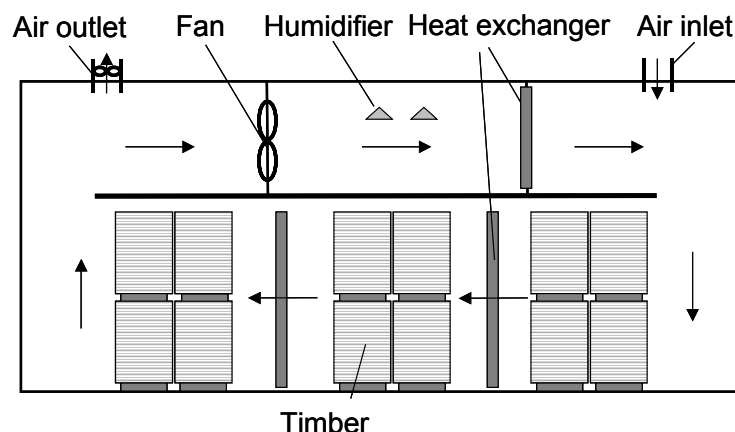


Figure 18: An example of a predryer [194].

Predryers operate at constant drying conditions with humidity and temperature control and forced ventilation [16]. The drying climate is kept at low temperatures between 20 and 40 °C (see also chapter 2.2.1.1). The relative humidity is kept either at a constant level of 70 % or varies at a high level between 50 and 80 %. The partially recirculated drying air has a low air velocity between 0.4 to 0.8 m/s between the single board layers [16]. Low temperature drying with constant climatic conditions is, similar to solar drying, an intermediate step between ambient air drying and artificial drying.

Predrying timber in a low temperature dryer reduces drying defects compared to ambient air drying and reduces energy consumption compared to high temperature drying. This results in an undoubted economic advantage of predrying. Combining predrying and high temperature drying can reduce the drying costs by about 30 % compared to exclusively high temperature drying [194]. Therefore, predryers are widely distributed in Australia and the United States of America for the drying of sensitive hardwoods like eucalypts from green to fibre saturation point (20-25 % d.b.) [30].

3.4 Medium Temperature Dryer

Medium temperature dryers like heat pump and vacuum dryers are operated at temperatures between 45 and 90 °C (see also chapter 2.2.1.1).

Heat Pump Dryer

Heat pump dryers have a similar structure as high temperature dryers, **Figure 19**. However, the heating process of the drying air is quite different. To start with, the drying air is preheated at the beginning of the drying process. Then the air is recirculated within the drying chamber without adding fresh air. The warm and humid drying air is sucked partially away from the timber stack and directed towards the evaporator of the cooling unit of the heat pump. There, the liquid cooling medium evaporates by absorbing the thermal energy. Through the temperature drop of the drying air, the air moisture condenses and the water is drained. The dry air is then reheated at the condenser and added again to the drying process.

The drying air temperature in heat pump dryers is limited by the available cooling mediums to approximately 60 °C. Thermal energy reduction of between 50 to 70 % compared to high temperature dryers can be reached.

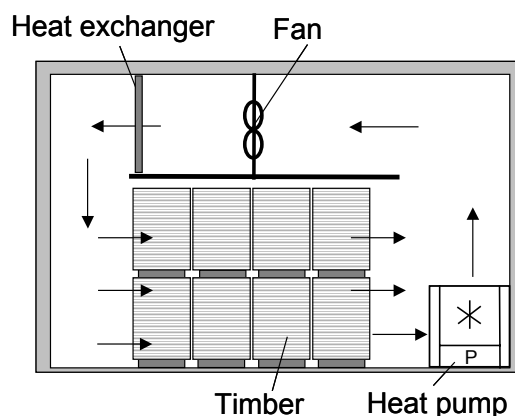


Figure 19: Example of a heat pump timber dryer [29; 195].

With drying chamber capacities of up to 150 m³, heat pump dryers are often used for pre-drying of sensitive hardwoods. Afterwards, the wood is dried in high temperature dryers to the final moisture content. However, small heat pump dryers are used for the whole drying process. Heat pump dryers have a relatively low market share due to extensive drying times and a high technical complexity. Besides this, heat pumps are much more expensive and prone to corrosion than simple air heater with the same power [31; 195-197].

Vacuum Dryer

Vacuum drying takes advantage of the fact that the boiling point of water is reduced with decreasing pressure which facilitates the wood moisture movement in and the evaporation from the timber. The air pressure in the drying chamber of a vacuum dryer is reduced by a vacuum pump. To withstand the pressure difference between the drying chamber and the ambient air, vacuum dryers are often either build as a tube or have a very thick and strong cover, **Figure 20**. Because the transport of thermal energy is complicated at vacuum, vacuum dryers are separated into two classes - continuous and discontinuous dryers. Discontinuous dryers use vacuum free intervals to transport the heat energy with air to the timber. Continuous dryers use either heating panels between the boards or unsaturated water vapour to supply heat energy to the timber. Meanwhile, most vacuum dryers use recirculating water vapour for drying. The drying air is preheated at the beginning of the drying process. Then the drying cycle is closed and the evaporated wood moisture is condensed at specific condensers.

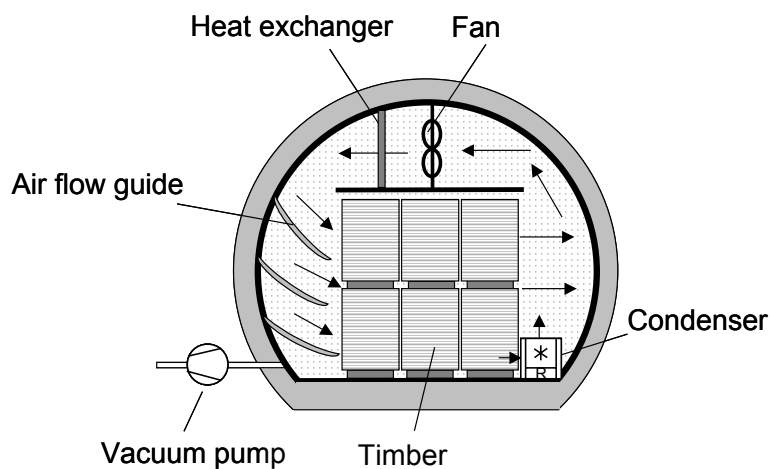


Figure 20: Continuously operated vacuum dryer [29].

Vacuum dryers can accelerate the drying process for timber significantly at relatively low temperatures and high timber quality. However, the energy costs due to a high electrical energy consumption and high investment costs due to a complex technology are still very high [198]. Until the 1990's, the drying volume of vacuum dryers was limited to 25 m³ which caused extremely high investment costs per m³ timber volume compared to high temperature dryers [30]. Meanwhile, drying chambers with a wood capacity of 100 m³ and

more are available, so that vacuum drying is competing in some areas with high temperature dryers resulting in increasing market shares [199-201].

3.5 High Temperature Dryer

High temperature dryers can be operated at temperatures as high as 130 °C (see also chapter 2.2.1.1). The timber capacity of one drying chamber varies between a few m³ up to 150 m³. Transverse ventilated dryers can even contain up to 4.000 m³ of sawnwood. Small dryers are completely finished devices while dryers with a high wood capacity are installed at the desired location. The structure and cover of all high temperature dryers, produced in industrialised countries, are meanwhile highly insulated by aluminium or stainless steel supported sandwich plates with 60 to 100 mm thick polyurethane foam with a heat transfer coefficient between 0.4 and 0.5 W/m²·K. The dryers used in developing countries are still stonewalled with a heat transfer coefficient of approximately 1.8 W/m²·K, **Figure 21**.

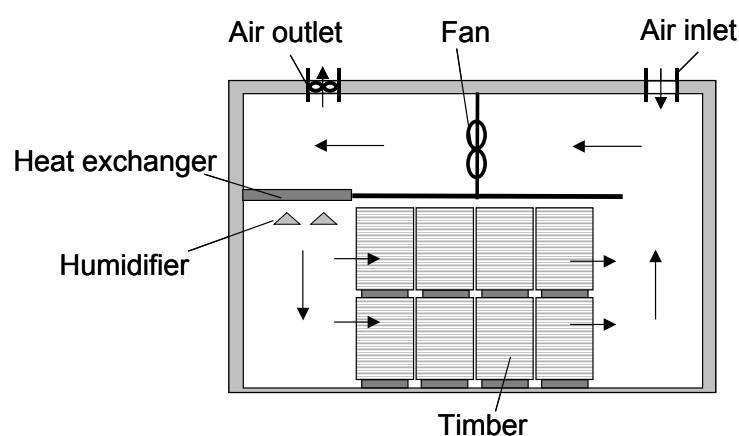


Figure 21: Typical sophisticated high temperature dryer [29].

Axial flow fans are mostly installed above the ceiling of the drying chamber to ensure a uniform ventilation. A heat exchanger, a humidifier and exhaust fans are installed for the control of the drying climate. Automatic control of the drying air conditions like the temperature, the relative humidity and the air velocity is meanwhile state of the art in high temperature dryers. Wood loading is done from the front or from the side with rail wagons or forklifts [31; 58; 196; 197; 202-207].

Suitable drying schedules for high temperature dryers exist already for most wood species. Normally, only one wood species with the same board thickness and moisture content is dried at the same time. A drying regime for high temperature drying of sawnwood is normally divided into a heating phase (phase 1), drying phases above and below fibre saturation point (phase 2 and 3), a reconditioning phase (phase 4) and a cooling phase (phase 5). At the beginning, the sawnwood is heated up uniformly to the desired drying temperature, while the relative humidity of the drying air is kept high between 90 and 100 % to prevent drying, **Figure 22**. When the timber is heated up, the drying process starts with a high relative humidity and a relatively low temperature until the fibre saturation point is reached. Below fibre saturation point, the drying process is accelerated by increasing the temperature and decreasing the relative humidity until the final moisture content is reached. If necessary, a reconditioning phase at high temperature and high relative humidity is initiated to equalise the moisture distribution inside the timber and to reduce drying stress. Afterwards, the sawnwood is cooled down to ambient air temperature inside the dryers to prevent checking through fast cooling [29; 49; 84]. The drying time in a high temperature dryer for a definite wood species and board thickness can be estimated by the initial and desired final wood moisture content and the drying air temperature [29; 208; 209]. However, the drying time depends not only on the wood characteristics and the drying air conditions but also on the dryer's design and operational factors like the wood stacking method or the professional skills of the operator [210]. Drying times vary between a few days for softwood at temperatures of up to 90 °C and several weeks for hardwood at a maximum temperature between 40 and 50 °C.

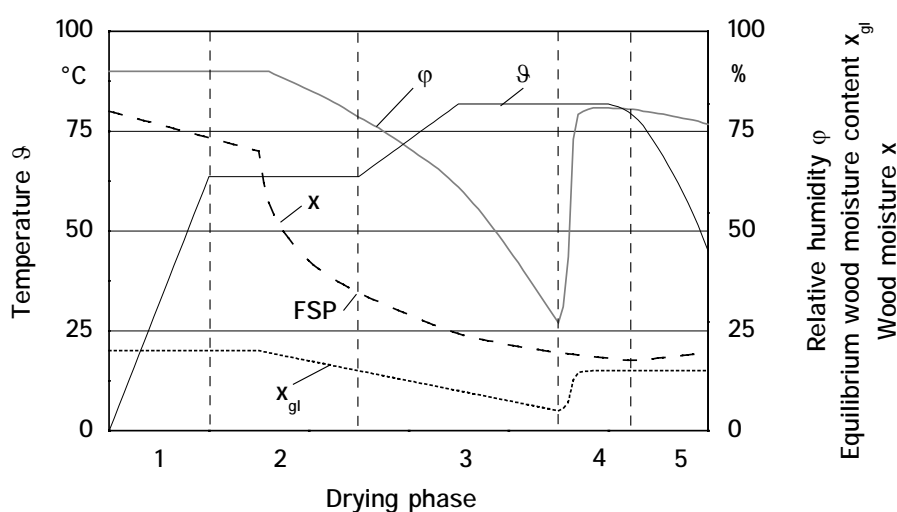


Figure 22: Typical drying schedule for high temperature timber dryers [30].

Up to 70 % of the total thermal and electrical energy consumption during wood processing from the log to the final wood product is consumed by the drying process in high temperature dryers [30; 84; 132; 211-213]. Thereby, the largest part of the thermal energy is required for the evaporation of the moisture, for the air exchange with the ambient and to compensate heat losses at the dryer surface [197; 212]. A thermal energy demand of 4.5 MJ for softwood and 6.2 MJ for hardwood is specified for the evaporation of one kg wood water [84; 146]. Firewood, wood chips, oil, gas or electricity is mainly used as thermal energy source. Highly insulated drying chambers were developed to reduce the thermal energy demand. Furthermore, methods like the connection of various drying chambers by an air duct to allow an air exchange between the different drying chambers were developed. This method can in fact reduce the thermal energy consumption between 10 and 30 % but demands a highly complex control unit [92; 214; 215]. However, all systems for a thermal energy reduction are linked with higher investment costs, which makes them only economical at high drying air temperatures. The biggest part of the electrical energy consumption is needed for the operation of the fans. Here, electrical energy savings between 50 and 60 % can be reached by the melioration of the air flow inside the drying chamber, a high efficiency of the used fans, the length of the timber stack and by adjusting the fan rotation at every drying phase [92; 197; 206; 216; 217].

Artificial drying is still the most expensive step during sawnwood production. This is, next to the high investment costs for high temperature dryers, the labour intensity of operation and losses in quality, mainly due to the high thermal and electrical energy consumption [84; 211]. Improvements of the dryers construction, machine equipment and insulation of the drying chamber did not reduce these high drying costs significantly [92; 216].

High temperature dryers are the most common artificial drying method world-wide with a market share of over 90 % due to a relatively simple technology and a wide range of possible fields of application. All wood species, including eucalypts, are dried with high temperature dryers whereby degradation rates between 30 and 40 % are reported for sensitive eucalypt species at industrial scale [118].

4 OPERATING PERFORMANCE OF THE SOLAR-ASSISTED TIMBER DRYER

A fully automatic, solar-assisted dryer with an internal solar collector, for drying tobacco and sawnwood was developed between 1991 and 1998 by Bux at the Institute of Agricultural Engineering in the Tropics and Subtropics of the University of Hohenheim [37-39]. This solar dryer consists basically of an air bubble foil covered greenhouse construction, fans for forced ventilation of the drying air, a supplementary heater, a humidifying system and a microcomputer control. Its suitability for drying of sensitive hardwoods was shown by preliminary investigations [218]. To evaluate the potential and the possibilities linked with this type of solar dryer, the operating behaviour of both the single components and the entire solar dryer was investigated during this research work.

4.1 Material and Methods

4.1.1 Design of the Solar-Assisted Timber Dryer

The substructure of the solar-assisted timber dryer consists basically of a simple greenhouse construction in order to reduce the high investment costs. The vertical side walls have a height of 3.40 m and the span roof, with an inclination angle of 22°, has a ridge height of 5.40 m, **Figure 23**. The analysed solar dryer has a width of 10 m and a length of 18 m. Since it is designed in a modular way, an infinite expansion or reduction of the dryer length in segments of 2 m is easily realisable. The framework of the dryer consists of corrosion resistant 80 by 50 mm rectangular aluminium profiles. To protect the construction from mechanical damage during loading and unloading, concrete walls 2 m in height are installed on the length side between the aluminium girders. Black coated and corrugated aluminium sheets are installed horizontally in the height of the eaves. They do not only separate the drying chamber from the attic for air circulation purposes but do also serve as absorber for solar radiation. Since the solar dryer is installed close to the equator, the incident solar radiation reaches the dryer mainly in a vertical direction. This means that significantly more solar energy is added to the solar dryer at the span roof than at its transparent side walls and gables. Therefore, the transparent roof and the attic of the timber dryer can be defined as the relevant solar collector. Up to 250 m³ of sawnwood can be loaded in the drying chamber of the investigated dryer. Thereby, timber stacks with 40 mm thick

boards and 15 mm thick stacking laths have to be arranged over the whole width of the dryer of 10 m, at a length of 14 m and at a height of 3.20 m. To guarantee that the entire drying air passes the timber stacks, sealing foils are installed between the side walls and the absorber sheets of the solar dryer on one side and the piled timber stacks on the other side. For timber loading and unloading, two revolving doors are installed at the front side of the dryer over the full width of the drying chamber.

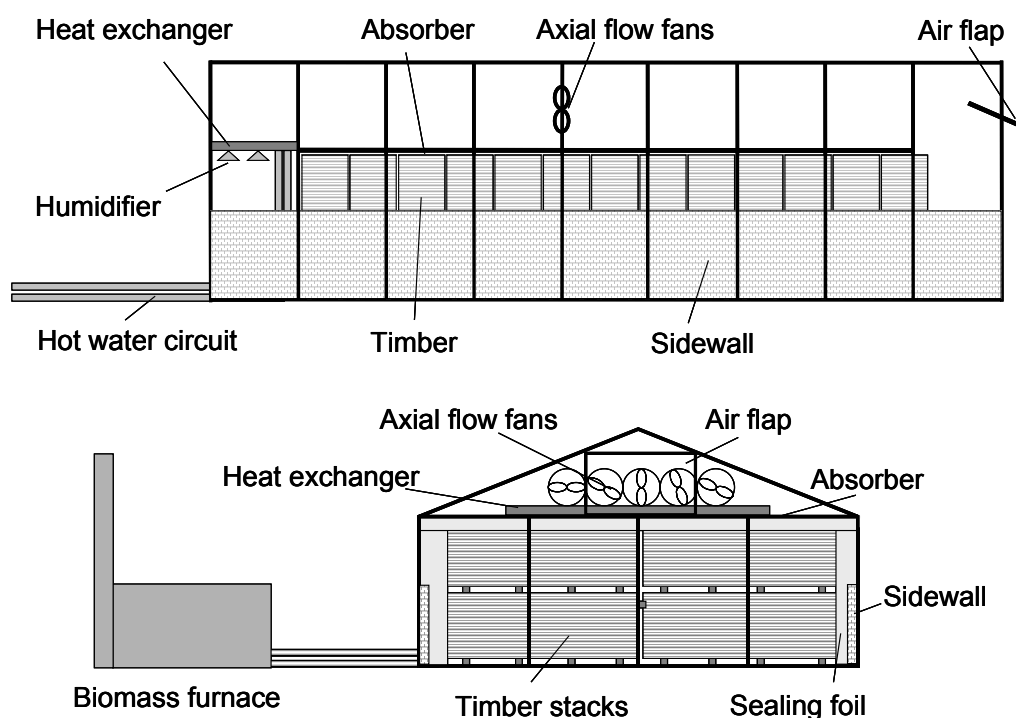


Figure 23: Longitudinal and cross section of the solar-assisted timber dryer [37].

The substructure of the solar dryer is covered with a transparent, highly UV-stabilised air bubble foil, **Figure 24**. The 8 mm thick bubble sheeting is a three-ply composite sandwich-material of polyethylene (PE) and ethylene vinyl acetate copolymer (EVA) foil. Due to the combination of these two components, its mechanical strength is higher, and its radiation transmitting capacity in the long wave IR range is lower than that of the constituent components. The transmission ratio of the foil is 83 % for beam and 68 % for diffuse solar radiation. The bubbles in the central deep-drawn layer, approximately 1000 per m², are heat formed in a calender, occluded by a 200 μm thick outer layer and bonded with a 80 μm thick inner layer [219; 220]. Weather strips are welded along both sides of the 2 m wide foil sheets which can be pulled into PVC fastening profiles with a maximum temperature resistance of 95 $^{\circ}\text{C}$, fixed on the girders by self drilling screws. Due to the high me-

chanical strength of the foil and the fixing system, the cover of the solar dryer can withstand even wind speeds of up to 140 km/h and 0.5 m high snow loads without any risk of damage. Long term experience gained under moderate climatic conditions showed that a life span of at least 15 years can be expected even under tropical conditions. The gable ends of the drying chamber are covered with polycarbonate sheets with a twin wall design. The heat transfer coefficient U of the air bubble foil and the polycarbonate twin wall sheets is given at $3.2 \text{ W}/(\text{m}^2 \cdot \text{K})$, which is a relatively low value compared to other transparent cover materials like simple glass or plastic foil with U - values between 6 and $10 \text{ W}/(\text{m}^2 \cdot \text{K})$. A low U - value reduces the heat losses through the dryer cover and prevents the condensation of water vapour at the inside of the cover during the drying process. This gives the air bubble foil priority over other transparent cover materials [219-221].

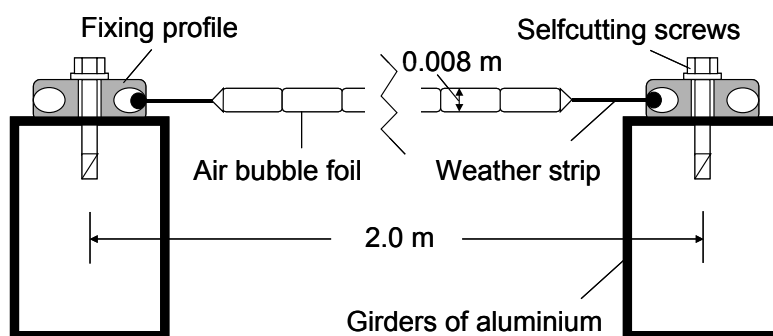


Figure 24: Cross section of the air bubble foil with fixing profile and aluminium girders.

If the desired drying air temperature cannot be reached by solar energy during night-time and adverse weather conditions, the drying air is heated additionally by a supplementary heater. The supplementary heating system consists of a biomass furnace, a boiler, a hot water pump and a heat exchanger. The biomass furnace is installed close to the dryer and generates hot water with a maximum temperature of $95 \text{ }^\circ\text{C}$ from waste material from the sawmill such as sawdust and wood chips. The ribbed-tubes heat exchanger is installed horizontally in the height of the eaves at the rear end of the drying chamber and is designed for a maximum heating capacity of 250 kW. The hot water pump has a power consumption of 1.4 kW at a pumping capacity of $10 \text{ m}^3/\text{h}$ and a pressure drop of 2.5 bar which results in an efficiency of about 50 %.

For the regulation of the relative humidity of the drying air and for remoistening cycles, a humidifying system is installed horizontally below the heat exchanger. The two-stage hu-

midifier consists of a water pump, a water filter and stainless steel pipes with eight equally distributed corrosion resistant spraying nozzles. Every humidifying stage is controlled by a magnetic valve. The cold water pump has a power consumption of 0.4 kW at a volume flow of 0.3 m³/h and a pressure drop of 1 bar.

Five axial flow fans with a diameter of 1 m are installed in the attic and generate a permanent airflow in order to promote the circulation of the drying air inside the dryer. Every fan has a maximum nominal power demand of 1.65 kW and generates a volume flow of 15 000 m³/h at a pressure drop of 140 Pa [222]. A digital rotation control allows the fan rotation respectively the drying air velocity to be adjusted to the specific wood species and board thickness at any phase of the drying cycle to reduce the electrical energy consumption. An air flap at the front side of the solar dryer regulates the air exchange between the inside of the dryer and the outside. It is moved at the centreline by a servomotor with a torque of 30 Nm and power consumption of 10 W. Various measuring and control units like temperature and humidity sensors, magnetic valves and a microprocessor unit for the control of the drying conditions have a total power consumption of about 100 W. The maximum total power demand of the entire solar dryer is about 10.2 kW.

4.1.2 Functional Principle of the Drying Process

The axial flow fans force a horizontal current of drying air over the absorber from the front to the rear end side of the solar dryer where it passes through the heat exchanger down to the drying chamber. Then, the air is forced through the timber stacks in horizontal direction to the front side of the dryer where it moves back to the attic. By this, a permanent air circulation is guaranteed inside the dryer. During daytime the circulating drying air is heated by solar energy while passing the absorber. The preheated air moves over the heat exchanger where it is heated additionally to the desired drying air temperature if necessary. As the drying air passes the timber load, the moisture is evaporated which causes a temperature decrease and simultaneously an increase of the relative humidity of the drying air along the load. This results in a higher relative humidity and lower temperature at the air outlet from the timber stack than at the air inlet. When the humidity of the circulating drying air exceeds the set maximum value, a part of the drying air is substituted by outside air. By opening the air flap, humid drying air leaves the dryer while comparatively dry external air is sucked into the drying chamber. Thereby, the relative humidity and the temperature

of the drying air decreases due to a lower water content and temperature level of the external air. If the relative humidity decreases below the set minimum value, the air flap is closed. The humidifying system is either used to maintain the relative humidity of drying air when ever it falls below the minimum value or to increase the humidity level during the remoistening intervals.

4.1.3 Control of the Drying Conditions

Since the control of the drying conditions is essential for quality drying, fully automatic control devices are state of the art in sophisticated high temperature dryers. In solar dryers, however, computer control was rarely used due to a higher complexity resulting from weather influences. Besides this, most systems were too small to justify the investments of a complex climate control (see also chapter 3). During this research work, the newly developed software for the microprocessor control had to be adapted to the specific conditions and was tested during various drying cycles. The microcomputer has six inputs for measured data and eight outputs for controlled variables. The measurands describe the real conditions of the drying climate and are provided by an analog voltage signal from different sensors. The actual state is compared with the set and calculated values from the drying schedule which are typed in at a small menu-guided keypad. The output signal depends on the relationship between the desired and the real state, which means that the relays of the different controlled variables are energised or de-energised during the whole drying process.

Table 5 shows the six available measurands, the set values from the drying schedule, the values calculated in the microprocessor and the seven controlled variables. The single parameters are self explaining and will not be described in detail.

Table 5: Required parameters for the control of the solar dryer.

Input (measured data)
<ul style="list-style-type: none"> • Temperature of the drying air \mathcal{G}_i • Relative humidity of the drying air φ_i • Temperature of the ambient air \mathcal{G}_e • Relative humidity of the ambient air φ_e • Wood moisture content x • Water temperature of the heating system \mathcal{G}_W
Set and calculated values
<ul style="list-style-type: none"> • Set temperature of the drying air \mathcal{G}_{i-set} • Minimum temperature of the drying air \mathcal{G}_{i-min} • Maximum temperature of the drying air \mathcal{G}_{i-max} • Dew point temperature of the drying air \mathcal{G}_{dew} • Set relative humidity of the drying air φ_{i-set} • Minimum relative humidity of the drying air φ_{i-min} • Maximum relative humidity of the drying air φ_{i-max} • Water content of the drying air x_i • Water content of the ambient air x_e • Maximum temperature increase until the dew point is reached $\Delta\mathcal{G}_{i,e-max}$ • Range of opening of the air flap • Surface temperature of the air bubble foil \mathcal{G}_F • Wood moisture equilibrium x_{eq} • Maximum allowable temperature difference between dryer and ambient \mathcal{G}_{con} • Set wood moisture content
Output (controlled variables)
<ul style="list-style-type: none"> • Servomotor air flap (open) • Servomotor air flap (close) • Heating pump (on/off) • Humidifying pump (on/off) • Magnetic valve of the humidifier A (on/off) • Magnetic valve of the humidifier B (on/off) • Axial flow fans (rotation speed)

Figure 25 illustrates the position of the different measurands and controlled variables at the solar dryer for the control of the drying air conditions. The temperature and the relative humidity of the drying air is measured inside the dryer at the second timber row. To take into consideration the local climate conditions during the drying process, these parameters are also quantified at ambient air. The wood moisture content is measured every second timber row at six locations. A further sensor measures the water temperature of the supplementary heating system. The controlled variables regulate the heat exchanger, the humidifier, the air flap and the axial flow fans.

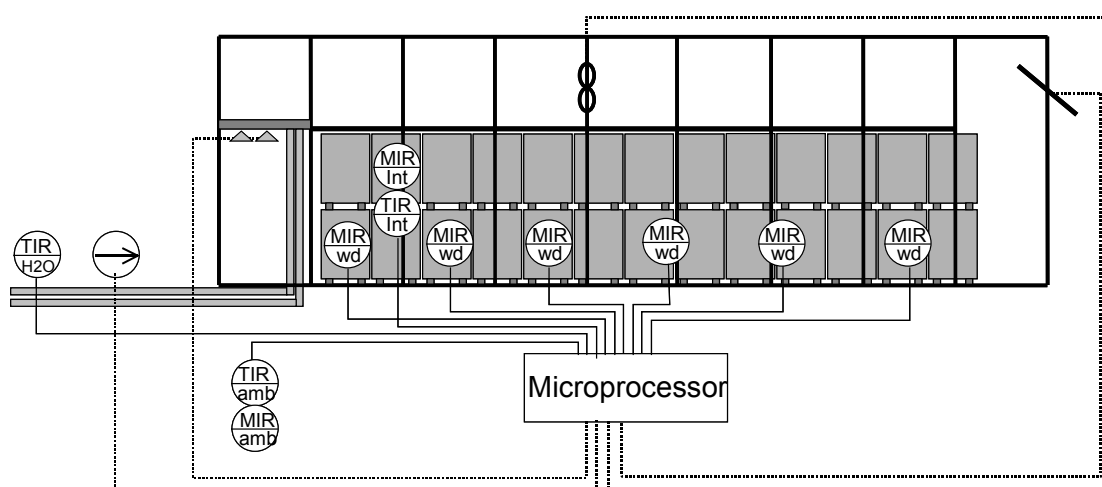


Figure 25: Location of the sensors for the control system inside and outside of the solar dryer. Input = filled line, Output = dashed line.

4.1.4 Data Acquisition

Data for all measured, calculated, set and control values was recorded and stored by the microprocessor over the whole drying process (Table 5). Additional parameters were registered by two computer assisted data acquisition units (FLUKE, Hydra) with 20 channels each. Besides this, various manual measurements like air velocity or air pressure were done. The different parameters are shown in **Figure 26**. The measurands are described in detail in **Table A2** in the appendix.

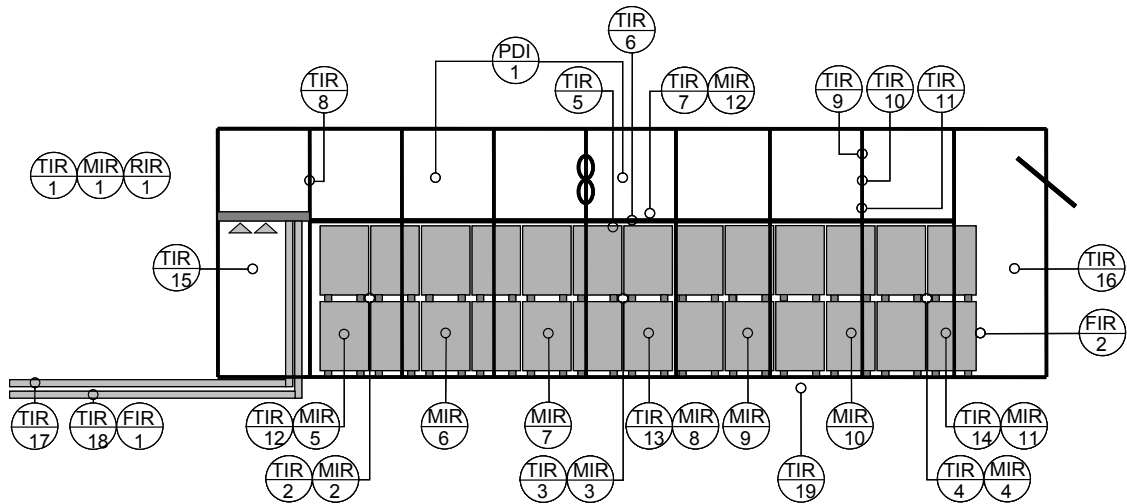


Figure 26: Schematic diagram showing the different locations of the sensors inside and outside the solar dryer.

R – Insolation F – Flow P – Pressure
T – Temperature M – Humidity

4.1.5 Methods of Calculation

4.1.5.1 Heat Transfer at the Air Bubble Foil

A heat transfer coefficient U of $3.2 \text{ W}/(\text{m}^2 \cdot \text{K})$ can be defined for the air bubble foil under standardised test conditions by following the industrial standard DIN 4108 [220; 223]. Since this standard does not consider the permanent air flow that exists inside the solar dryer, the heat transfer coefficients were calculated depending on the velocity of the passing drying air. Calculations were mainly done according to Bohl and Wagner [89; 224].

Generally, the U - value of the three-layer foil can be deduced from the thickness of the two polyethylene coats d_F and the enclosed air layer d_A , their corresponding thermal conductivities λ and the convection heat transfer coefficients h at the inner and outer foil surfaces by [86]:

$$\frac{1}{U} = \frac{1}{h_i} + \left(\frac{d_{i,F}}{\lambda_{pe}} + \frac{d_A}{\lambda_A} + \frac{d_{e,F}}{\lambda_{pe}} \right) + \frac{1}{h_e} \quad (7).$$

Since this equation determines the heat transfer coefficient for a single air bubble and not for the entire air bubble foil with its inhomogeneous structure, it was simplified by using

the thermal conductivity for the entire foil with $0.064 \text{ W/m}\cdot\text{K}$ which was specified by the manufacturer. Thereby, the U - value of the foil depends on its thickness d with 0.008 m , the thermal conductivity of the foil λ_F and the convection heat transfer coefficients h [86; 220]:

$$\frac{1}{U} = \frac{1}{h_i} + \frac{d}{\lambda_F} + \frac{1}{h_e} \quad (8).$$

Outside the solar dryer, neither the velocity nor the flow direction of the wind can be defined for a certain point in time over the whole dryer surface. However, the average wind velocity v_{wi} at the outer foil surface of the solar dryer is sufficient to determine the convection heat transfer coefficient h_e in $\text{W}/(\text{m}^2\cdot\text{K})$ between the air bubble foil and the ambient air [225]:

$$h_e = 2.8 + 3 \cdot v_{wi} \quad (9).$$

Sufficiently uniform air flow conditions exist inside the solar dryer for the calculation of a convection heat transfer coefficient h_i between the drying air and the air bubble foil. Where, the heat conductivity λ_A of the air with $27.16 \times 10^{-3} \text{ W/m}\cdot\text{K}$ at 1 bar and the overflown length l in m are required:

$$h_i = \frac{\text{Nu} \cdot \lambda_A}{l} \quad (10).$$

In the above equation, the Nusselt number Nu at longitudinal flow on a plane surface at laminar flow with a Reynolds number $Re < 1 \times 10^5$ is defined by:

$$\text{Nu} = 0.664 \cdot \sqrt{\text{Re}} \cdot \sqrt[3]{\text{Pr}} \quad (11),$$

whilst at turbulent flow with $Re \geq 5 \times 10^5$ by:

$$\text{Nu} = \frac{0.037 \cdot \text{Re}^{0.8} \cdot \text{Pr}}{1 + 2.443 \cdot \text{Re}^{-0.1} \cdot (\text{Pr}^{2/3} - 1)} \quad (12).$$

For an air temperature between 0 and 100 °C, the Prandl number Pr is 0.7. The Reynolds number is defined by the air velocity v at the foil surface in m/s and the overflowed length l in m by:

$$Re = \frac{v \cdot l}{\nu} \quad (13),$$

with the kinematic viscosity ν of the air in m^2/s depending on the temperature T at a corresponding pressure of 1 bar by the following relationship:

$$v = 42.6 \cdot 10^{-10} \cdot \frac{T^{\frac{3}{2}}}{1 + \frac{123.6}{T}} \quad (14).$$

The point, where the laminar flow changes in turbulent flow is called the critical point S_{crit} . It was calculated by using the air velocity v , the kinematic viscosity ν and the critical Reynolds number Re_{crit} of 3.2×10^5 by:

$$S_{crit} = \frac{v \cdot Re_{crit}}{\nu} \quad (15).$$

Analysing the specific air flow conditions in the solar dryer allowed the subdivision of the dryer in different modules with similar drying air velocities respectively similar U -values.

4.1.5.2 Condensation of Moisture at the Air Bubble Foil

To investigate the problems linked to condensation of the water vapour on the inner dryer surface, the surface temperature of the air bubble foil ϑ_F on the inside of the dryer was calculated by utilising the drying air temperature ϑ_i , the ambient air temperature ϑ_e , the convection heat transfer coefficient h_i and the heat transfer coefficient U by [86]:

$$\vartheta_F = \vartheta_i - \left(\frac{1}{h_i} \cdot U \cdot (\vartheta_i - \vartheta_e) \right) \quad (16).$$

It is possible to define the dew point temperature ϑ_{dew} from the saturation vapour pressure at the dew point $p_{dew,S}$ in Pa by the following equation [226]:

$$\vartheta_{dew} = 100^{\circ}\text{C} \cdot \left(\left(\frac{p_{dew,S}}{288.68\text{Pa}} \right)^{\frac{1}{8.02}} - 1.098 \right) \quad (17),$$

whereby the saturation vapour pressure at the dew point $p_{dew,S}$ can be deduced from the atmospheric pressure p of 1 000 mbar and the water content of the drying air x_i in kg/kg by [86; 227]:

$$p_{dew,S} = \frac{x_i \cdot p}{(0.622 + x_i)} \quad (18).$$

The water content of the drying air x_i was calculated by the relative humidity of the air φ , the atmospheric pressure p of 101 300 Pa and the saturation vapour pressure $p_{v,S}$ of the drying air in Pa by [86; 227]:

$$x_i = 0.622 \cdot \frac{\varphi \cdot p_{S,A}}{p - \varphi \cdot p_{S,A}} \quad (19).$$

Hereby, the saturation vapour pressure $p_{v,S}$ of the drying air in Pa was derived from the drying air temperature ϑ_A by [226] :

$$p_{v,S} = 288.68\text{Pa} \cdot \left(1.098 + \frac{\vartheta_A}{100^{\circ}\text{C}} \right)^{8.02} \quad (20).$$

4.1.5.3 Efficiency of the Solar Collector

The thermal efficiency η_c of the solar collector consisting of the span roof of the dryer and the absorber was analysed as a major evaluation criteria. Since the ridge was orientated in North-South direction, the roof surfaces with an inclination β of 22° were orientated to the East and West. The maximum transmission rate of the transparent polyethylene air

bubble foil was given with 83 % for direct and 68 % for diffuse solar radiation [219; 220]. Due to the inclined transparent side panels of the roof, the beam solar radiation could cross the plastic foil with a relatively steep angle during the morning and the evening which equalised the heat availability during the day. Almost all the ground plan of the solar dryer is covered with black aluminium sheets. Since solar energy is not only absorbed by the aluminium absorber but also by the heat exchanger and the small area in front of the air flap for air circulation purposes, the absorber area A_C was defined as 180 m². Since the drying air is passing above and below the corrugated absorber, an excellent heat transfer from the aluminium to the drying air is guaranteed. The calculation of the thermal efficiency of the solar collector was mainly done by following Duffie and Beckman [228].

The thermal efficiency of a solar collector is defined by the relationship between the usable energy flow \dot{Q}_{use} and the received energy flow \dot{Q}_{rec} :

$$\eta_C = \frac{\dot{Q}_{use}}{\dot{Q}_{rec}} \quad (21),$$

whereby the received energy \dot{Q}_{rec} in kW was deduced from the global solar radiation G_{glob} in kW/m² and the collector area A_C by:

$$\dot{Q}_{rec} = G_{glob} \cdot A_C \quad (22).$$

The received energy \dot{Q}_{rec} to the solar collector is a sum of the thermal losses $\dot{Q}_{L,th}$, the optical losses $\dot{Q}_{L,opt}$, the stored thermal energy \dot{Q}_{st} and the useable energy \dot{Q}_{use} :

$$\dot{Q}_{rec} = \dot{Q}_{L,th} + \dot{Q}_{L,opt} + \dot{Q}_{st} + \dot{Q}_{use} \quad (23).$$

Due to a good thermal conductivity, a small mass and a good cooling of the thin aluminium sheets, the proportion of the stored thermal energy \dot{Q}_{st} could be neglected.

All optical losses $\dot{Q}_{L,opt}$ can be defined by the share of light transmission at the transparent air bubble foil and the share of light absorption at the absorber, the so called transmission-

absorption-product ($\tau_F \cdot \alpha_{Ab}$). Thereby, the degree of transmission depends on the character of the solar radiation. Diffuse radiation G_{diff} is transmitted in a different way than beam radiation G_{beam} . The proportion of the diffuse radiation G_{diff} was estimated from the global radiation G_{glob} which was measured during this research work and the hourly clearness index k_C by:

$$G_{diff} = \begin{cases} G_{glob} \cdot (1 - 0.249 \cdot k_C) & \text{for } k_C < 0.35 \\ G_{glob} \cdot (1.557 - 1.84 \cdot k_C) & \text{for } 0.35 < k_C < 0.75 \\ G_{glob} \cdot 0.177 & \text{for } k_C > 0.75 \end{cases} \quad (24).$$

Thereby, the hourly clearness index k_C describes the correlation between the global radiation G_{glob} and the extraterrestrial radiation G_0^* :

$$k_C = \frac{G_{glob}}{G_0^*} \quad (25).$$

Considering the distance between the sun and the earth which depends on the number of the day n , the extraterrestrial radiation G_0^* on a horizontal surface can be estimated from the solar constant $G_0 = 1.353 \text{ kWh/m}^2$ by:

$$G_0^* = G_0 \cdot \left(1 + 0.033 \cdot \cos\left(\frac{2 \cdot \pi \cdot n}{365}\right) \right) \cdot (\cos \phi \cdot \cos \delta \cdot \cos \omega + \sin \phi \cdot \sin \delta) \quad (26),$$

Then, the share of the beam radiation from the global radiation is:

$$G_{beam} = G_{glob} - G_{diff} \quad (27).$$

While 65 % of the diffuse solar radiation is transmitted at the polyethylene air bubble foil independently from the sun angle [229], the beam solar radiation is transmitted depending on the angle of incidence. The angle of incidence θ_C between the beam radiation and the normal to the roof surface was given by the declination δ , the geographical latitude ϕ , the slope β of the solar collector, the hour angle ω and the surface azimuth angle γ by:

$$\begin{aligned}
\cos\theta_c &= \sin\delta \cdot \sin\phi \cdot \cos\beta - \sin\delta \cdot \cos\phi \cdot \sin\beta \cdot \cos\gamma \\
&+ \cos\delta \cdot \cos\phi \cdot \cos\beta \cdot \cos\omega \\
&+ \cos\delta \cdot \sin\phi \cdot \sin\beta \cdot \cos\gamma \cdot \cos\omega \\
&+ \cos\delta \cdot \sin\beta \cdot \sin\gamma \cdot \sin\omega
\end{aligned} \tag{28},$$

where, the geographical latitude ϕ on the test location of the solar dryer in Brazil was 19.19° , the surface azimuth angle γ of the solar collector was -90° for the East roof and 90° for the West roof and the slope β of the solar collector 22° . The declination δ was calculated from the number of the day of the year n by:

$$\delta = 23.45 \cdot \sin\left(360 \cdot \frac{284 + n}{365}\right) \tag{29}.$$

The hour angle ω depends on the solar time by:

$$\omega = 0.25 \cdot (720 - \text{Solartime}) \tag{30},$$

whereby the solar time depends on the standard time, the geographic longitude of the standard meridian of the locale time zone $\varphi_{S_{\tan}}$ with -45° and the geographic longitude of the solar dryer φ_{Loc} with -45.14° by:

$$\text{Solar time} = \text{Standard time} + 4 \cdot (\varphi_{S_{\tan}} - \varphi_{Loc}) + E \tag{31}.$$

The equation of the time E was calculated from the factor B by:

$$\begin{aligned}
E &= 229.2 \cdot (0.000075 + 0.001868 \cdot \cos B - 0.032077 \cdot \sin B \\
&- 0.014615 \cdot \cos 2B - 0.04089 \cdot \sin 2B)
\end{aligned} \tag{32},$$

and the factor B from the number of the day of the year n by:

$$B = (n - 1) \cdot \frac{360}{365} \tag{33}.$$

Observing the slope β and the distance between the ridge and the absorber, the area of the absorber reached by beam radiation during a definite time of the day can be defined.

The proportion of transmission of the beam radiation at the air bubble foil was calculated from the angle of incidence of the solar collector θ_C by [229]:

$$\tau = 81 + 0.1 \cdot \theta_C - 0.002 \cdot \theta_C^2 - 0.0001 \cdot \theta_C^3 \quad (34),$$

while the absorption coefficient α_{Ab} of the black aluminium sheet was given with 0.93 [221].

Thermal losses $\dot{Q}_{L,th}$ from the solar collector consist mainly of losses through thermal radiation and losses through convection. No heat losses existed from the absorber sheets downwards to the timber load because all energy was utilised for heating. Heat losses upwards through the roof were mainly caused by heat radiation from the absorber plates and through convection at the air bubble foil.

Losses through infrared radiation \dot{Q}_{Rad} from the absorber plate were calculated from the heat transfer coefficient from the absorber to the sky h_{Ab-Sky} , the collector area A_C , the temperature of the absorber T_{Ab} and the temperature of the sky T_{Sky} by [221]:

$$\dot{Q}_{Rad} = h_{Ab-Sky} \cdot A_C \cdot (T_{Ab} - T_{Sky}) \quad (35),$$

whereby the heat transfer coefficient from the absorber to the sky h_{Ab-Sky} was deduced from the transmission coefficient for thermal radiation at the air bubble foil τ_F of 0.4 at a temperature of 50 °C, the emission coefficient for black aluminium sheet ε of 0.64, the radiation coefficient (Stefan-Boltzmann constant) σ of $5.67 \cdot 10^{-8} \text{ W}/(\text{m}^2 \cdot \text{K}^4)$, the temperature of the absorber T_{Ab} and the temperature of the sky T_{Sky} by [221]:

$$h_{Ab-Sky} = \frac{\tau_F \cdot \varepsilon \cdot \sigma \cdot (T_{Ab}^4 - T_{Sky}^4)}{T_{Ab} - T_{Sky}} \quad (36).$$

From the measured ambient air temperature T_e and the dew point temperature T_{dew} deduced from equation (17) to (19), the temperature of the sky T_{sky} was calculated by:

$$T_{sky} = T_e \cdot \left(0.8 + \frac{T_{Dew} - 273}{250} \right)^{1/4} \quad (37).$$

The convective heat losses at the air bubble foil \dot{Q}_{Conv} result from the heat transfer coefficients U , the collector area A_C , the temperature of the drying air T_i and the ambient air temperature T_e by [86]:

$$\dot{Q}_{Conv} = U \cdot A_C \cdot (T_i - T_e) \quad (38).$$

4.1.5.4 Electrical Energy Demand

The product of the voltage U and the amperage I is the electrical power P of a single-phase motor [230]:

$$P = U \cdot I \quad (39).$$

For three-phase motors, the electric energy demand P is calculated by the voltage U , the amperage I and the phase difference φ by using the following equation [230]:

$$P = U \cdot I \cdot \cos \varphi \cdot \sqrt{3} \quad (40).$$

The efficiency of the axial flow fans is the ratio between the delivery rate P_C and the driving power P [231]:

$$\eta = \frac{P_C}{P} \quad (41).$$

Thereby, the delivery rate P_C is the product of the total pressure drop Δp_A in Pa and the volume flow \dot{V} in m³/s [231]:

$$P_C = \Delta p_A \cdot \dot{V} \quad (42).$$

The volume flow \dot{V} of the fans was measured at filled dryer with an air flow anemometer at a grid pattern. The grid was fixed at the aperture from the drying chamber to the attic on the side of the air flap.

The efficiency of the hot and cold water pump was calculated following equation (40) and (41) [86; 232].

4.2 Results

4.2.1 Operating Behaviour of the Solar Collector

An accurate determination of the solar collector's efficiency is a quite complicated problem due to a high number of influencing variables. However, reliable results can be achieved by using a simplified model of the solar collector and limiting the energy balance to the most relevant parameters.

Generally, the efficiency of a solar collector is defined as the ratio between the useable Q_{use} and the received solar energy Q_{rec} . Solar energy is received as global radiation on the total ground plan of the solar collector. The useable energy is the difference between the received energy and the optical and thermal losses and the stored energy. In the analysed solar collector, however, the amount of stored energy is very low due to the low mass of the absorber and was therefore neglected. Optical losses $Q_{L,opt}$ are mainly found through reflection of the solar radiation at the outer cover of the solar collector and at the absorber surface. Thermal losses $Q_{L,th}$ result primarily from heat radiation from the absorber surface and convection.

The efficiency of the investigated solar collector η_C was analysed during a typical drying day with clear weather conditions. Since the reflection of the solar radiation at the transparent collector cover depends on the type of radiation, the share of beam and diffuse solar radiation was estimated from the measured global solar radiation G_{glob} and the calculated extraterrestrial solar radiation G_o^* , **Figure 27**.

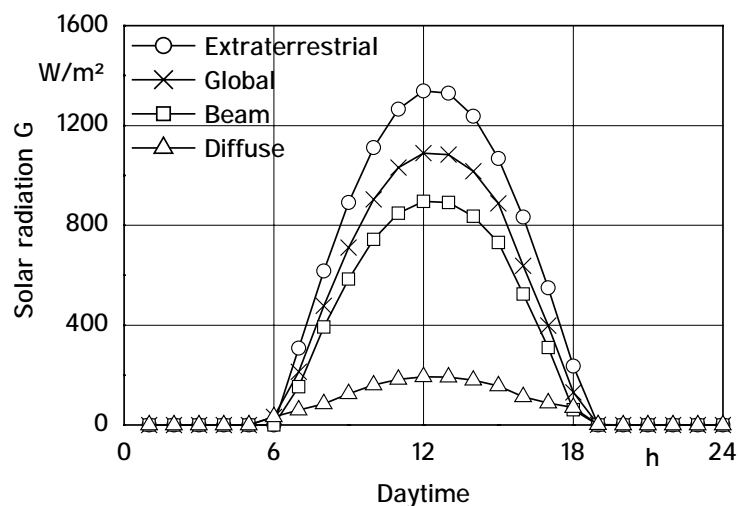


Figure 27: Solar radiation during a clear drying day, in December the 12th, at a southern latitude of 20 °.

The transmission of the diffuse solar radiation at the transparent air bubble foil of the solar collector is independent from the angle of incidence and was 68 % during the whole drying time, **Figure 28**. At a high global solar radiation of about 1100 W/m² during noon-time about 12 kW of solar energy was received per hour by the solar collector through diffuse solar radiation.

Since the solar collector consists of the span roof of the timber dryer, its transparent outer cover is not arranged parallel to the horizontal absorber plates. This results in different angles of incidence of the beam solar radiation on the East and West side of the roof at a certain point of time. Therefore, the angle of incidence was calculated separately for each side of the roof depending on the surface azimuth angle γ . The corresponding absorber area was defined for each roof side by the shadow of the ridge for each time interval. The lowest rate of transmission was found during morning (7:00 a.m.) and evening hours (6:00 p.m.) with about 60 % of the total beam radiation while the highest transmission with about 80 % was available during noon-time (12:00 a.m.). However, the highest absolute optical losses through reflection of the available beam radiation of about 35 kW over the whole collector area was measured at 10:00 a.m. and 3:00 p.m.. This corresponds to a share of 26 % of the total beam radiation and was mainly due to the unfavourable combination of the two different angles of incidence on the sides of the solar collector. During noon-time, the absolute optical losses were lower with about 30 kW respectively 19 % of the total beam radiation due to a relatively steep angle of incidence on both sides of the

dryer roof. Thus, about 160 kW of solar energy was supplied to the solar collector by the transmitted beam solar radiation.

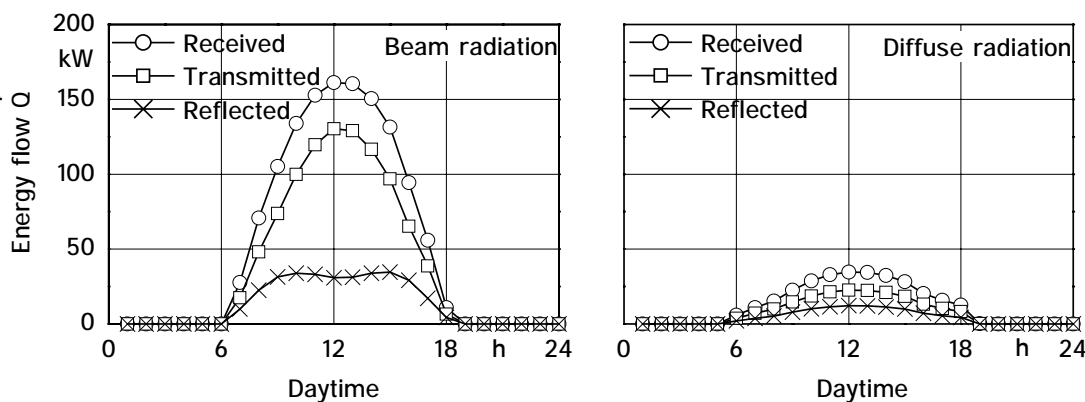


Figure 28: Received, transmitted and reflected energy flow at the entire solar collector for beam and diffuse solar radiation on December the 12th.

A maximum of 93 % of the transmitted solar radiation was absorbed by the black aluminum sheets. This absorbed solar energy was either converted into thermal radiation or increased the temperature of the absorber plates. Therefore, thermal energy losses from the solar collector were found as losses through heat radiation from the absorber and losses through thermal convection from the warm drying air to the ambient air.

The thermal energy flow from the collector surface to the ambient air through heat radiation is mainly influenced by the thermal emission coefficient of the absorber sheets ε , the transmission coefficient of the air bubble foil τ_F , the absorber temperature T_{Ab} and the clear sky temperature T_{sky} . During night-time the temperature of the absorber sheets was about 24 K higher than the clear sky temperature, **Figure 29**. During daytime the temperature of the absorber surface increased up to a maximum of 65 °C due to a high rate of insolation and was thereby about 44 K higher than the clear sky temperature. Therefore, the thermal energy loss through heat radiation at the entire solar collector was with about 15 kW per hour more than two times higher during day-time than during the night with about 6 kW.

The thermal losses through convection from the solar collector result from the temperature difference between the drying air and the ambient air and the heat transfer coefficient of the air bubble foil U . Since the drying air temperature in the solar dryer is controlled de-

pending on the ambient air temperature, the temperature difference was always about 15 K during the whole drying day. Therefore, the total thermal energy loss from the solar collector through convection was with about 10 kW per hour only slightly higher during the day than during the night with 7 kW.

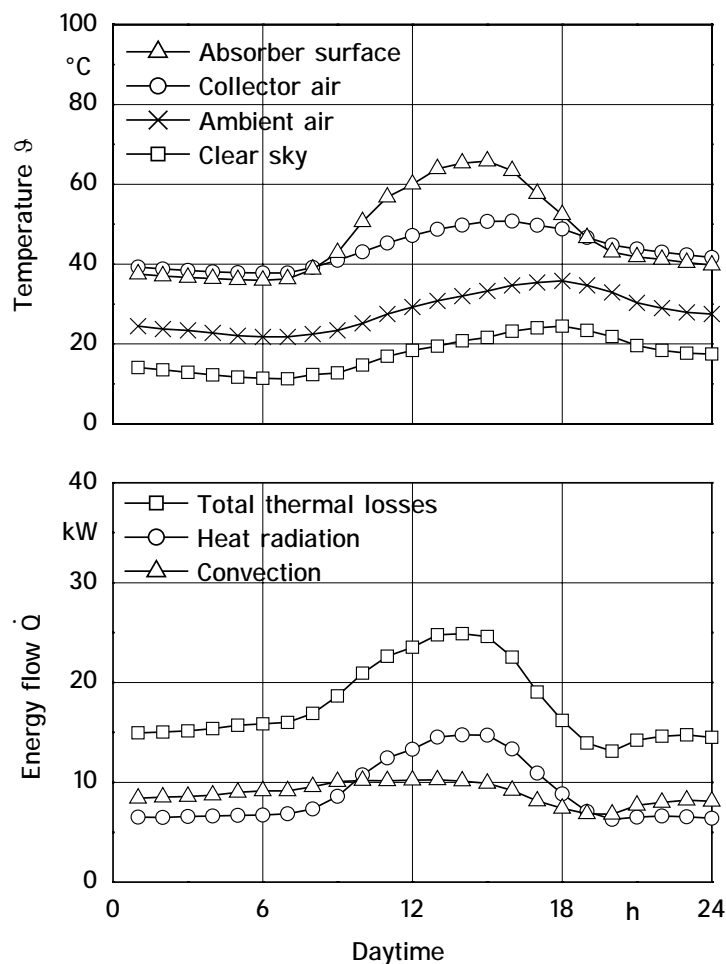


Figure 29: Temperature profile and corresponding thermal energy losses at the solar collector on December the 12th.

The resulting energy balance shows that the optical losses through reflection were about two times higher during daytime than the thermal losses through heat radiation and convection, **Figure 30**. The relatively low energy loss through heat radiation was caused by a good heat transfer from the absorber plates to the drying air due to a permanent high air flow above and below the absorber sheets. Thereby, maximum temperature differences of about 15 K were found between the absorber sheets and the collector air during the highest insolation at noon-time, Figure 29. No thermal energy losses existed bellow the absorber sheets, since all emitted energy was used for the heating of timber. The high volume flow

of the drying air above the absorber plates was also responsible for a low temperature difference between the drying air and the ambient air, which reduced the thermal energy losses through convection. Therefore, the efficiency of the analysed solar collector was relatively high compared to common flat-plate solar collectors that have low optical losses but high thermal losses due to a low volume flow of the heating medium. A low volume flow causes a high temperature difference between the absorber surface respectively the collector air and the ambient air which increases the heat losses through radiation and convection. The highest efficiency of about 60 % was found at the solar collector of the timber dryer during noon-time due to a high insolation and a steep angle of incidence of the beam radiation at the transparent collector cover.

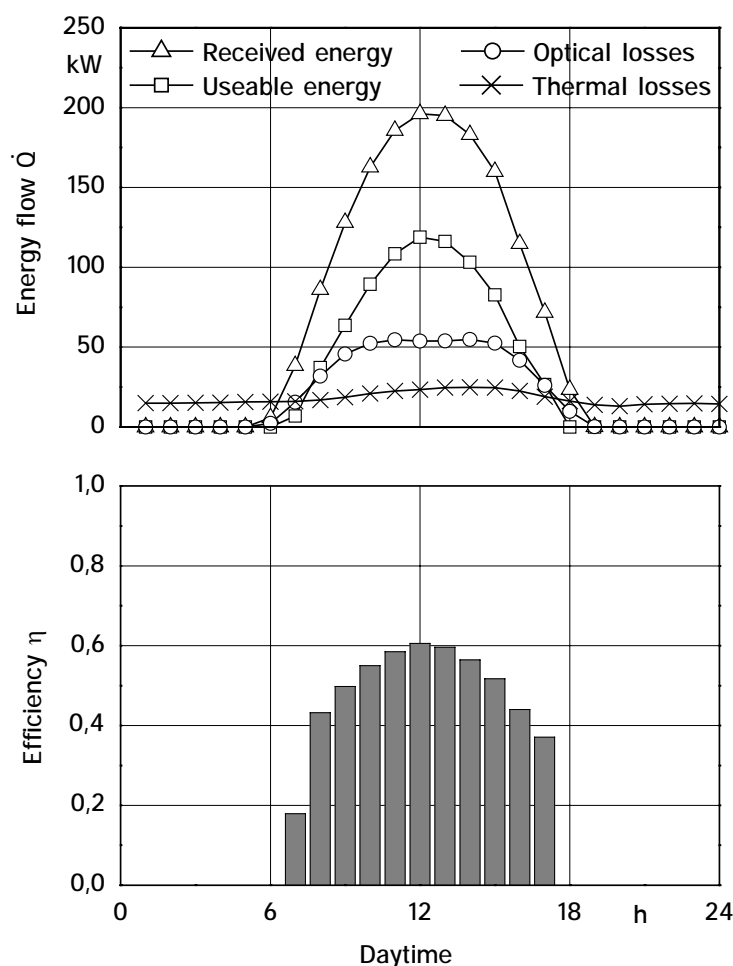


Figure 30: Energy balance and efficiency of the solar collector during a clear drying day at December the 12th and a southern latitude of 20 °.

4.2.2 Operating Behaviour of the Supplementary Heater

The circuit water of the supplementary heating system was heated by a biomass furnace to a maximum temperature of about 95 °C. Then, the hot water was either stored in a boiler or directly pumped into the heat exchanger of the solar dryer.

The heating capacity of the installed ribbed tubes heat exchanger was not a constant value since it was not only influenced by its proper design but also by the volume flow of the circuit water and the temperature difference between the passing drying air and the heating water. Thereby, the volume flow of the circuit water in the heating system was about 10 m³/h and the temperature difference between the drying air and the heating water was about 70 K at the beginning and about 40 K at the end of the drying process. This was due to the increasing air temperature along the drying process. However, an useable heating capacity of about 180 kW was found as a reliable average value over the whole drying process.

The pressure drop of the circulating drying air at the heat exchanger is a further important criteria since it has a significant influence on the specific energy consumption of the axial flow fans. The low measured pressure drop of less than 10 Pa at maximum air flow showed that the design of the heat exchanger allowed the use of low pressure axial flow fans. These fans are characterised by a high air flow per amount of required electrical energy.

The biomass furnace, the boiler and the hot water pump were not further investigated since they had no direct influence on the operating behaviour of the solar dryer and were installed independently by the Brazilian partner outside the dryer.

4.2.3 Operating Behaviour of the Humidifying System

Cold water was temporary sprayed by the humidifying system into the solar dryer to increase the relative humidity of the drying air. The volume flow was thereby about 0.2 m³/h for one activated humidifier stage with 8 spray nozzles and 0.3 m³/h for two activated stages with 16 spray nozzles.

The efficiency of the humidifier which is defined as the ratio between added and vaporized water was mainly influenced by the spraying behaviour. During normal drying phases, the humidifier was activated for short time intervals to adjust the relative humidity of the drying air in a small range. Thereby, small amounts of water were sprayed into the solar dryer that moistened the surface of the dryer structure, the ground and the sawnwood. Most of the water evaporated directly from the moistened surfaces and was absorbed by the passing drying air, resulting in a high efficiency of the humidifying system. However, when a high amount of water was sprayed within a short time period during the remoistening intervals, the efficiency was quite low since most of the water was drained into the ground. Since the measurement of the drained water was not possible under the given layout of the dryer, the average efficiency of the humidifier was calculated by an energy balance. The method of calculation of the energy balance is described extensively in chapter 5. An efficiency of 60 % was found as an average value over all analysed drying experiments.

4.2.4 Operating Behaviour of the Axial Flow Fans

A minimum drying air velocity of about 1.5 m/s is required between the single board layers for proper timber drying (see chapter 2.2.1.3). The air velocity results not only from the volume flow of the drying air, but also from the open cross section of the timber load. The open cross section depends on the size of the boards and the arrangement of the timber stacks inside the solar dryer. Loading the dryer with 4.5 m long and 27 mm thick boards with 15 mm thick stacking laths resulted in an open cross section of 10.7 m². Drying 4.5 m long and 42 mm thick boards with the same stacking laths reduced the open area to 8.3 m². Therefore, a higher volume flow had to be supplied by the axial flow fans for 27 mm thick boards to get the same air velocity as for 42 mm thick boards. For the air velocity of 1.5 m/s, a volume flow of about 12.5 m³/s was required for the thick boards and 16.0 m³/s for the thin boards, **Figure 31**.

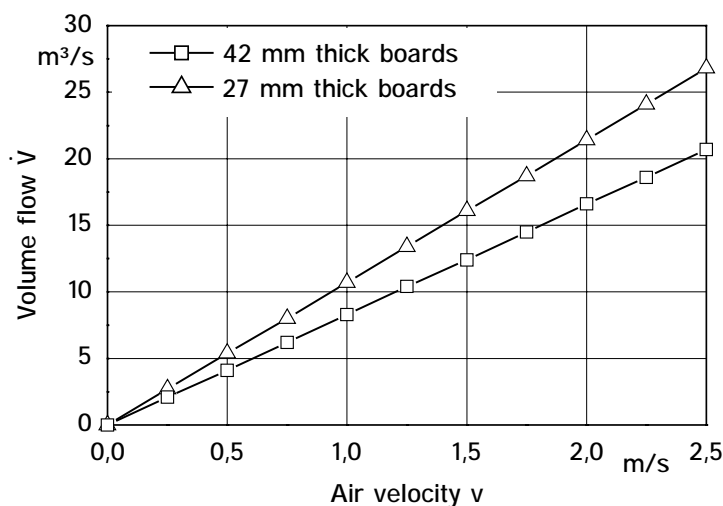


Figure 31: Required volume flow of the drying air for different air velocities between the board layers.

The volume flow of 16 m³/s for 27 mm and 12.5 m³/s for 42 mm thick boards could be reached by the same fan rotation respectively an equal electrical energy consumption of 4.2 kW for all five fans. The total pressure drop of the drying air was thus 78 Pa for the 42 mm and 54 Pa for the 27 mm thick boards. Furthermore, the fan efficiency was about 28 % for the 42 and 20 % for the 27 mm thick boards. At maximum fan rotation, a average air flow velocity of approximately 2.1 m/s was measured for 42 mm boards and of 1.9 m/s for 27 mm boards. This corresponds with a volume flow of 20.5 m³/s (73 800 m³/h) for the thin boards and of 17 m³/s (61 200 m³/h) for the thick boards. Thereby, the air velocity varied between 1.6 and 2.4 m/s for 42 mm boards and between 1.5 and 2.2 m/s for 27 mm boards. The total pressure drop reached a maximum of 120 Pa for the 42 mm thick boards and 90 Pa for the 27 mm thick boards. This relatively low pressure drop resulted mainly from the low maximum air velocity and the design of the solar dryer with a low air resistance at the attic and the heat exchanger. This allowed the use of highly efficient low pressure axial flow fans with a total electrical energy consumption of 6.2 kW for all five fans at maximum rotation speed. Thereby, the efficiency of the fans was approximately 40 % for 42 mm boards and 30 % for the 27 mm boards. If the average air velocity for the 42 mm thick boards was reduced to 1.9 m/s like for 27 mm boards, the energy consumption of the fans was reduced to 5.3 kW and the pressure drop decreased to 105 Pa, which reduced mechanical stress at the air bubble foil, **Figure 32**.

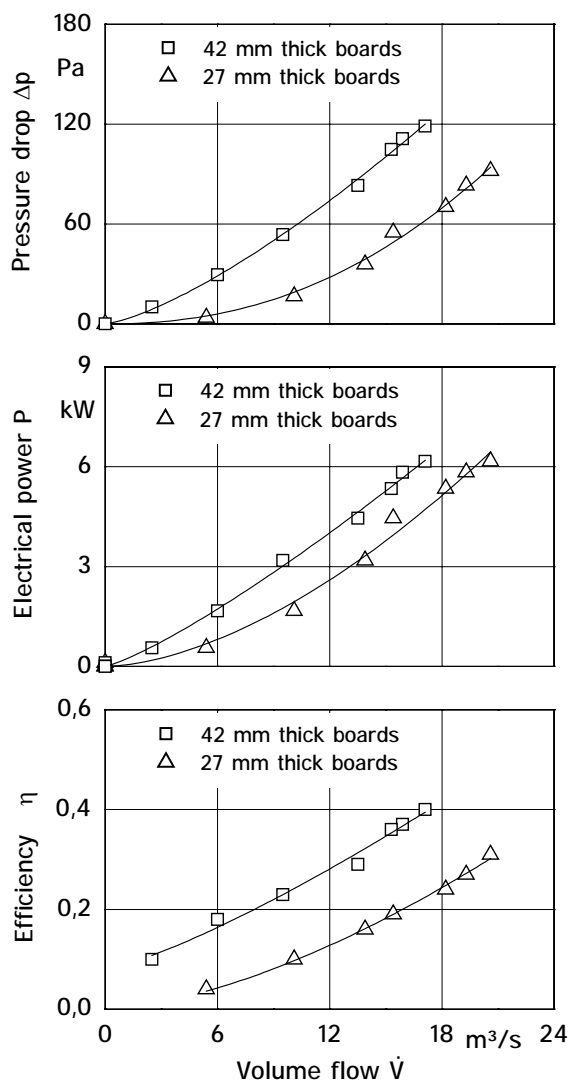


Figure 32: Pressure drop of the drying air, electrical energy consumption and efficiency of the five axial flow fans depending on the volume flow at different timber loads.

The correlation between the efficiency of the analysed axial flow fans and the total pressure drop is shown in **Figure 33**. A comparison of the measured data with nominal data shows that the maximum efficiency is reached at a pressure drop of 120 Pa. This value was measured at maximum fan rotation with 42 mm thick boards and 15 mm thick stacking laths. Therefore, and for stability reasons of the air bubble foil, it was recommended to use thicker stacking laths for a board thickness higher than 42 mm.

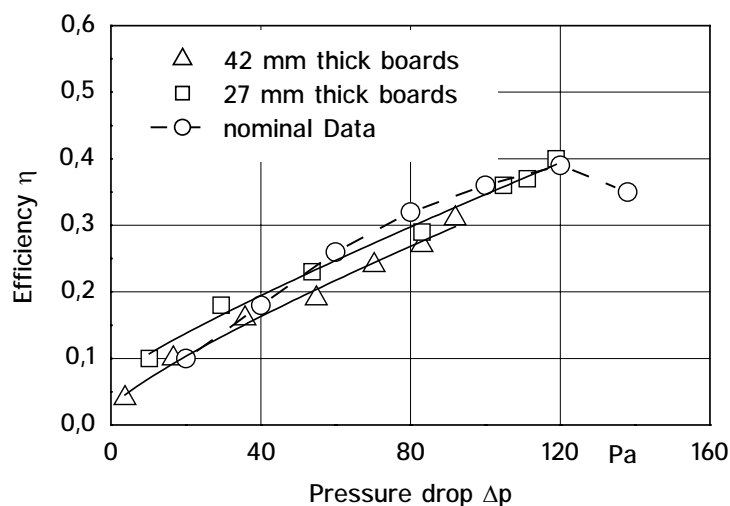


Figure 33: Correlation between the total pressure drop of the drying air and the efficiency of the axial flow fans [222].

In general, reducing the open cross section at the timber load without changing the rotation velocity of the fans, increased the pressure drop of the drying air which caused a lower volume flow. However, a lower volume flow of the drying air reduced the air velocity between the board layers only at low fan rotation while at high rotation the drying air velocity was even increased. Besides this, reducing the open cross section increased the efficiency of the axial flow fans only up to a maximum pressure drop of 120 Pa.

4.2.5 Operating Behaviour of the Whole Dryer

Heat Loss through the Cover

The heat transfer through the cover of the solar dryer depends not only on the used material but also on the air velocity inside and outside the dryer. While the wind velocity of the surrounding air is not predictable for a certain position and time, the air flow distribution inside the solar dryer is quite stable and is only influenced significantly by the position of the air flap. The circulating drying air above the absorber passes in a higher distance to the aluminium sheets at closed air flap than at open air flap, **Figure 34**. This was expected to reduce the heat transfer from the absorber surface to the drying air which would result in higher absorber temperatures and therefore higher energy losses through heat radiation. However, the affected absorber sheets are also cooled by the drying air that passes below them. In addition, the thermal energy is transferred excellently by the aluminium sheets to

colder areas of the absorber. Therefore, a considerable temperature difference could not be found. Furthermore, the installation of an air duct to eliminate this zone would have caused additional flow resistance and therefore an increase of the electrical energy demand. The other part of the absorber surface was cooled perfectly by the circulating drying air. Turbulences existed in the expansion area in front of the timber load on the side of the heat exchanger. However, this had no negative influence on the air flow distribution in the timber stack.

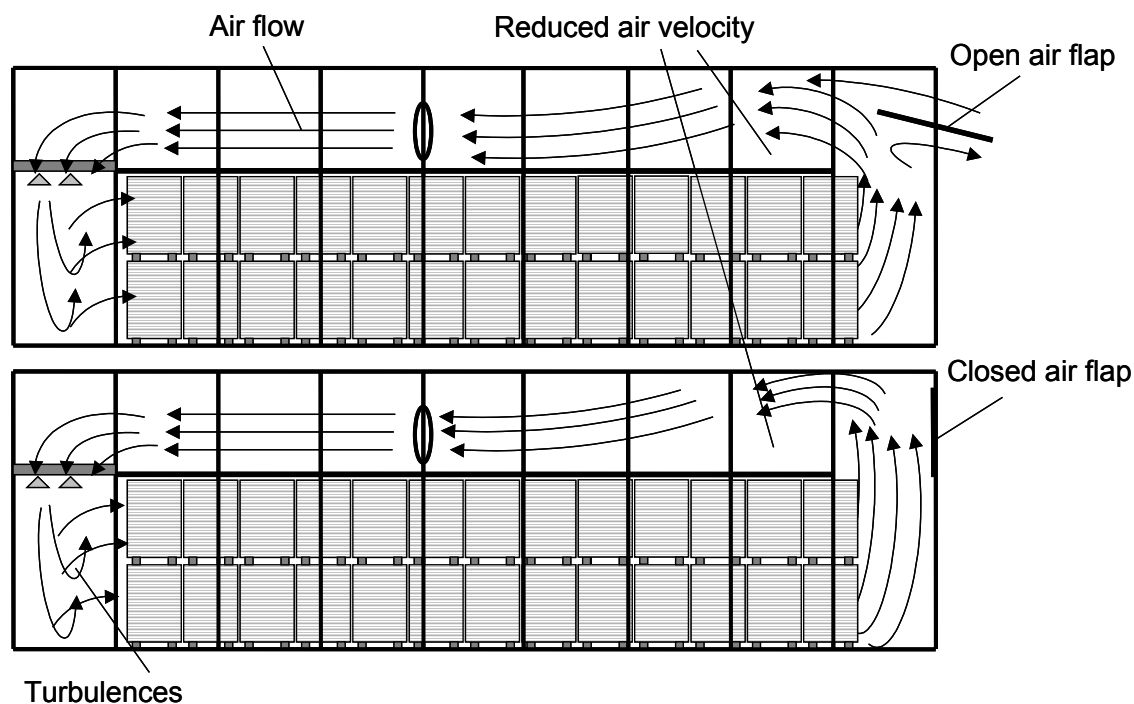


Figure 34: Measured distribution of the air flow inside the solar dryer at open and closed air flap.

The heat transfer coefficient U of the air bubble foil depends not only on the thickness and thermal conductivity of the plastic foil but also on the convection heat transfer coefficient h at its surface. The convection heat transfer coefficient at a plane surface can either be estimated empirically by the mean air velocity or can be calculated by the air velocity, the heat conductivity of the air, the overflowed length and the Nusselt number. The Nusselt number results from the Reynolds number and the Prandtl number. The Reynolds number depends on the air velocity, the overflowed length and the kinematic viscosity of the air. The critical point, where the laminar flow changes in turbulent flow can be estimated by the air velocity, the kinematic viscosity of the air and the critical Reynolds number. These correlations allowed the determination of a specific U -value depending on the drying air velocity at every position of the solar dryer.

The aluminium girders of the solar dryer form a barrier to the circulating drying air in a distance of 2.0 m in horizontal and of 1.0 m in vertical direction. This means that the drying air restarts to pass the plane plastic foil close behind a girder. Thereby, an insulating boundary layer is generated that increases with increasing distance from the barrier. This windless air layer reduces the heat transfer from the foil to the drying air which causes a decreasing U -value. Due to a maximum air velocity of 2.0 m/s and a maximum distance between two girders of 2.0 m, the critical point was not reached which means that the boundary layer was not destroyed by turbulences. Since the heat transfer coefficient changes with overflowed distance, an average U -value was calculated for each field between two aluminium girders by measuring the air velocity every 10 cm close to the foil surface.

Finally, the solar dryer could be subdivided into five different zones with similar velocities of the drying air close to the inner foil surface: the span roof in front of the axial flow fans, at the side of the air flap where the air bubble foil is bent inwards due to a low air pressure, the span roof behind the fans where the foil is curved outwards due to an overpressure, the two gables and the side walls of the dryer, **Table 6**.

Table 6: Division of the solar dryer in different air flow zones with corresponding average air velocity close to the foil surface in m/s and heat transfer coefficient U in W/m^2K .

Air flow zone	Average air flow velocity	U-value
Span roof after the fans	0.9	2.6
Span roof in front of the fans	2.0	3.1
Gable – heat exchanger	0.8	2.8
Gable – air flap	1.0	3.0
Side walls	0.5	2.1

The highest average drying air velocity at the inner dryer cover was measured with 2 m/s in front of the axial flow fans. The lowest air velocity with 0.5 m/s existed at the side walls due to the installed sealing foils. The air velocity was lower on the gable at the side of the

heat exchanger than at the side of the air flap. Altogether, the different air velocities resulted in U -values between 2.1 and 3.1 W/m²K and were therefore noticeable lower than the cited value of 3.2 W/m²K. However, it must be pointed out that the air flow distribution in the solar dryer is very inhomogeneous and had to be generalised within this calculation method.

Condensation of Moisture Inside the Solar Dryer

The transparent cover of the solar-assisted timber dryer has a significantly lower thermal insulation than that of a high-temperature dryer. The resulting high influence of the ambient air temperature complicates the control of the drying climate since water vapour condenses at low temperatures on the internal surface of the plastic foil (see also chapter 3.2). The consequential decrease of the relative humidity of the drying air cannot be stopped by humidifying. As a result, thermal energy is consumed to immediately evaporate water that condenses on the plastic cover. Therefore, the air temperature inside the solar dryer has to be adapted to the ambient air temperature and the relative humidity of the drying air. **Figure 35** shows the maximum permissible temperature difference between the drying air and the ambient air for different relative humidities of the drying air. The outside temperature is hereby 20 °C. However, the temperature level at the analysed range does not have a significant influence on the demonstrated temperature differences.

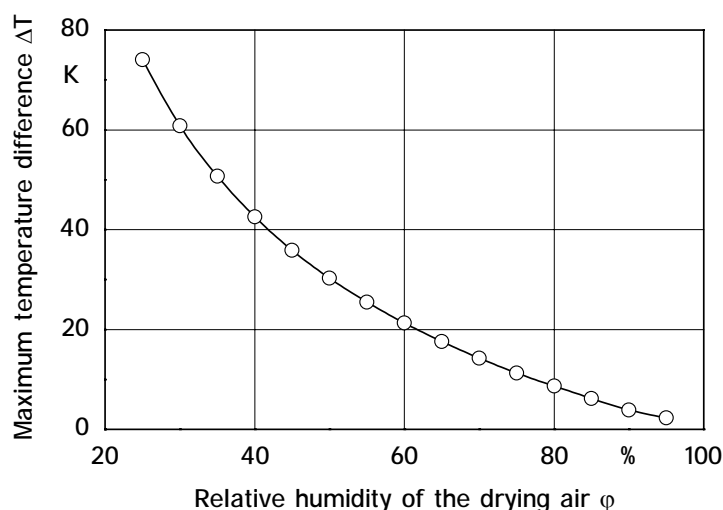


Figure 35: Maximum temperature difference between the drying air and the ambient air depending on the relative humidity of the drying air at an ambient air temperature of 20 °C to avoid condensation at the cover.

For example, a needed relative humidity of the drying air of 75 % allows a maximum temperature difference to the ambient air of 11 K. Generally, the higher the relative humidity of the drying air, the lower the temperature difference has to be in order to avoid condensation. This explains why drying schedules for high temperature dryers cannot be applied to the analysed solar dryer. Consequently, the drying air temperature has to be kept low or has to follow the ambient air temperature which results in daily temperature oscillations.

4.3 Evaluation of the Results

The functional principle of the investigated solar-assisted timber dryer is basically similar to that of a high temperature dryer as circulating drying air absorbs the wood moisture and humid drying air is replaced by dry ambient air. However, the solar dryer is more economical due to a relatively simple design, the utilisation of solar energy as a thermal energy source and the applicability of highly efficient low pressure axial flow fans. Furthermore, the length of the timber stack is much higher resulting in a lower specific air flow per m³ of timber. The transparent span roof can be used very efficiently as a cheap solar collector which reduces costs for additional heating. Besides this, the solar-assisted dryer is, in contrast to most previous solar dryers, equipped with a supplementary heating system, a humidifying system, a regulated air flap and a microprocessor control. This additional equipment reduces the dependence on local weather conditions and allows the application of adequate drying schedules for different wood species. However, the control of the drying climate in the solar dryer is more complicated than in a high temperature dryer, due to a lower thermal insulation of the transparent cover. A higher influence of the ambient air temperatures facilitates the condensation of water vapour on the inside of the solar dryer. Therefore, drying schedules with a high relative humidity have to be applied with a low temperature difference to the ambient air. This can result in extended drying times compared to high temperature dryers. To reduce this disadvantage, the drying air temperature should oscillate by following the ambient air temperature.

5 SOLAR-ASSISTED DRYING OF EUCALYPTWOOD IN BRAZIL

5.1 Material and Methods

5.1.1 Location and Climate

The solar-assisted timber dryer was installed at the Brazilian wood company in Martinho Campos in the federal state of Minas Gerais in Brazil. The sawmill is located in the central West of Brazil at a Western longitude of 45.14° and a Southern latitude of 19.19° . The distance to Belo Horizonte, the capital of Minas Gerais, is about 180 km and about 660 km to the Brazilian capital Brasilia [233]. Extensive information about the local climate was available from satellite observations by NASA and from meteorological measurements close to the sawmill [234-239]. The climate at the test location can be described as a typical subtropical climate with distinct rainy and dry season. None the less, the relative humidity of the ambient air is relatively high throughout the year with approximately 80 %, **Figure 36**. The medium air temperature is with 22°C about 4 K higher during the rainy season than during the dry season. The daily average of global solar radiation is about $5\text{ kWh/m}^2\cdot\text{d}$ during the rainy season and about $4\text{ kWh/m}^2\cdot\text{d}$ in the dry season. A maximum of $9\text{ kWh/m}^2\cdot\text{d}$ can be measured during the rainy season at cloudless weather conditions. The average midday solar radiation is about 700 W/m^2 in both the rainy and the dry season. The temperature difference between day and night is with 15 K in the dry season two times higher than in the rainy season with about 7 K.

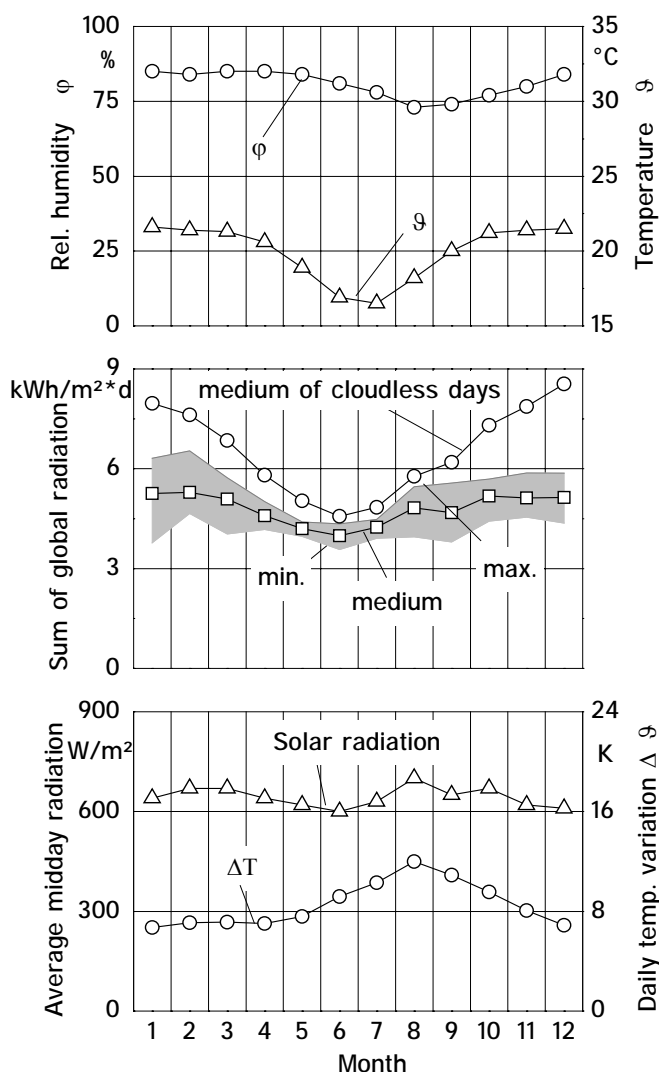


Figure 36: Climate diagram of the test location in Martinho Campos, Minas Gerais, Brazil showing the temperature and the relative humidity of the air, the daily global radiation, the midday solar radiation and the daily temperature variations [234-239].

5.1.2 Raw Material

The timber for the drying tests was produced from eucalypt plantations that were originally planted and managed for charcoal production. Therefore, the quality of the raw material was quite low with regard to the desired characteristics for sawnwood. In addition, a high genetic variability of the eucalypt trees was found since the trees were grown from seeds and not from selected clones. Furthermore, attention was rather given to a high growth rate than to increase the wood quality by breeding and forest management. This shows that the available raw material was an extraordinary difficult wood for the production of high quality sawnwood.

The main timber production in the sawmill were boards with a thickness of 18, 27, 32 and 42 mm, a length of 3.0 m and a width between 5 and 20 cm. The boards were cut from 8 to 10 year old trees of *Eucalyptus grandis* with a log diameter between 14 and 25 cm. The logs were harvested in the eucalypt plantations and transported to the sawmill within two weeks. In the sawmill, the sideware of the logs was removed by a band-saw. Afterwards, the logs were sawn in one direction with a circular saw. This type of log processing is normally used for softwood and is not suitable for quality production from sensitive hardwoods. Adequate sawing methods for hardwood allow the production of true quartersawn (growth rings at right angles to the board face) or true backsawn timber (growth rings parallel to the board face) and permit the removal of the low quality wood at the pith of the log [18], **Figure 37**. However, these methods are more sophisticated and therefore more cost intensive.

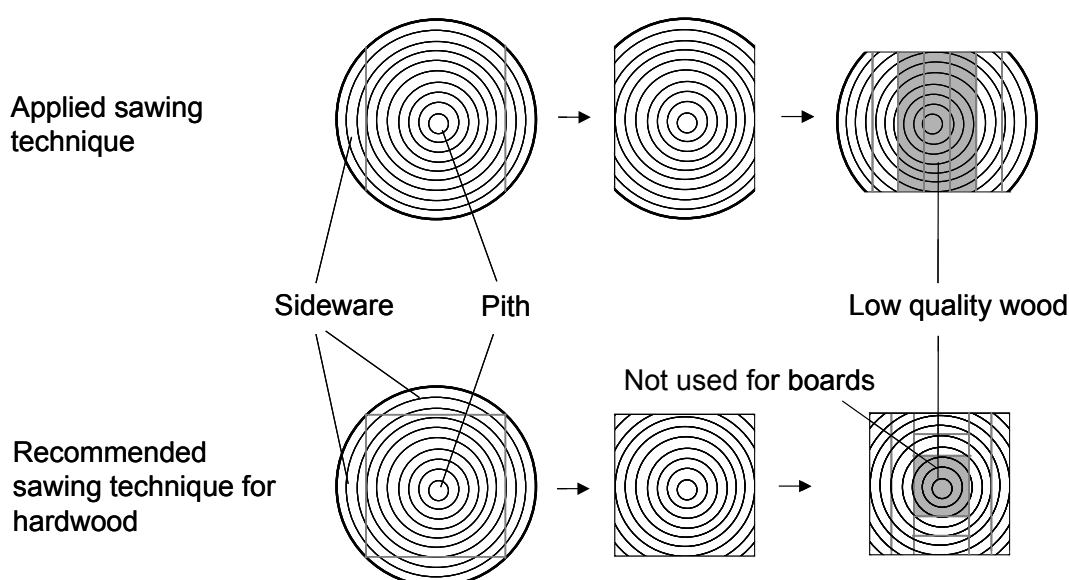


Figure 37: Applied and recommended sawing technique for low-diameter hardwood logs.

5.1.3 Test Conditions

5.1.3.1 Solar-Assisted Dryer

Production Drying Tests

Most drying tests in the solar-assisted dryer were done with an entire timber load of approximately 200 m³ within the normal production flow of the Brazilian sawmill. This

means that the drying experiments were performed under realistic industrial conditions. However, no extreme drying conditions could be applied at this test arrangement in order to establish the limits of the drying process. The position of the wood stacks in the solar dryer is shown in Figure 23.

Additional Drying Tests

To investigate the influence of the drying air velocity between the board layers on the drying rate, three small timber stacks were arranged in a different way inside the drying chamber with an additional fan, **Figure 38**. The timber stacks were 1.00 m high, 1.00 m wide and 1.80 m long and were loaded inside the solar dryer behind the timber load on the side of the air flap. The drying experiments were done with 27 mm thick boards and the application of a typical drying schedule. Thus, different drying air velocities could be applied to the wood stacks under the same temperature and humidity level of the drying air.

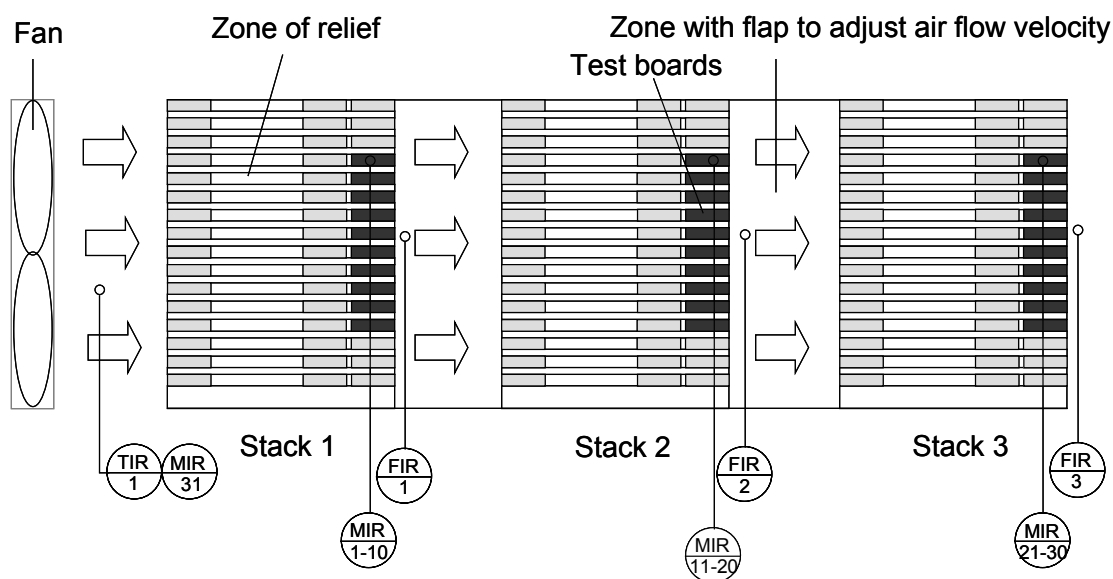


Figure 38: Test conditions for the investigation of the influence of the drying air velocity on the drying rate.

F – air velocity T – temperature M – humidity

Air velocities between 0.5 and 7 m/s were applied during different drying tests. First, high air velocities of 7.0 m/s, 6.0 m/s and 3.0 m/s, assuring a turbulent flow, were compared with low air velocities of 1.5 m/s and 0.5 m/s, presenting a laminar flow, to estimate the air velocity where the drying rate is decelerated significantly. Afterwards, different low air

flow velocities of 0.5 m/s, 1.0 m/s and 1.5 m/s were compared to find the required minimum air velocity for timber drying.

5.1.3.2 Ambient Air

Complete or partial ambient air drying still is the predominant drying method for eucalypt hardwood within the Brazilian timber industry. Ambient air drying depends primarily on the existing weather conditions. However, the arrangement of the timber stacks allows a certain but limited control of the drying conditions. Mounting the timber stacks in large distances increases the drying rate due to a higher insolation and a stronger influence of the wind. Severe drying conditions cause high drying stress in the timber which results in drying defects. Therefore, the available young and sensitive eucalypt timber was dried under controlled ambient air conditions for a comparison to the drying process in the solar-assisted timber dryer. Thereby, the timber stacks were arranged close to another near to the solar dryer to protect them from wind and direct insolation.

5.1.4 Timber Quality

Due to still missing international quality standards for dried sawnwood, an evaluation method was elaborated and standardised for the special needs and properties of eucalypt timber. The basis for this was the EDG-Recommendation “Assessment of drying quality of timber” proposed by Welling [40; 41].

5.1.4.1 Sample Strategy

Different minimum quantities of wood samples are defined in literature to evaluate the average wood moisture content of a timber load. The suggested CEN standard-drafts prEN 175-13.01 and prEN 12169 are not applicable in industrial practise due to an unacceptably high number of required single measurements. Following ISO 2859, a 4 m long and 65 mm thick board would have to be measured at 24 locations which also excludes this standard for the industry [41]. Therefore the European pre-standard „prEN175.092“ was proposed for industrial purposes. Thus, the number of required samples depends either on the number of single boards or on the number of wood stacks in a timber load. From a load of more

than 40 stacks a minimum of 6 stacks have to be taken and from a load with more than 10 000 boards a minimum of 80 boards have to be measured [240].

Observing this instruction, the number of wood samples which were taken from the dried timber load were defined by results from various drying tests with a high number of samples. For the determination of the average wood moisture content, the moisture distribution and casehardening of 70 boards were evaluated per timber load with approximately 12 000 boards, whereby, 10 boards were taken from each sample stack that was selected from every second row in the solar dryer, **Figure 39**. For the evaluation of warp, fissuring and collapse a model stack was placed in the middle of the dryer. This model stack contained 50 selected boards which were analysed for the described parameters before and after the drying process. A corresponding model stack was also placed under ambient drying air conditions for comparison.

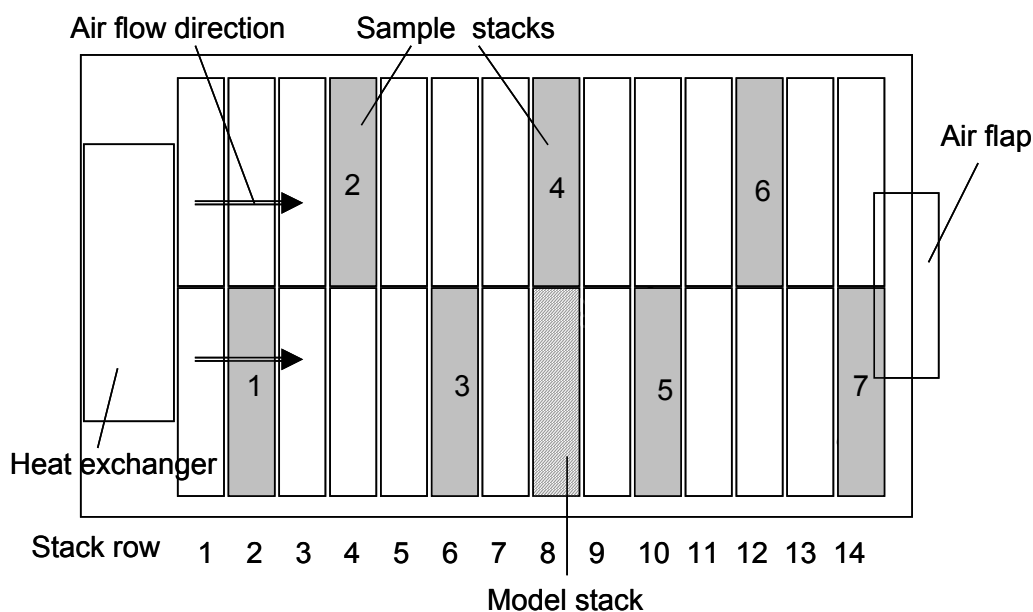


Figure 39: Solar dryer with the arranged timber stacks, the sample stacks and the model stack.

5.1.4.2 Wood Moisture Content

Sawnwood for the furniture industry has to be dried to the required equilibrium wood moisture content. An average equilibrium wood moisture content of 13.6 % was given for Belo Horizonte and the region close to the sawmill [97-99]. Since timber swells less with increasing moisture content than it shrinks with decreasing wood moisture, the eucalypt

wood was dried to a final wood moisture content of 12 % when it was produced for the Brazilian timber market. Timber that was produced for the export market was used as parquet in a heated environment and was therefore dried to a final wood moisture content of 8 %. The wood moisture content was determined by both measuring the electric resistance of the wood tissue with an instrument and cutting samples for the oven-dry method.

Electric Moisture Meter

A moisture meter allows the fast determination of the wood moisture content by measuring either the electrical or the capacitive resistance. Capacitive resistance instruments measure the dielectricity constant of the timber by holding them against the board surface. This allows the determination of the wood moisture content without puncturing the samples. However, correct values can only be received if there is a homogeneous moisture distribution in the wood. Electrical resistance instruments measure the electrical conductivity between two electrodes that are driven into the timber. These instruments permit the determination of a moisture gradient by measuring in different depths of the wood sample. The electrical resistance correlates with the wood moisture content whereby the electrical resistance decreases with increasing moisture content and vice versa. However, the electrical resistance is not only influenced by the moisture content but also by the temperature and the anatomical wood structure. Therefore, an automatic temperature compensation and a correction factor for different wood species are included in the instruments. Both instruments contain a higher error level above than below fibre saturation point. Reliable values can be measured between 5 and 30 %. In this research work a resistance instrument of the type „Greisinger GHH 91“ for manual measurements and of the type „Greisinger HF 91“ for stationary measurements was used [206; 241-243].

A method to estimate the correct average wood moisture content with the electrical resistance method is given in a draft (prEN 13183-2) for an European Standard. Thereby, measuring with insulated electrodes in a depth of 0.3 times the board thickness in more than 5 boards per stack is sufficient for an exact determination. For statistical reasons, however, it was decided to measure 10 boards per stack. Besides this, the wood moisture content was also measured in the centre and close to the board surface to determine the moisture gradient [244].

Oven-Dry Method

An exact and standardised method for the determination of the wood moisture content is the oven-dry method. The draft prEN 13183-1 suggests a European standard following the DIN 52 183 respectively ISO 3130-1975 [245]. The oven-dry method is a destructive and time consuming method and therefore it is less frequently used in industrial practice. However, this method provides a safe comparison to the electrical measurements and for this reason it was applied to all 70 wood samples chosen for wood moisture determination (see chapter 5.1.4.1). The wood samples were cut at a distance of 0.30 m from the top of the analysed boards and weighed on a laboratory balance with an accuracy of 0.1 g. Preliminary tests showed that the moisture content of these samples did not differ significantly from wood samples in the middle of the eucalypt boards. Then, the samples were dried at a temperature of $103\text{ }^{\circ}\text{C} \pm 2\text{ }^{\circ}\text{C}$ to constant weight i.e. to zero moisture content and were re-weighed. Since eucalypt wood does not have a high content of volatile compounds like ethereal oils or resin, the drying process had not to be carried out in an exsiccator [29; 245; 246].

The wood moisture content x in % was then calculated from the wet weight m_{wet} and the oven dry weight m_{dry} by:

$$x = 100 \cdot \frac{(m_{\text{wet}} - m_{\text{dry}})}{m_{\text{dry}}} \quad (43).$$

5.1.4.3 Casehardening

Two methods exist for the quantitative evaluation of casehardening in timber: the fork test and the slicing test. During this research work, however, the fork test was preferred due to its wide distribution and simple application. The fork test was carried out by cutting a fork from 40 % of the boards sample selected for moisture determination respectively 28 samples per load following the sketch in **Figure 40**. When the outer wood layers are separated from the inner layers, the fork closes or opens immediately corresponding to residual compression or tension stress. In addition to the evaluation of the residual drying stress, the evaluation of casehardening includes also the effect caused by a moisture gradient between

the core and the surface layer. Therefore, the fork values were measured with a calliper after 24 hours [41; 101; 247].

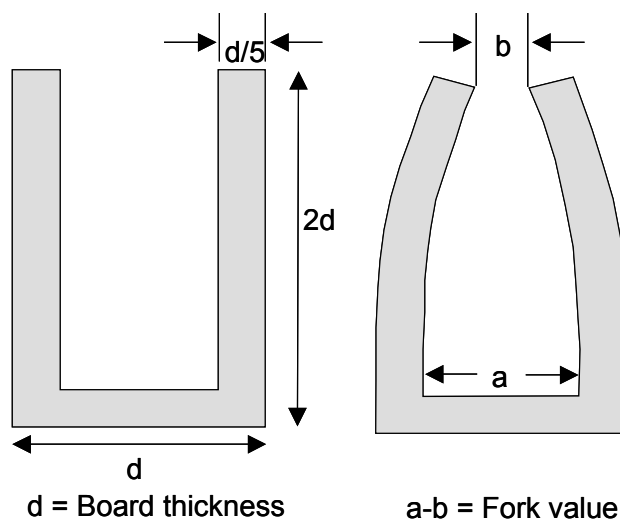


Figure 40: Sketch of the fork test for the evaluation of casehardening [41; 247].

The degree of casehardening was evaluated by comparing the measured fork values with maximum fork values for a definite quality grade. The maximum fork values were derived for four different board thicknesses from a template described by Welling [247], **Table 7**.

Table 7: Maximum fork value in mm for different grade of drying stress.

Drying stress	Light	Medium	Strong
18 mm	3	7	18
27 mm	5	11	27
32 mm	6	13	32
42 mm	8	16	40

5.1.4.4 Warp

The different types of warp (see chapter 2.2.2.3, Figure 13) were measured with a line and a ruler at 50 boards from two model stacks before and after the drying process.

5.1.4.5 Fissuring

Fissuring was measured with a ruler at 50 boards from the model stack before and after the drying process. Surface checks were only evaluated if the boards were not influenced by the pith. This means that the boards had to be cut in a minimum distance of 5 cm from the log centre.

5.1.4.6 Cell Collapse

Cell collapse was measured with a ruler at the 50 boards from the model stack before and after the drying process. Since collapse can often only be separated from natural shrinkage on a microscopic level, an exact evaluation of boards that contained a part of the pith was not always possible.

5.1.4.7 Discolorations

Discolorations were evaluated visually at the 50 boards from the model stack before and after the drying process. A quantitative evaluation was not possible.

5.1.4.8 Quality Classification of the Sawnwood

The quality assessment of drying defects like warp, fissuring, cell collapse and discolorations is still done visually in the industry due to missing objective methods. The introduction of a classification system for these parameters had been attempted several times without success due to the complexity and different quality demands of each wood manufacturer. Therefore, these quality parameters were described qualitatively and quantitatively but were not classified in this research work. However, a quality classification of casehardening, average wood moisture content and moisture distribution of a dried timber load is sufficient to describe the quality of a drying process [41]. The applied classification system for these parameters was derived from the EDG-Standard „Drying quality“ [40] and adapted to the special needs of eucalypt wood and the Brazilian furniture industry. Thereby, the wood quality was separated in four classes: extra class, 1. class, 2. class and 3. class, **Table 8**. The average wood moisture content could vary within the given limits from the defined final moisture content to be classified in the specified quality class. The

moisture distribution in the timber load was determined by the variation of the single measurements. Since timber is a natural product, only 90 % of the measured values had to be within the defined range. Casehardening was classified by the different quality grades (see chapter 5.1.4.3).

Table 8: Adapted quality classification for eucalypt sawnwood for different board thicknesses d.

	3. Class	2. Class	1. Class	Extra
Average wood moisture content*				
d ≤ 40 mm	Without limit	+3 % / -3 %	+2 % / -2 %	+1.5 % / -1.5 %
d > 40 mm	Without limit	+3 % / -3 %	+2.5 % / -2,5 %	+2 % / -2 %
* Allowed deviation of the measured average wood moisture content from the defined average wood moisture content.				
Wood moisture distribution**				
d ≤ 40 mm	Without limit	+4 % / - open	+3 % / -3 %	+2 % / -2 %
d > 40 mm	Without limit	+6 % / - open	+4 % / -4 %	+3 % / -3 %
** 90 % of all measured values are allowed to vary within the given range from the measured average wood moisture content.				
Casehardening***				
	Strong	Strong	Medium	Light
*** The quality grades are deduced from the fork value.				

5.1.5 Energy Balance

The most relevant energy flows at the solar-assisted timber dryer during the drying process are shown in **Figure 41**. Energy flows with a negative sign signify a temperature decrease of the drying air while energy flows with a positive sign result in an increase of it. The drying air temperature is mainly increased by the absorbed solar radiation $+\dot{Q}_s$, by the heat exchanger $+\dot{Q}_{He}$ and by the waste heat of the axial flow fans $+\dot{Q}_{Fa}$. The drying air temperature is either decreased by removing sensible heat from the solar dryer or by converting sensible heat into latent heat by water evaporation. Water is either evaporated at the timber to reduce the wood moisture content $-\dot{Q}_{Eva}$ or at the humidifying system to in-

crease the relative humidity of the drying air $-\dot{Q}_{Hu}$. Sensible heat is removed from the solar dryer by exchanging the drying air with outside air $-\dot{Q}_{Ae}$, by convection at the dryer surface $-\dot{Q}_{Con}$ and by thermal radiation from the absorber surface $-\dot{Q}_{Rad,th}$. The quantitative determination of the different energy flows was done according to chapter 4.1.5 and 5.1.7.

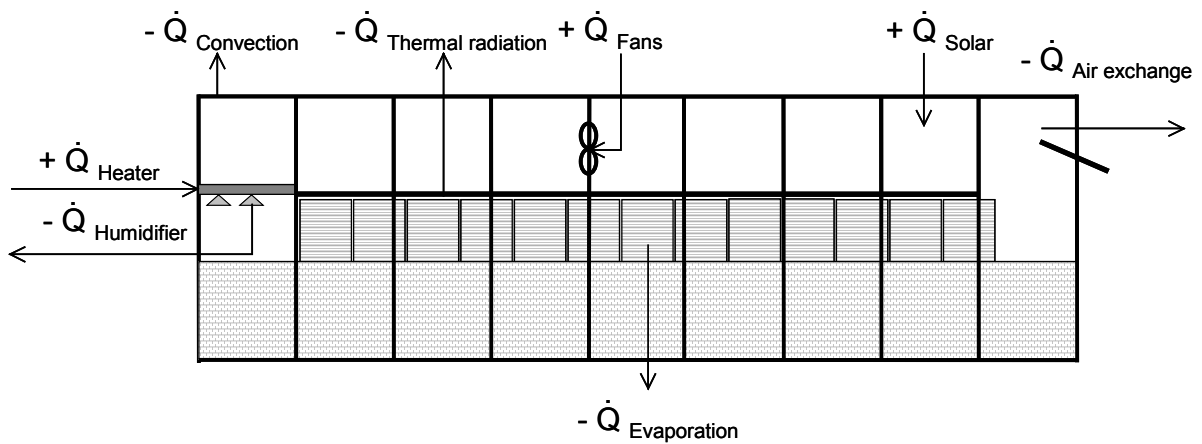


Figure 41: Energy balance of the solar-assisted timber dryer.

5.1.6 Data Acquisition

The data acquisition was mainly done according to chapter 4.1.4. Additionally, manual measurements of the air velocity, the consumption of the wood chips and the gravimetric determination of the wood moisture content were carried out in given intervals during the drying process. The sawnwood quality was evaluated before and after each drying experiment.

5.1.7 Methods of Calculation

5.1.7.1 Energy Flow

Heat Exchanger

The heat flow from the heat exchanger to the drying air \dot{Q}_{He} results from the flow pipe temperature ϑ_{Fl} , the return pipe temperature ϑ_{Re} , the mass flow of the hot water \dot{m}_W and the specific heat capacity of water $c_{p,W}$ by:

$$\dot{Q}_{He} = \dot{m}_W \cdot c_{p,W} \cdot (\vartheta_{Fl} - \vartheta_{Re}) \quad (44),$$

whereby the heat capacity of water is 4.2 kJ/kg·K for a temperature between 0 and 100 °C and a pressure between 0 and 4 bar [86; 248].

Water Evaporation

The mass of the evaporated water from the timber depends on the average wood density of *Eucalyptus grandis* ρ with 600 kg/m³ and the average wood moisture content at the beginning and at the end of the drying process. The energy demand for water evaporation \dot{Q}_W is a product of the evaporation enthalpy of water r_W with 2430.7 kJ/kg at a temperature of 30 °C and the mass flow of the water \dot{m}_W [86]:

$$\dot{Q}_W = r_W \cdot \dot{m}_W \quad (45).$$

Air Exchange

The loss of sensible heat through the exchange of the drying air with the outside air \dot{Q}_{Ae} depends on the heat capacity of the air $c_{p,A}$ with 1.007 kJ/kg·K at a temperature between 0 and 40 °C, the density of the drying air ρ_A with 1.168 kg/m³ at 25 °C, the temperature difference between the dryer and the ambient ΔT and the volume flow of the exchanged air \dot{V} by:

$$\dot{Q}_{Ae} = c_{p,A} \cdot \Delta T \cdot \dot{V} \cdot \rho_A \quad (46).$$

The volume flow was calculated by the difference of the water content of the drying air and the ambient air (see chapter 4.1.5) and the amount of the evaporated and discharged water.

5.1.7.2 Statistics

Analysis of the Variance with Equal Group Frequency

The analysis of the variance allows the comparison of two and more sample means. Since this test can only be applied if the data set is normally distributed, a test on normal distribution was done primarily according to the Lilliefors diagram [249].

Samples with equal group frequencies have m groups of treatment with n repetitions. The sum of the square deviations SQ_b between the groups is defined by:

$$SQ_b = \sum_{i=1}^m (y_{i\cdot} - \bar{y}_{\cdot\cdot})^2 \quad (47),$$

whereby the degrees of freedom DF_b are:

$$DF_b = m - 1 \quad (48)$$

and the variance s_b^2 is:

$$s_b^2 = \frac{SQ_b}{DF_b} \quad (49).$$

The sum of the square deviations SQ_e within the groups can be determined by:

$$SQ_e = \sum_{i=1}^m \sum_{j=1}^n (y_{ij} - \bar{y}_{i\cdot})^2 \quad (50),$$

whereby the degrees of freedom DF_e are deduced by the difference between the total number of measurands N and the number of groups m by:

$$DF_e = N - m \quad (51).$$

The variance s_e^2 is the ratio between the sum of the square deviations SQ_e and the degrees of freedom DF_e :

$$s_e^2 = \frac{SQ_e}{DF_e} \quad (52).$$

The F-value F is the ratio between variance s_b^2 between the groups and the variance s_e^2 within the groups:

$$F = \frac{s_b^2}{s_e^2} \quad (53).$$

The calculated F-value is compared with the F-value from the table of probability of the F-distribution F_{α, DF_b, DF_e} . The null hypothesis is rejected in favour of the alternative with the level of error of the first kind α , if the calculated F-value is bigger than the given F-value. Thereby, the null hypothesis means that the samples are from the same parent populations that have the same mean, which signifies that there is no significant difference between the sample means.

Analysis of the Variance with Unequal Group Frequency

An unequal group frequency means that there are m groups of treatment with a different number of repetitions n within each group. The calculation is similar to the one used for equal group frequencies. However, the sum of the square deviations between the groups SQ_b follows the function:

$$SQ_b = \sum_{i=1}^m n_i (\bar{y}_i - \bar{y})^2 \quad (54)$$

and the sum of the square deviations within the groups SQ_e is calculated by:

$$SQ_e = \sum_{i=1}^m \sum_{j=1}^{n_i} (y_{ij} - \bar{y}_i)^2 \quad (55).$$

Rank Sum Test by Wilcoxon

The Wilcoxon rank sum test is used whenever the samples are not normally distributed and the samples are independent from each other. All the observations $N = n_1 + n_2$ are organised by size whereby the smaller of the both samples has the lower rank sum T_1 . The significance level is then:

$$u = \frac{T_1 - \frac{n_1 \cdot (n_1 + n_2 + 1)}{2}}{\sqrt{\frac{n_1 \cdot n_2 \cdot (n_1 + n_2 + 1)}{12}}} \quad (56).$$

If the value of the approximation $|u|$ is bigger or equal to the value from the normal distribution $u_{\alpha/2}$, the null hypothesis is rejected, which means that the samples are significantly different.

Matched Pair Rank Test by Wilcoxon

The Wilcoxon matched pair rank test is valid for samples that are not normally distributed and the samples are linked one to another. The absolutes of the differences between the n measurands available as pairs are sorted with increasing size. The rank sum of the negative and positive differences are built and the smaller of both rank sums is used as the test variable. An approximation of the significance level is calculated from the matched pair rank sum V by:

$$u = \frac{V - \frac{n \cdot (n + 1)}{4}}{\sqrt{\frac{n \cdot (n + 1) \cdot (2 \cdot n + 1)}{24}}} \quad (57).$$

If the value of the approximation $|u|$ is bigger or equal to the value of the normal distribution $u_{\alpha/2}$, the null hypothesis is rejected, which means that the samples are significantly different.

Box and Whisker Plot

Whenever the measured data were not normally distributed, the results were described by a box and whisker plot [249]. This diagram illustrates the median, the mean, the maximum and minimum value, the 1st and 3rd quartile and the 10 % and 90 % percentile of the sample, **Figure 42**.

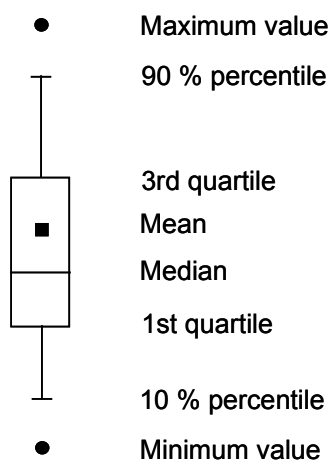


Figure 42: Box and whisker plot [249].

5.2 Results

5.2.1 Drying Performance

Over 80 drying experiments with more than 16 000 m³ of sawnwood from *Eucalyptus grandis* were carried out in the solar dryer during this research work. Thereby, the wood quality, the drying time, the energy consumption and the drying costs were measured and evaluated. Adequate drying curves for 18, 27, 32 and 42 mm thick boards were devised under observation of the retrieved results and the special needs of the solar dryer (see also chapter 4.2.5). The generated drying schedules have some special characteristics which will be described in the following chapters.

5.2.1.1 Gradient of the Drying Conditions Along the Timber Stack

The timber was stacked in the solar dryer at a length of 14 m. Due to a missing air flow reversion, a gradient of the relative humidity and the temperature of the drying air respectively the drying conditions between the air inlet and the air outlet of the wood stack was expected and analysed. **Figure 43** shows a typical gradient of the drying climate along the drying chamber during the drying of 27 mm thick boards of *E.grandis* from 60 to 12 % wood moisture content. The difference of the temperature and the relative humidity of the drying air was higher at the beginning of the drying process due to a higher water evaporation from the timber. Thereby, a maximum temperature difference of approximately 2 K was found at the beginning of the drying process. This value decreased continuously during the drying run. At the end of the drying process, the drying air temperature at the air outlet equalised to the temperature at the air inlet or was occasionally higher. The relative humidity of the drying air was about 15 % lower at the air inlet than at the air outlet at the beginning but approximated at the end of the drying process. The diagram shows that the relative humidity decreased continuously at the air inlet along the drying time following the set course. This was due to the fact that the control sensor was installed at the side of the air inlet. On the other side, the relative humidity at the air outlet oscillated during the day whereby the variations were lower at the beginning and higher at the end of the drying process.

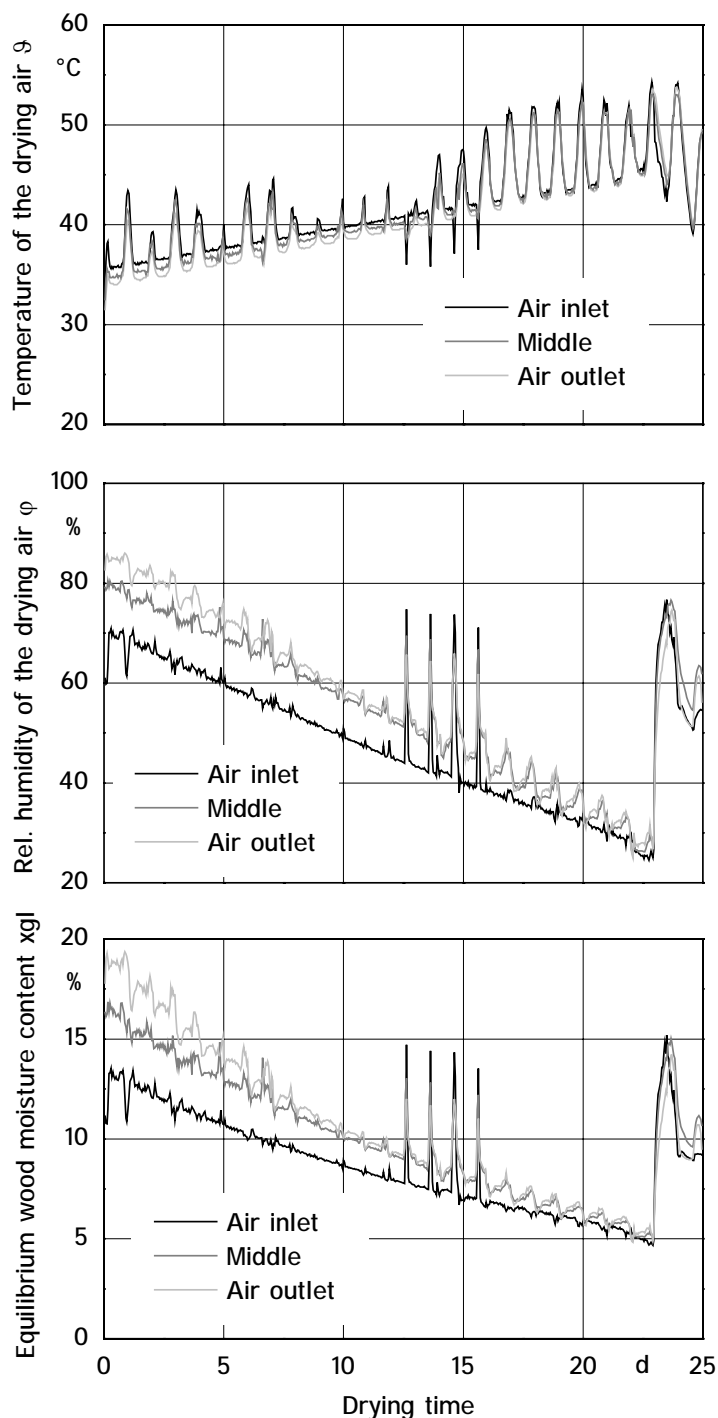


Figure 43: Comparison of the temperature, the relative humidity and the equilibrium wood moisture content of the drying air at the air inlet, in the middle and at the air outlet of the timber stack during the drying of 27 mm thick eucalypt boards.

This behaviour resulted from the intentionally allowed temperature oscillations of the drying air during day and night and will be explained in detail in chapter 5.2.1.2 by selected drying days. Nevertheless, the relative humidity at the air outlet was about 6 % higher during the morning but equalised during the day and was even lower during the afternoon than

at the air inlet. It has to be observed that the relative humidity and the temperature of the drying air in the middle of the wood stack was more similar to the conditions of the drying air at the air outlet than of the air inlet during the whole drying process. This is attributed to the fact that the influence of the heat exchanger and the humidifier was highest at the first timber row at the air inlet. Altogether, it was found that the equilibrium wood moisture content of the drying air was almost always lower at the air inlet than at the air outlet and almost the same in the middle of the wood stack and at the air outlet. Other drying runs showed that the faster the drying process the higher was the humidity and temperature gradient of the drying air. But normally the drying cycles were even slower, especially for thicker boards. The peaks downwards for the drying air temperature and upwards for the relative humidity of the drying air in Figure 43 between drying day 13 and 17 are due to the executed reconditioning cycles for stress relief in the timber.

5.2.1.2 Daily Temperature Oscillations

Figure 44 shows a selected time period of six days from two different drying runs. One drying run with low temperature oscillations on the left side and one drying run with high temperature oscillations on the right side. These sections show the consequences of the allowed maximum daily temperature oscillations, which are the most prominent difference to conventional high temperature dryers. On the left side of the diagram, a drying run of 27 mm thick eucalypt boards at a temperature level between 38 and 50 °C at the air inlet and a daily temperature oscillation of approximately 8 K is shown. The difference of the temperature and the relative humidity between the air inlet and the air outlet was high due to a high drying rate. An increasing drying air temperature during the morning induced the closing of the air flap. If sufficient water for the increase of the water content of the drying air could not be supplied by the timber, additional water was sprayed by the humidifier. If the water, added from the timber and the humidifier, was not sufficient, the relative humidity of the drying air decreased below the set value causing a small peak downwards. The water, supplied by the humidifier, evaporated at the side of the heat exchanger and increased the water content of the drying air. The drying air that passed along the colder timber stack, cooled down and its relative humidity increased in direction to the air outlet. If the ambient air and therefore the drying air temperature decreased during the evening, the air flap opened to keep the relative humidity at the desired level. The drying air cooled down mainly by mixing with the colder outside air. The colder drying air was heated up

when passing the timber stack and its relative humidity decreased in the direction of the air outlet. The steep increase of the relative humidity at the side of the heat exchanger was caused by the two hour long re-humidifying cycles. It may be observed that humidification caused a steep increase of the relative humidity at the air inlet but only a small increase at the air outlet. This means, the faster dried timber at the air inlet was moistened more than the one at the air outlet, thus equalising the drying conditions inside the solar dryer.

The right side of the diagram shows a drying run of 42 mm thick eucalypt boards with a lower temperature level between 27 and 42 °C at the air inlet but with high temperature oscillations of about 15 K. The difference of the temperature and the relative humidity between air inlet and air outlet was low due to a slow drying process. Due to the high temperature oscillations and the low drying rate, the humidifier system sprayed more frequently. It was switched on mainly during the morning when the temperature level increased inside the solar dryer by following the ambient air temperatures. However, the water supply by the humidifier was not sufficient to equalise the steep temperature increase. Therefore, the set high values for the relative humidity of the drying air could not be reached at the air inlet. However, the relative humidity of the drying air at the air outlet increased due to the temperature reduction of the drying air along the timber stack (see the explained correlation for 27 mm thick boards). During the evening, the relative humidity of the drying air was even lower at the air outlet than at the air inlet due to a temperature increase along the timber stack. This means that the drying conditions were more severe at the air outlet than at the air inlet. Generally, the higher the daily temperature oscillations the more water had to be added by the humidifier during the day and the higher was the deviation of the relative humidity from the set values.

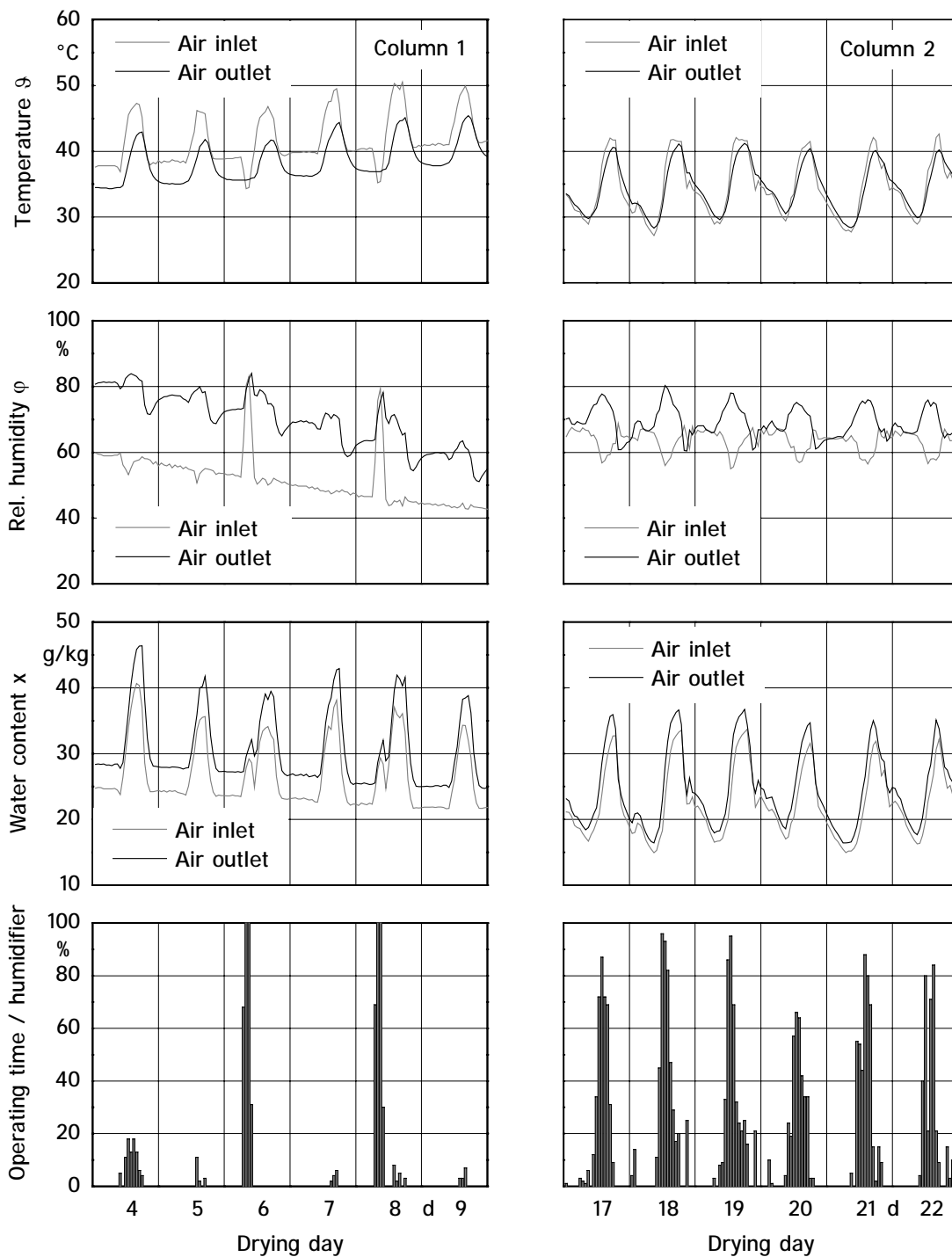


Figure 44: Comparison of the temperature, the relative humidity, the water content and the running time of the humidifier during the drying of 27 mm eucalypt boards with low temperature oscillations of 8 K (column 1) and of 42 mm eucalypt boards with high temperature oscillations of 15 K (column 2).

5.2.1.3 Drying Air Velocity

Significant electrical energy savings are possible by adapting the drying air velocity to the drying process (see chapter 2.2.1.3). However, an uncontrolled decrease of the fan power can reduce the absorption of the wood moisture by the drying air. This can decelerate the drying process significantly and can increase the difference of the drying conditions between the air inlet and the air outlet of the timber stack [217]. Therefore, the influence of the drying air velocity on the drying rate of *E.grandis* wood was analysed. First, high air velocities of 3 and 6 m/s were compared with low air flow velocities of about 1.5 m/s, **Figure 45**. It was shown that the drying rate could not be accelerated by an air velocity higher than 3 m/s under the analysed conditions. On the other side, the drying rate was significantly lower at an air velocity of 1.5 m/s compared to the air velocities above 3 m/s. While the average wood moisture content was the same for all treatments at the beginning of the drying test, it was significantly higher for the air velocity of 1.5 m/s between the 15th and the 30th drying day. However, no significant difference of the average wood moisture content was found for all air velocities at the end of the drying process due to the relatively long drying time of 42 days.

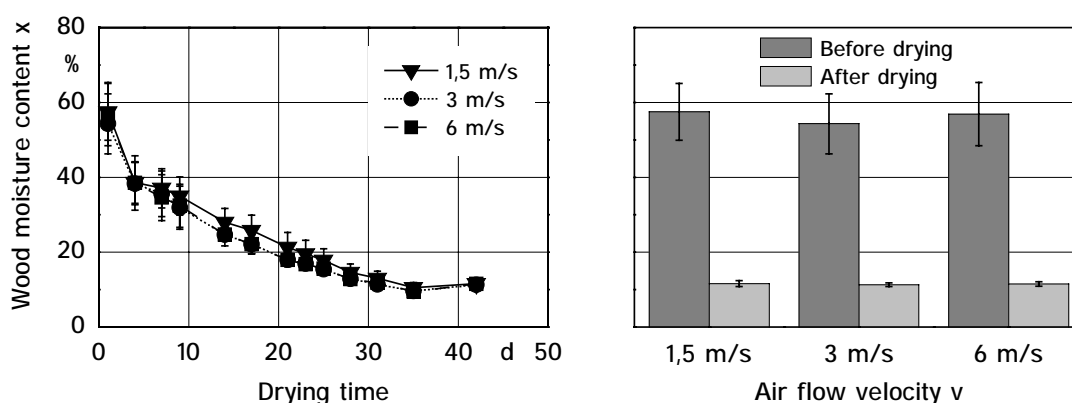


Figure 45: Wood moisture decrease and initial and final wood moisture content at a drying process with air flow velocities between 1.5 and 6.0 m/s.

Reducing the drying air velocity further below 1.5 m/s did not cause a significant deceleration of the drying rate, **Figure 46**. The drying rate was even at an air velocity of 0.5 m/s the same as with 1.5 m/s. Thereby, no significant difference between the different air velocities was found for the drying rate during the drying process and the final wood moisture content. This showed that hardwoods like eucalypts can be dried even at low drying air veloci-

ties. However, the lower the velocity of the drying air the higher is the drying gradient along the timber stack.

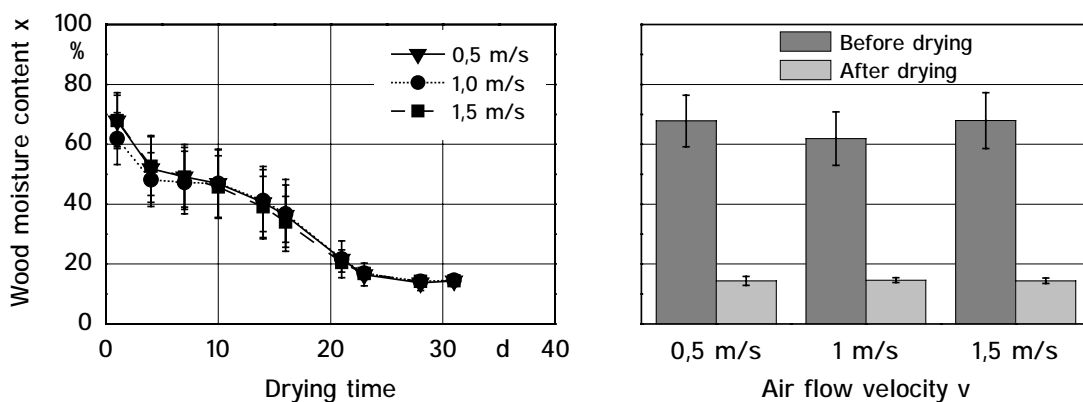


Figure 46: Wood moisture decrease, initial and final wood moisture content at a drying process with air velocities between 0.5 and 1.5 m/s.

5.2.1.4 Wood Temperature

The temperature of the 27 and 42 mm thick eucalypt boards was measured during the drying process at the surface and in the core. No temperature difference between the core and the surface could be measured in 27 mm thick boards. Small temperature differences were measured in 42 mm thick boards, **Figure 47**.

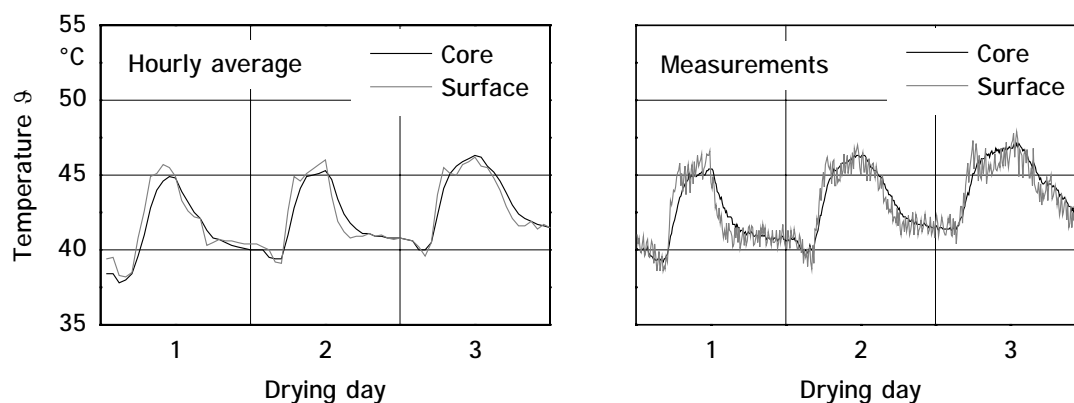


Figure 47: Hourly average and single measurements of the sawnwood temperature in the core and at the surface of 42 mm thick eucalypt boards.

The hourly average values show that the surface temperature was at a maximum of 2 K higher than the core temperature whilst the solar dryer was heated up in the morning. The core temperature was at a maximum of 1 K higher whilst the dryer cooled down during the

evening. The measurements every five minutes indicate that the surface temperature varied decidedly more than the core temperature due to the varying drying air temperature.

Figure 48 shows the temperature in the wood core of 27 mm thick boards at the air inlet and the air outlet of the timber stack. The temperature difference between the timber at the air inlet and the air outlet was higher at the beginning of a drying process (day 1 to 3) than at the end of the drying cycle (day 17 to 19). At the beginning of the drying process, the wood temperature was always about 2 K higher at the air inlet than at the air outlet during day and night. At the end of the drying run, the wood temperature was only about 2 K higher whilst the dryer was heated up during the morning. During the rest of the day and night, the wood temperature at the air inlet was the same or even lower than at the air outlet. Generally, the temperature of the timber during the whole drying process, varied always more at the air inlet than at the air outlet, due to both a stronger influence of the heat exchanger and the heat storage capacity of the timber.

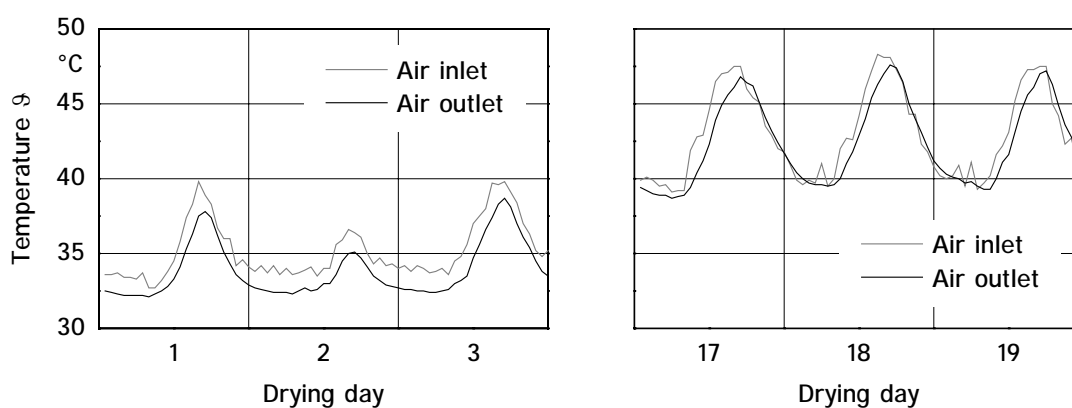


Figure 48: Comparison of the wood temperature in the core of 27 mm thick eucalypt boards over the length of the solar dryer at the beginning and at the end of the drying process.

5.2.1.5 Wood Moisture Content

A low moisture gradient between the surface and the core of a board allows a uniform moisture transport in the timber during the whole drying process and prevents drying defects like casehardening and deformations. This means that the moisture gradient can serve as an indicator for drying stress. **Figure 49** shows the wood moisture content at the surface and in the core of 27 and 42 mm thick eucalypt boards during one drying run. The moisture gradient between the surface and the core was with a maximum of 16 % significantly

higher in 42 mm thick boards than in the thinner boards with a maximum of 6 %. This value describes the total difference of the measured wood moisture content. However, more important than the total moisture gradient is the moisture gradient below the fibre saturation point since shrinkage starts below this point (see chapter 2.1.4). Therefore, the moisture content above FSP was always set as 27 % which means that only the relevant moisture gradient was given. This ensured that the gradient for 42 mm thick boards was 6 % and for 27 mm thick boards 5 %. This showed that the two board thicknesses were exposed basically to the same drying stress.

The right side of the diagram shows that approximately 65 m³ water was evaporated from the timber load during the drying process of 200 m³ eucalypt boards for both board thicknesses. This amount was evaporated from 27 mm boards in 27 drying days and from 42 mm boards in 62 days.

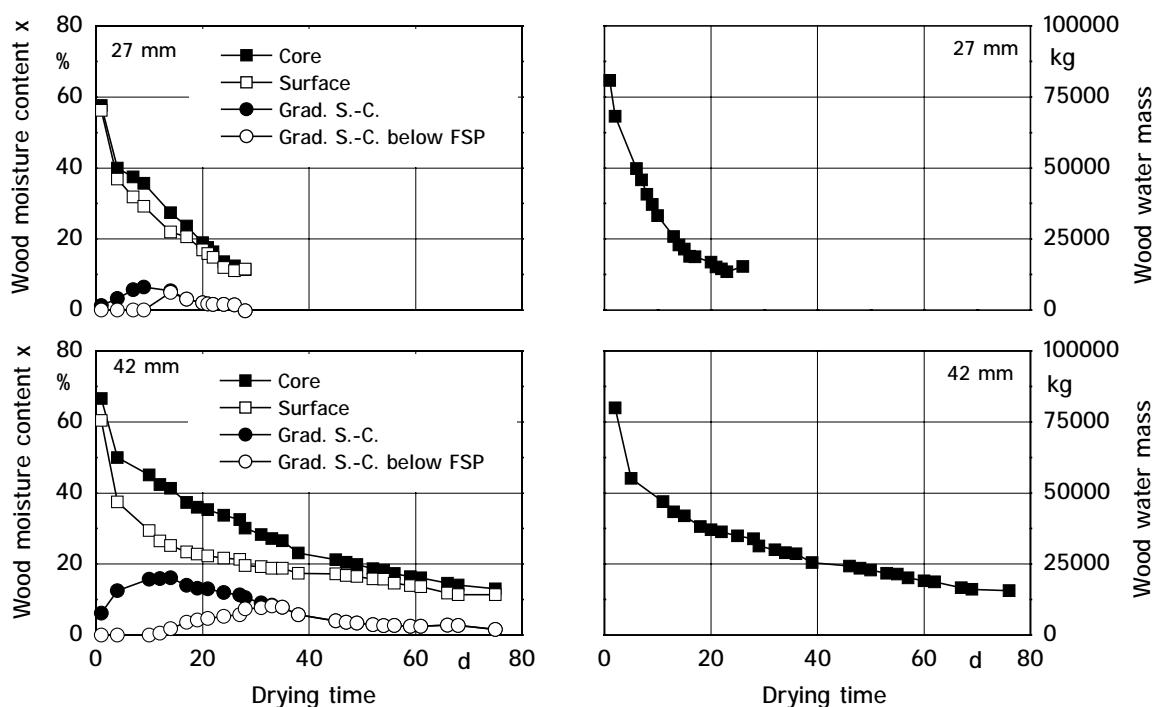


Figure 49: Course of the wood moisture content at the surface and in the core of 27 and 42 mm thick eucalypt boards during drying. The resulting moisture gradient is either shown as the difference of the measured values or as the difference of the moisture contents below FSP and the FSP (FSP = 27 %). The right column shows the course of the wood water mass of a timber load of 200 m³ during the drying of 27 and 42 mm thick boards.

Figure 50 compares the drying rate of 27 mm thick eucalypt wood in the solar dryer with controlled ambient air drying. Equal drying rates for ambient and solar drying were found at the beginning of the drying process at high wood moisture contents. While the drying process in the solar dryer slowed down but continued with decreasing wood moisture content, the drying rate at ambient air drying declined significantly and almost stopped close to the fibre saturation point. Thereby, a moisture content of 25 % was reached after 28 drying days at ambient air while 12 % was reached in the solar dryer in the same time. This confirms the disadvantages of ambient air drying.

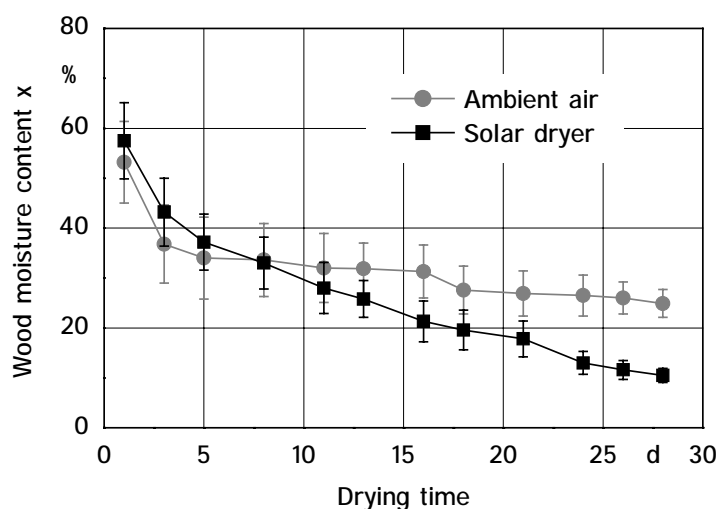


Figure 50: Course of the average wood moisture content during the drying process of 27 mm thick eucalypt boards under ambient climate conditions and in the solar dryer.

5.2.1.6 Drying Time

The average drying time for the investigated eucalypt sawnwood increased with increasing board thickness, in both solar drying and ambient air drying, **Figure 51**. This was due to the fact that the moisture gradient from the core to the surface of the board had to be kept at an acceptable level during the drying process in order to prevent drying defects (see also 5.2.1.5). While 18 mm thick boards could be dried in 22 days, 42 mm thick boards required about 65 days to dry from green to a uniform final wood moisture content of 12 %. The drying time for 27 mm thick boards in the solar dryer was about 27 days which was similar to the drying times known from conventional drying for this eucalypt species. Drying times between 20 and 35 days for 25 and 32 mm thick boards of *E. grandis* are cited in the literature [50; 114; 116; 119]. However, these drying experiments were normally real-

ised under laboratory conditions which is why the results are not offhand transferable to industrial big-scale plants. If the 27 mm thick eucalypt boards were dried at ambient air, the drying time was with 60 days about twice as long as in the solar dryer, and reached only a wood moisture content of about 18 %. Also the 42 mm thick eucalypt boards needed twice the time respectively about four months.

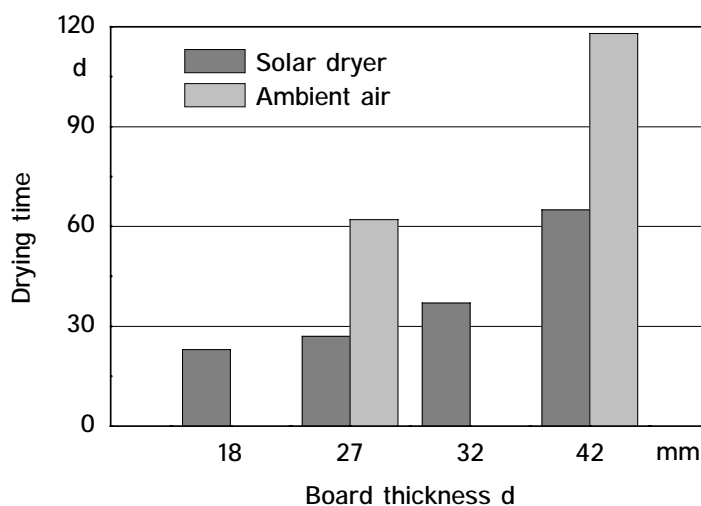


Figure 51: Average drying time for different board thicknesses at ambient air and solar drying of *Eucalyptus grandis*.

The required drying time t_{dry} for a certain board thickness in a high temperature dryer can be estimated by the initial wood moisture content x_{in} , the desired final wood moisture content x_f , the board thickness d , the drying air temperature ϑ and the drying coefficient α_D for hard- and softwood by [29; 208]:

$$t_{dry} = \frac{1}{\alpha_D} \cdot \ln\left(\frac{x_{in}}{x_f}\right) \cdot \left(\frac{d}{25}\right)^{1,5} \cdot \left(\frac{65}{\vartheta}\right)^{1,5} \quad (58).$$

This common method results in relatively short drying times and an almost linear increase of the required drying time with increasing board thickness. However, the calculated drying times for the four investigated board thicknesses with the cited drying coefficient α_D of 0.0265 for hardwood were too short, **Figure 52**. An adapted drying coefficient of 0,0058 brought the drying times for 27 and 32 mm thick boards into line but did not get the right values for 18 and 42 mm thick boards. Besides this, drying sensitive eucalypt hardwood at low temperatures in the solar dryer resulted in an exponential increase of the drying time

with increasing board thickness due to a slow water transport from the core to the board surface. Therefore, a regression equation for the measured drying times was used to estimate the drying time for other board thicknesses d of *Eucalyptus grandis* in the solar dryer by:

$$t_{\text{dry}} = (4.11 + 3.43 \cdot 10^{-4} \cdot d^{2.5})^2 \quad (59),$$

whereby the correlation coefficient was 0.99.

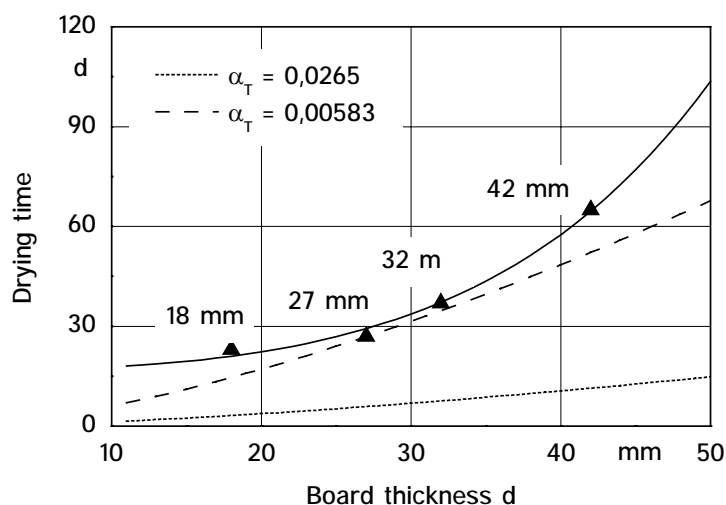


Figure 52: Comparison of the drying time for different board thicknesses of *Eucalyptus grandis* from 60 to 12 % wood moisture content.

5.2.1.7 Drying Schedules

A drying schedule was worked out which considered the specific demands of the solar dryer and the special requirements of the sensitive sawnwood from *Eucalyptus grandis* (see also chapter 2.2.3 and 4), **Figure 53**. It is separated in three phases: Filling of the drying chamber, the drying process which is further separated in a drying period before and after the fibre saturation point and the equilibration phase after drying. A phase for heating up and cooling down the timber at the beginning and at the end of the drying process, common in high temperature drying, is not necessary due to the low temperature level inside the solar dryer. User adjustments are possible at the transitions between the different drying phases. The desired relative humidity and temperature of the drying air changes automatically along the timeline between the transitions.

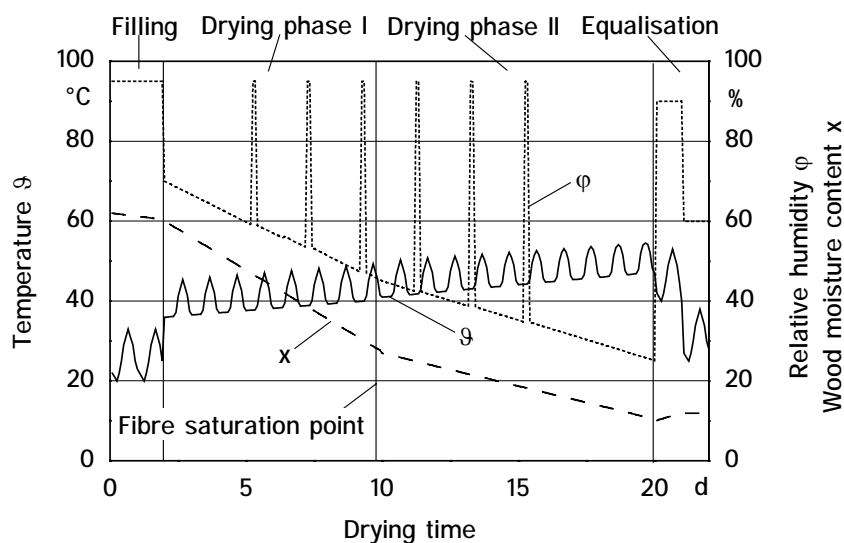


Figure 53: Model of a drying schedule for sensitive eucalypt timber in the investigated solar dryer.

Idealised drying schedules for 18, 27, 32 and 42 mm thick boards from the Brazilian eucalypt variety were derived from exemplary drying experiments, **Figure 54**. The required relative humidity of the drying air, the minimum and maximum drying air temperature, the drying time and the needed re-humidifying cycles were given for every stage of the drying process. These drying schedules proved to be suitable to dry Brazilian *E. grandis* timber in the investigated solar dryer with a maximum drying quality at minimum drying time. Green timber with an average initial wood moisture content between 60 and 80 % was dried with these schedules to a final moisture content of 12 % in 23, 27, 37 and 65 days with increasing board thickness. The drying times of the single experiments varied only slightly due to small weather variations of the subtropical climate.

Since the solar dryer could be filled in approximately four hours, the described filling phase was normally not necessary. However, when sufficient machine and manpower was not available, the dryer was run in the filling phase with a high relative humidity of 90 % and a low temperature level to prevent precipitated drying.

Generally, the drying air temperature in the solar dryer oscillated during the whole drying process resulting in elevated temperatures during the day and lower temperatures during the night, depending on the ambient air temperature. These temperature oscillations diminished the energy demand and prevented condensation on the air bubble foil on the dryer

inside (see also chapter 4). Slow drying conditions were adjusted at the beginning of the drying process above fibre saturation point at high wood moisture contents. Thereby, a maximum drying air temperature of 40 °C, a minimum temperature of 25 °C, a temperature difference to the ambient air of 10 K and a relative humidity between 70 for thin and 75 % for thick boards prevented collapse and casehardening. With decreasing wood moisture content, the drying process was intensified by increasing the temperature to a maximum of 45 °C, a minimum of 35 °C and a temperature difference of 15 K to the ambient air. The relative humidity was decreased to 45 % for thin boards and 60 % for thick boards to evaporate the bound water. Below fibre saturation point, the temperature was increased continuously to its maximum value of 55 °C, the minimum temperature to 50 °C and the temperature difference to 30 K. The relative humidity was decreased continuously to its minimum value of 25 % for all boards. The maximum temperature of 55 °C was limited by the durability of the air bubble foil. The minimum relative humidity of the drying air was defined by the climate control whereby the water content of the drying air had to be higher than the water content of the ambient air to allow the moisture discharge from the dryer.

The wood surface was re-humidified for a certain time period during defined time intervals by increasing the relative humidity of the drying air above 90 %. The drying air temperature was decreased in order to reach this high humidity level. The re-humidifying cycles were run every day for 2 hours for 18 mm thick boards, every second day for 3 hours for 27 and 32 mm thick boards and every third day for 4 hours for 42 mm thick boards. That way, the drying process could be accelerated without increasing the degree of drying stress.

The equilibration phase was divided into two periods and lasted one day for 18 mm thick boards and two days for the thicker boards. During the first period of the equilibration phase, the relative humidity was kept as high as possible and the temperature difference to the ambient air was kept at 20 K for all types of boards, to moisten the board's surface and to reduce still existing drying stress. During the second period, the temperature difference to the ambient air was kept at 5 K and the relative humidity was defined by the final equilibrium wood moisture content of 12 %, to cool down the timber and to homogenise the moisture distribution into the load.

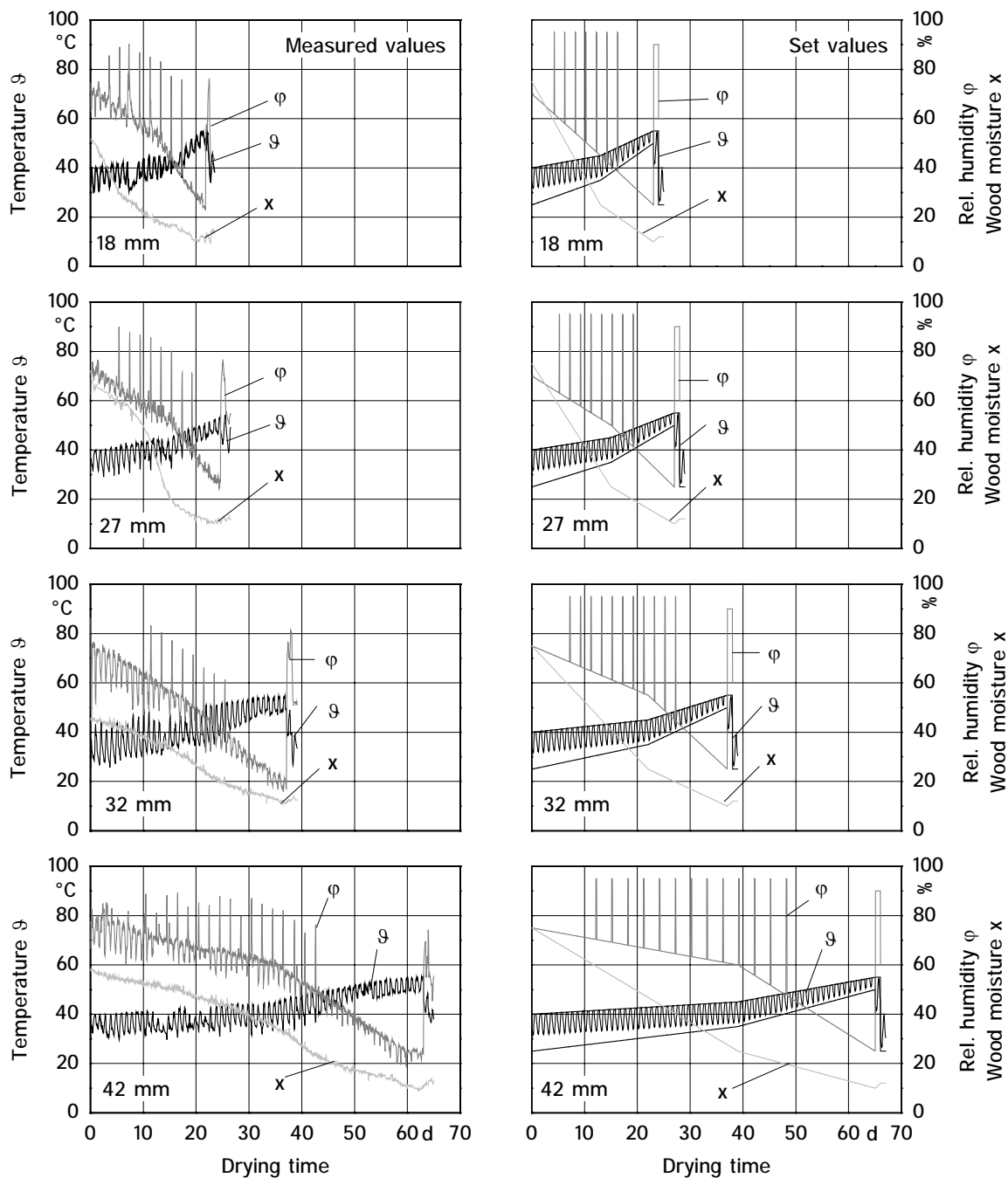


Figure 54: Measured values and generalised models of the drying schedules for 18, 27, 32 and 42 mm thick boards of *Eucalyptus grandis*.

The desired drying air temperature in the solar dryer was reached well due to an adequate heat supply from the solar collector and the biomass furnace, Figure 54. The set values of the relative humidity were reached with small deviations for small daily temperature oscillations and a high drying rate. This was usually the case for thin boards. However, the relative humidity differed more from the set values whenever there were high temperature oscillations and a low drying rate which was typical for thick boards (see also chapter

5.2.1.2). These small deviations from the desired humidity level, however, accelerated the drying rate but did not significantly reduce the drying quality (see also chapter 2.2.3). Also the desired high relative humidity during the re-humidifying cycles was not reached sufficiently. To reduce these deviations, either the efficiency of the humidifying system should be increased or the daily temperature oscillations should be reduced.

The typical drying conditions at ambient air at the test location are described in **Figure 55**. It shows that the relative humidity of the ambient air oscillated between 40 % and 80 % during one day. The ambient air temperature varied about 10 K during the day, which was equal to the temperature changes inside the solar dryer.

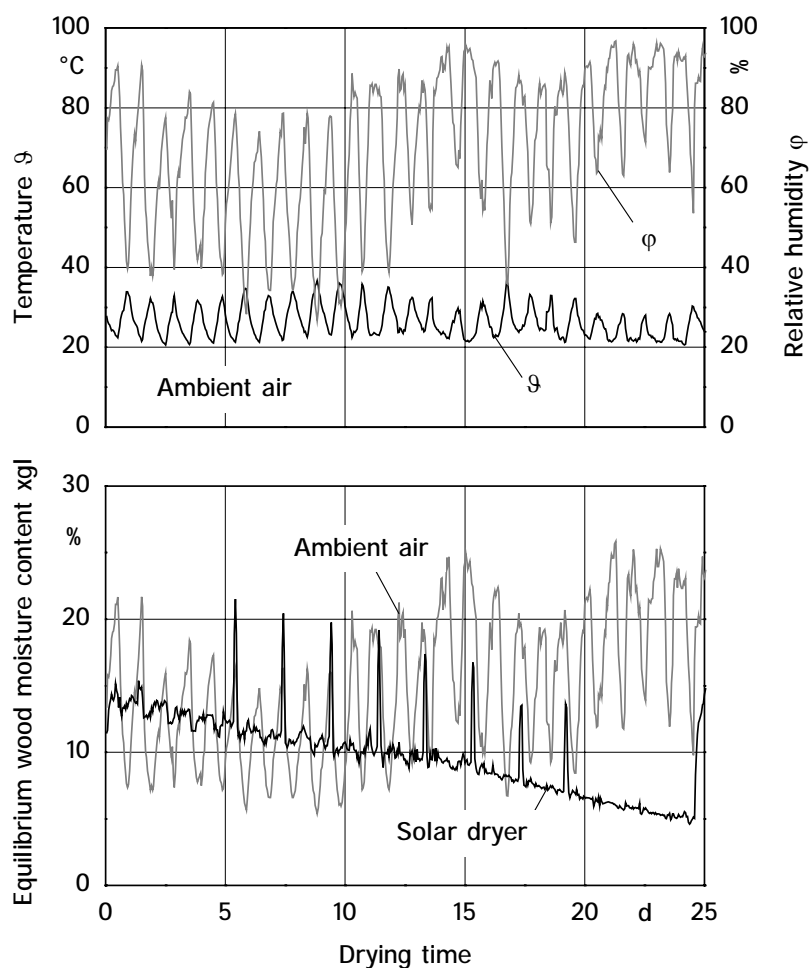


Figure 55: Typical course of the temperature and relative humidity of the ambient air at the test location and a comparison between the equilibrium wood moisture content at ambient air and in the solar dryer.

A comparison of the equilibrium wood moisture content between ambient air and the solar dryer demonstrates that the drying conditions were more severe at ambient air during day-

time, causing quality losses and less severe during night-time, reducing the drying stress compared to the conditions in the solar dryer at the beginning of the drying process. However, the drying conditions at ambient air were less severe at the end of the drying process which led to prolonged drying times.

5.2.2 Timber Quality

A reduction of the timber quality during the drying process is caused either by incorrect drying conditions or by the specific biological wood properties (see chapter 2). To evaluate the quality of the drying process, the inevitable quality losses caused by low quality raw material had to be eliminated. This was done by starting the investigations with mild drying schedules and intensifying respectively accelerating the drying schedules until significant quality losses were noticed. For comparison, the quality of naturally dried timber was analysed. However, no quantitative quality evaluation of conventionally dried timber was available for this eucalypt variety.

5.2.2.1 Wood Moisture Content

Slightly higher values (on average about 1 %) were measured for low final wood moisture contents with the moisture meter than with the oven-dry method. This small difference was taken into account when the final timber quality was classified with the used rigorous evaluation method. Higher deviations were found for higher wood moisture contents due to the known inaccuracy of the electrical instruments above fibre saturation point.

Average Wood Moisture Content

The average wood moisture content of all drying runs of 27 mm thick boards from *Eucalyptus grandis* was only about 0.3 % higher than the desired final wood moisture content of 12 % and 0.8 % higher than the desired moisture content of 8 %, **Figure 56**. For 42 mm thick boards, the final average wood moisture content was about 0.4 % lower than the desired final moisture content of 12 %. This proved that each wood moisture content could be reached with small deviations by using the investigated solar dryer. On the other hand, only wood moisture contents of 17 and 18 % for 27 and 42 mm thick boards could be reached with high drying times (see chapter 5.2.1.6) at ambient air. These results con-

firmed the available information from the literature. Thereby, a average wood moisture content of about 14 % could be reached in 27 mm thick boards of *E. grandis* in 70 days under Brazilian weather conditions with unprotected timber stacks. When the timber stacks were protected or re-humidified to improve the quality, the final wood moisture content that could be reached within this time period was much higher. But nevertheless, pre-drying eucalypt timber to a wood moisture content of about 30 % at ambient air under controlled conditions was recommended by certain authors [19; 50]. However, the low wood moisture contents, needed in the furniture industry, of 12 respectively 8 % cannot be reached at ambient air drying under Brazilian weather conditions.

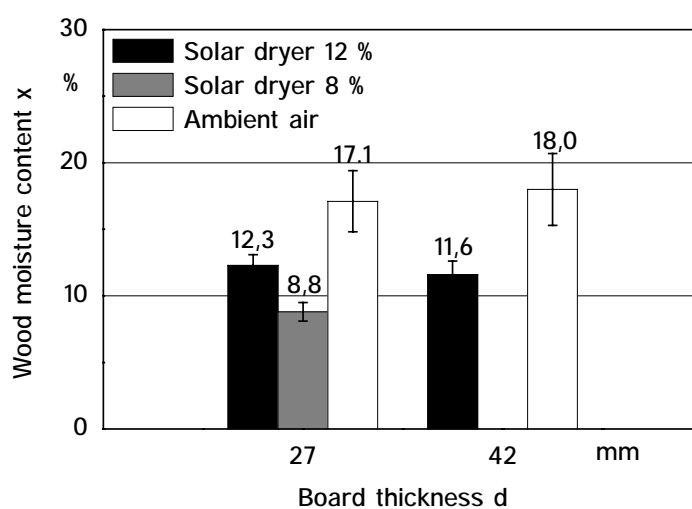


Figure 56: Final average wood moisture content for different board thicknesses from *Eucalyptus grandis* in the solar dryer and at ambient air.

The described average wood moisture content of the more than 80 drying tests in the solar dryer provided information about the continuity of the achieved timber quality. However, more information about the correct function of the solar dryer is provided when the final wood moisture content of the timber load is demonstrated for each drying process. **Figure 57** shows the classified distribution of the final average wood moisture contents of all drying experiments with 27 and 42 mm thick eucalypt boards. The moisture content for 42 mm thick eucalypt boards varied between 10 and 13 % if it was dried to a final moisture content of 12 %. On the other hand, the average moisture contents of ambient air dried timber had a variation between 15.5 and 22.5 % with a drying time of up to four months. If 27 mm thick boards were dried in the solar dryer to a desired final wood moisture content of 8 %, the average wood moisture contents ranged from 7 to 10 %. For a desired final

moisture content of 12 %, the average moisture contents varied between 10.5 and 14 % whereby more than 80 % of the drying experiments could be assigned between 11.5 and 13 %. The final average wood moisture content of 27 mm thick ambient air dried timber varied between 14.5 and 21.5 % after two months.

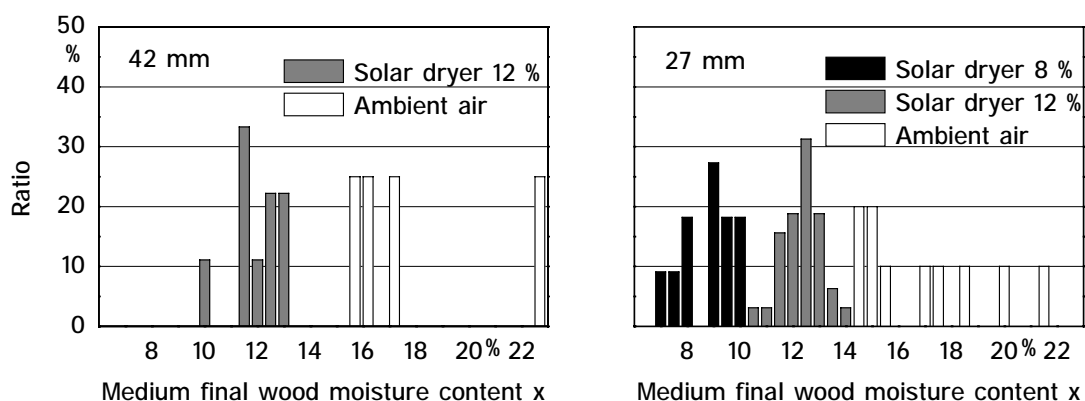


Figure 57: Distribution of the average final wood moisture content in 27 and 42 mm thick eucalypt boards after solar and ambient air drying.

Wood Moisture Distribution

Since the variability of the wood moisture content in a timber dryer results from its design and operation, the wood moisture distribution can serve as an indicator for the dryer quality [206; 250]. **Figure 58** describes the deviation of all single measurements from the final average wood moisture content of the timber dried in the solar dryer and at ambient air. When 42 mm thick eucalypt boards were dried to a final wood moisture content of 12 %, all single measurements varied between -5 and $+8$ % whereby over 90 % varied only ± 3 % from the average moisture content. If the same boards were dried at ambient air, a similar moisture distribution was found. However, the share of measurements that deviated more than 4 % from the average value was higher than that of the solar dried timber. If 27 mm thick boards were dried to a final moisture content of 12 %, the variation of all measurements was between -4 % and $+7$ % whereby over 90 % varied only ± 2 %. Compared to this, the wood moisture contents at ambient air drying varied between -8 % and $+12$ %. Meaning, 78 % of all measurements were located in the range of ± 2 %. If the timber was dried in the solar dryer to 8 %, the moisture distribution was even better. All measurements varied less than ± 4 % from the average value and over 95 % were in the limits of ± 2 %. Altogether, the highest moisture variation was found in the thick boards that were

dried to 12 % while the lowest variation existed in the thin boards that were dried to 8 %. These results support the information available from literature that ambient air dried timber has normally a higher moisture variation than artificially dried timber. For example, very high moisture variations can be found inside a timber stack of 25 mm thick eucalypt boards when it is exposed to extreme weather conditions. This high moisture variation can only be reduced to an acceptable level within more than six months [19; 27; 47]. Besides this, high wood moisture variations can also be found in high temperature dryers [250].

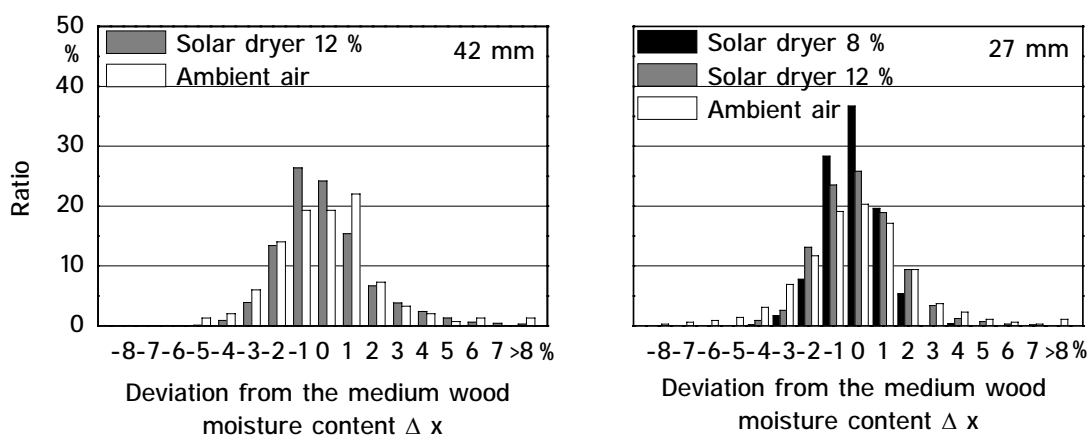


Figure 58: Variation of the final wood moisture content at different board thicknesses and final wood moisture contents at solar and ambient air drying.

Wood Moisture Gradient Along the Timber Load

Not only the average wood moisture content and the moisture distribution of the timber load is of importance, but also the wood moisture gradient along the timber load. This parameter was especially of interest for the investigated solar dryer, due to both a long timber stack and a missing reversion of the drying air. These circumstances caused temporarily a difference of the drying conditions between the air inlet and the air outlet of the timber load (see also chapter 5.2.1.1). **Figure 59** shows that the first stack row had a slightly lower final wood moisture content than the following stack rows. But almost the same final wood moisture content was measured from the fourth row up to the final row at the side of the air flap. The slight differences of the final wood moisture content between the single timber rows were not significant. This seemed surprising but could be explained by the slow drying process causing a slow but uniform drying rate compared to high temperature dryers. Besides this, the difference of the drying air conditions between air inlet, middle and air outlet of the timber stack was only significant at the air inlet at the first few timber

rows. These more severe drying conditions were thereby levelled out by the humidifier and the re-humidifying cycles as shown in Figure 43.

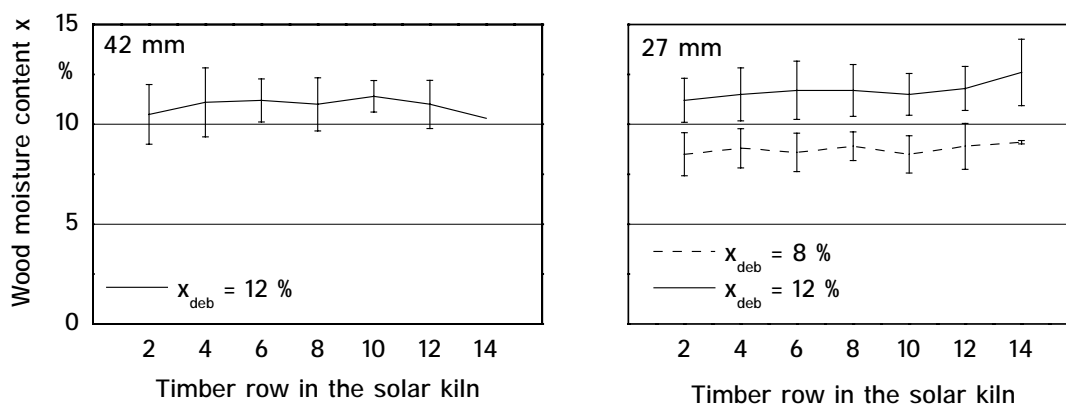


Figure 59: The final wood moisture content of each stack row along the drying chamber for different board thicknesses and different final wood moisture contents.

5.2.2.2 Casehardening

The fork values as an indicator for casehardening were logically higher for 42 mm thick boards than for 27 mm thick boards due to longer prongs and should not be misinterpreted as lower quality, **Figure 60**. However, the fork values from the ambient air dried timber with the same thickness were significantly higher than those from the solar dryer dried timber. This means that the ambient air dried boards that were exposed to more severe drying conditions during the drying process respectively suffered higher drying stress. The same results were observed for the 27 mm thick boards. Thereby, about 80 % of the fork values of the solar dried boards were less than 3 mm for the both final wood moisture contents of 8 and 12 %. In contrast to this only about 40 % of the ambient air dried timber had fork values less than 3 mm. This showed that casehardening could be reduced significantly through slow drying conditions and re-humidifying cycles in the solar dryer.

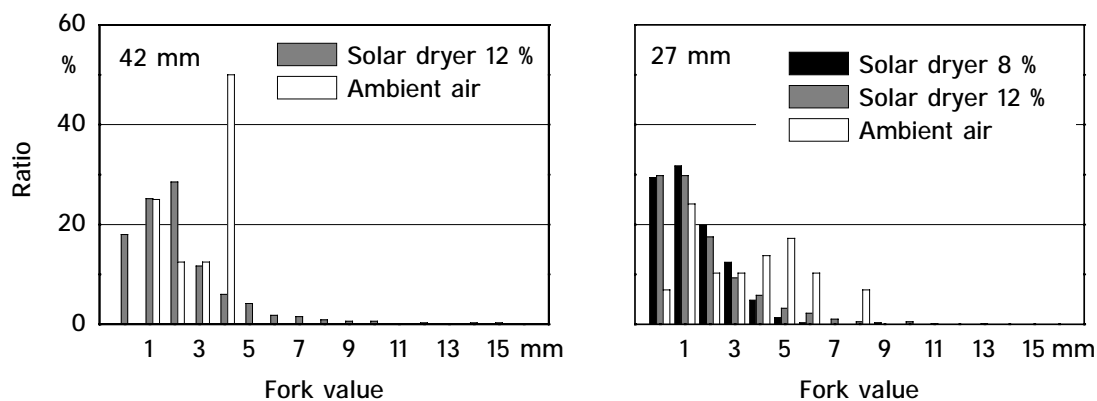


Figure 60: Fork values for different board thicknesses from drying tests in the solar dryer and in ambient air.

5.2.2.3 Warp

Warp was measured in 27 and 42 mm thick eucalypt boards. Accelerating the drying process was identical with more severe drying conditions which resulted in higher deformations. Therefore, warp could be used as an indicator for the suitability of the elaborated drying schedules. The influence of different drying times on warp will be shown exemplarily for the drying of 27 mm thick eucalypt boards. They were dried in 22, 25 and 28 days in the solar dryer to a final wood moisture content of 12 % and in ambient air in 62 days to a moisture content of 18 %.

Crook and Cup

Cup and crook were expressed by mm deformation per m board width and length respectively. Cup did not exist in the green boards while crook was present due to growth stress release resulting in longitudinal deformation, **Figure 61**. As a consequence of the drying process, cup was build-up and crook increased significantly at all drying experiments. The lowest average for cup was found in ambient air dried boards due to a higher final wood moisture content compared to the solar dried samples. However, neither cup nor crook was significantly influenced by different drying times in the solar dryer and at ambient air. This showed that these types of warp depended rather on natural shrinkage and therefore on the final wood moisture content than on the type of drying conditions within the investigated limits (see also chapter 2.1.4). Nevertheless, the high variation of the analysed parameters

between the single boards complicated the detection of slight differences without increasing the sample size enormously.

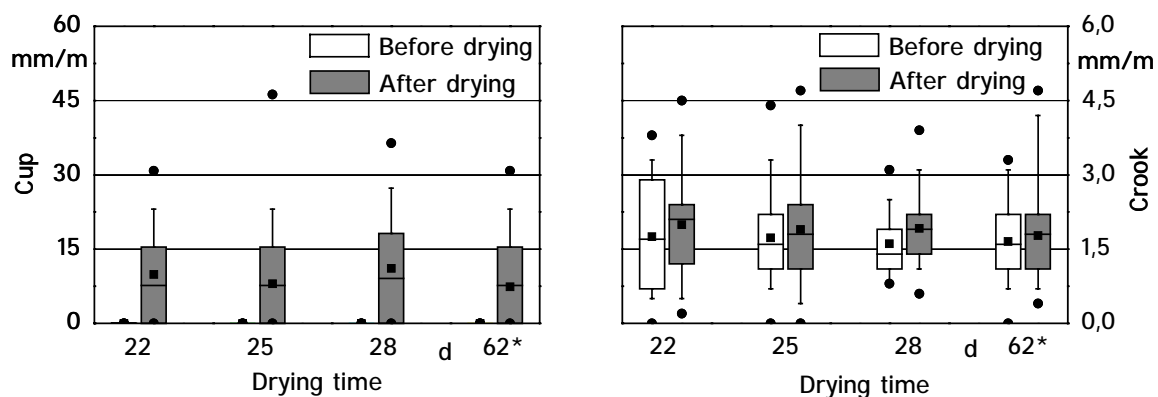


Figure 61: Influence of the drying time on cup and crook during the drying process of 27 mm thick boards from *E.grandis* to a final wood moisture content of 12 % in the solar dryer and in ambient air (*).

Twist

Twist was measured as mm deformation per m² board area since it is influenced by both the width and length of a board. No significant difference was found for twist between the investigated boards before the drying process, **Figure 62**.

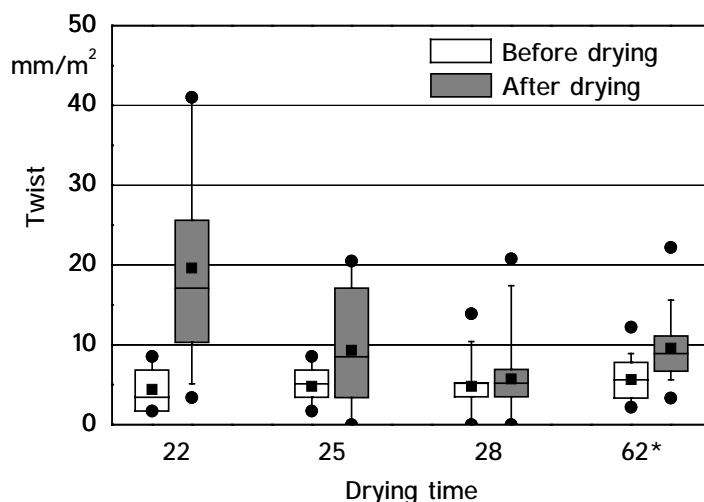


Figure 62: Influence of the drying time on twist during the drying process of 27 mm thick boards from *E.grandis* to a final wood moisture content of 12 % in the solar dryer and in ambient air (*).

Drying the 27 mm thick eucalypt boards in 22 and 25 days in the solar dryer and in 62 days at ambient air increased twist significantly. On the other side, a drying process of 28 days

in the solar dryer did not cause a significant rise of twist. This proved that the development of this type of warp could be limited to an acceptable level by the application of a slow and controlled drying process. Nevertheless, twist was found to be the most problematic deformation as consequence of the drying process due to an extreme spiral growth of the processed young eucalypt trees (see also chapter 2.2.3 and 5.1.2). Since twist was found as the limiting factor for an acceleration of the drying process, a reduction of the drying time will only be possible in future by using raw material with less spiral growth.

Bow

Bow is not a very problematic deformation in timber since it can be adjusted easily during the following manufacturing process (see also chapter 2.2.2). It is also generally known that bow is much more influenced by the stacking method than by the drying conditions. Bow can be reduced significantly either by adding weight to a timber stack or by arranging the single boards in terms of existing deformations [50; 114]. Since already the green eucalypt boards had bow due to high growth stress, the timber was stacked in a way that ensured that the bow of one board was arranged in the opposite direction to the board above or below. By this stacking method, existing bow, in mm deformation per m board length, could be reduced significantly, **Figure 63**. In contrast, unsorted timber showed a significant increase of bow. The drying time in the solar dryer and in ambient air drying had no direct influence on the development of bow.

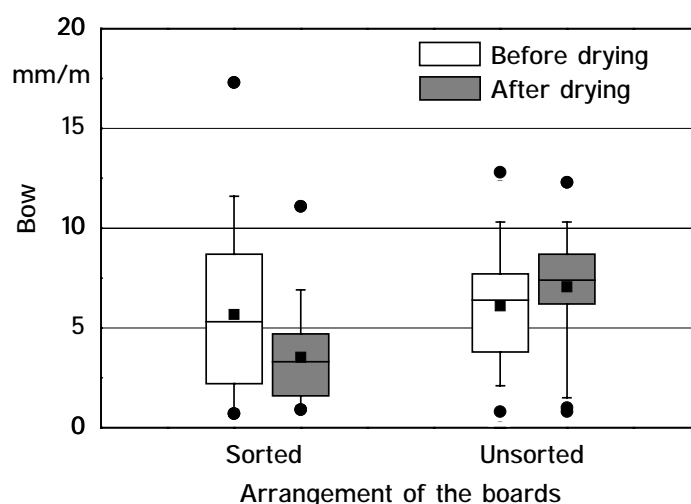


Figure 63: Influence of the stacking method on bow during the drying process of 27 thick boards of *E.grandis* to a final wood moisture content of 12 %.

5.2.2.4 Fissures

End and surface checks were measured before and after the drying process. Internal checks, resulting from very severe drying conditions respectively casehardening, were never found during all analysed drying tests.

End Checks

Since all end checks of the green boards were already cut off in the sawmill, the measured end checks resulted from the growth stress release during the time of evaluation. The checks in the base of the tree were significantly higher than in the top log, **Figure 64**. On the other side, neither the drying time in the solar dryer nor ambient air drying had a significant influence on the size of the end checks.

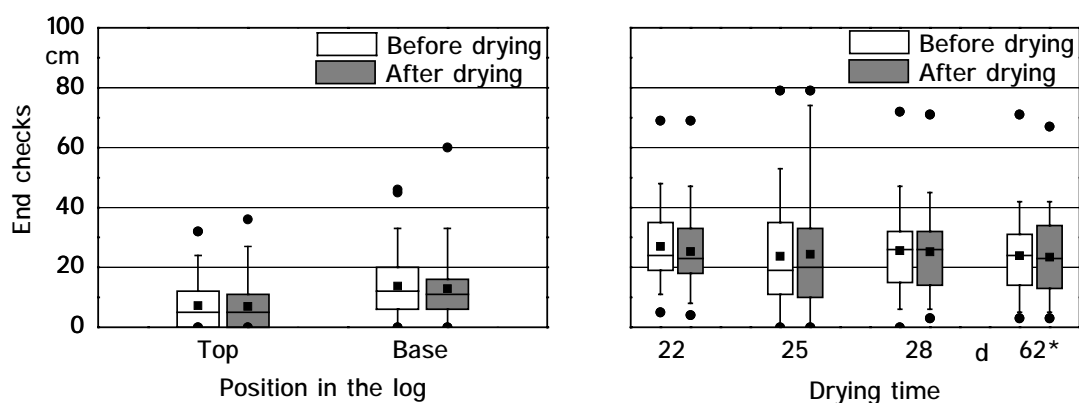


Figure 64: Size of the end checks in dependence on the position in the log and the influence of the drying time on the development of end checks during the drying process of 27 mm thick *E.grandis* boards to a final wood moisture content of 12 % in the solar dryer and in ambient air (*).

Surface Checks

Surface checking in eucalypts is normally much more serious in heartwood than in sapwood [102]. This was confirmed during this research work since surface checks were exclusively found in boards that were cut from the heartwood and contained a part of the pith. Therefore, only boards close to the pith were evaluated for surface checks. Most of the analysed boards had no surface checks. The impression that the share of the boards with surface checks before the drying process was higher for ambient air drying than for

solar drying could not be confirmed by statistical methods, **Figure 65**. While the length and the depth of the surface checks were reduced slightly by shrinkage during the drying process in the solar dryer, ambient air drying caused a significant increase of the check length and depth. Besides this, an extreme development of hair checks at the board surface was observed during ambient air drying if the boards were exposed directly to sun and rain. However, it was not possible to quantify these kind of checks with the available instruments during this research work.

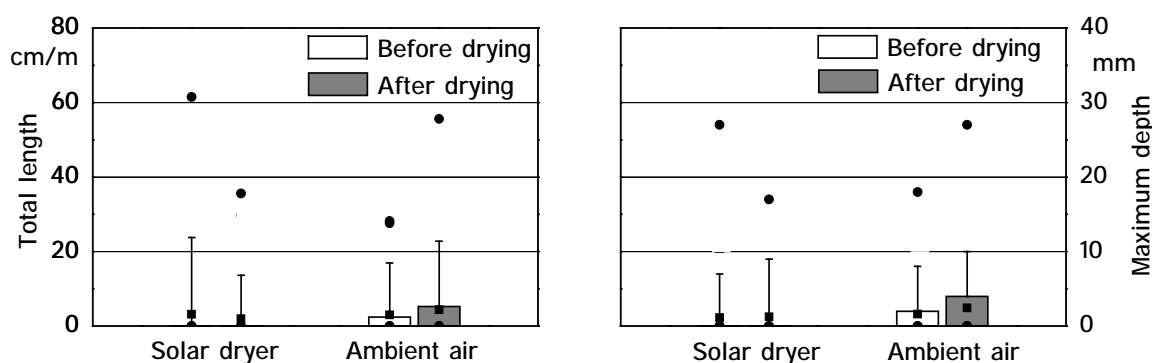


Figure 65: Development of the surface checks during the drying of 27 mm thick boards of *E. grandis* to a final wood moisture content of 12 % in the solar dryer and in ambient air.

5.2.2.5 Cell Collapse

Cell collapse was never observed during the drying tests in the solar dryer. Similar deformations were found at the board surface that resulted from differential shrinkage due to extreme wood density variations between heartwood and sapwood. This was proved by the fact that collapse develops at high temperatures above fibre saturation point while these deformations emerged at low wood moisture contents below fibre saturation point. Cell collapse could only be found at ambient air drying if the eucalypt boards were exposed to extreme insolation. However, a reliable differentiation in collapse shrinkage and shrinkage caused by density variations was macroscopically not possible.

5.2.2.6 Discolorations

If the eucalypt timber was loaded directly in the solar dryer after sawing, no noticeable discolorations Besides a slight darkening were observed as consequence of the drying process. Discolorations from bright red to brown and silver greyish at the board surface to

a depth of about 1 mm were primarily found at ambient air dried sawnwood through the influence of rain and sun. However, this had no important influence on further manufacturing.

5.2.2.7 Quality Classification

The quality of the drying process was evaluated with the classification system described in chapter 5.1.4.8. The results show that the highest possible drying quality could be reached during almost all drying tests. However, the total timber quality was negatively influenced by the low quality of the available raw material, which caused inevitable defects through e.g. shrinkage and growth stress.

Average Wood Moisture Content

With regard to the average wood moisture content, about 90 % of the 27 and 42 mm thick eucalypt boards that were dried to a final wood moisture content of 12 % was of extra quality, **Figure 66**.

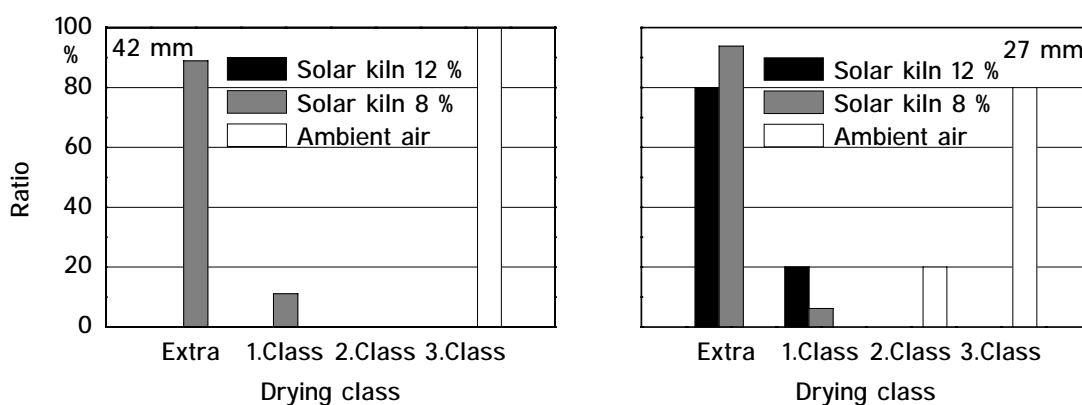


Figure 66: Quality classification for the average wood moisture content for different board thicknesses and final wood moisture contents from drying tests in the solar dryer and in ambient air.

The residual 10 % of this timber was classified as first class quality. 80 % of the 27 mm thick eucalypt boards that were dried to a final moisture content of 8 % were of extra quality and 20 % of first class quality. The quality reduction was rather due to insufficiently dried timber than to overdried timber. It has to be mentioned that only few drying cycles were conducted for this moisture content resulting in little drying experience. Altogether, it

was shown that each desired final wood moisture content could be reached sufficiently with the investigated solar dryer. The average wood moisture content found in ambient air dried timber was normally too high which is why almost all timber was evaluated as 3.class. This means that ambient air dried timber did not meet the requirements of the furniture industry.

Wood Moisture Distribution

Observing the wood moisture distribution within a timber load, about 80 % of the drying experiments in the solar dryer with 27 and 42 mm thick eucalypt boards that were dried to a final wood moisture content of 12 % were of extra class and about 20 % of first class, **Figure 67**. Whenever the 27 mm thick boards were dried to 8 %, the wood moisture distribution was completely classified as extra class. This was due to the prolonged drying time which allowed a better moisture equilibration in the timber load.

The timber that was dried in ambient air showed a good wood moisture distribution for 42 mm thick boards with almost 80 % extra quality and about 20 % of 2.class timber. This was mainly due to the long drying time of over four months. The classification of the 27 mm thick boards dried in ambient air was worse whereby only 40 % were of extra class, 20 % of 1.class and about 40 % of 2. class. These results confirmed the unpredictable influence of the weather in ambient air drying. However, no drying test was classified as 3.class neither for the solar dryer nor for ambient air drying.

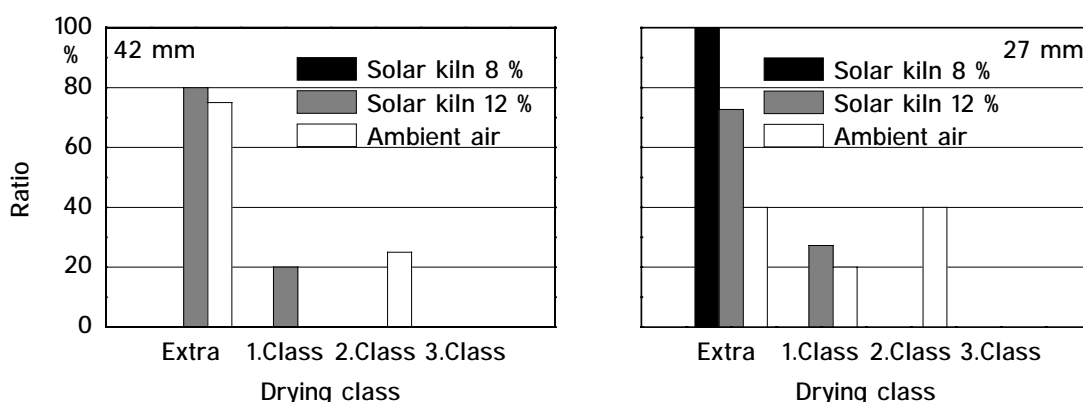


Figure 67: Quality classification for the wood moisture distribution for different board thicknesses and final wood moisture contents from drying tests in the solar dryer and in ambient air.

Casehardening

With regard to casehardening, the 27 and 42 mm thick eucalypt boards that were dried in the solar dryer to final wood moisture contents of 12 and 8 % were almost all classified as extra class, **Figure 68**. Even controlled ambient air dried timber of 42 mm thickness was all of extra class. However, about 80 % of the 27 mm thick ambient air dried timber was classified as extra class and about 20 % as 1.class. This showed that severe drying conditions existed neither in the solar dryer nor at controlled ambient air drying.

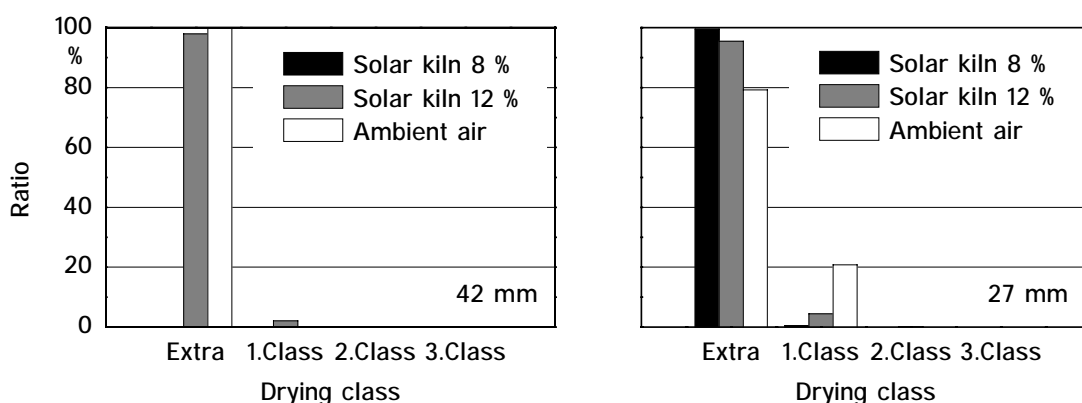


Figure 68: Quality classification for casehardening for different board thicknesses and final wood moisture contents from drying tests in the solar dryer and in ambient air.

5.2.3 Energy Balance

Figure 69 shows the energy balance for the drying of 27 mm thick eucalypt boards in the investigated solar dryer. About 80 % of the required thermal energy was supplied by biomass from the supplementary heating system and about 20 % by solar radiation. The total thermal energy demand for the drying of 1 m³ of eucalypt timber was about 1.39 GJ. This corresponded to a thermal energy demand for the evaporation of one kg wood water of about 4.6 MJ which is relatively low compared to the cited energy demand of 6.2 MJ for hardwood [84; 146]. The biggest part or almost 50 % of this energy was used for the drying process respectively the evaporation of the wood moisture. About 20 % of the total energy was lost by the air exchange at the air flap and also 20 % through the dryer cover by convection and heat radiation. About 14 % or 218 MJ of thermal energy were required to evaporate the water supplied by the humidifying system. The electrical energy demand

for the drying of 1 m³ of eucalypt timber was about 68 MJ whereby 21 MJ was needed for the forced circulation of the drying air.

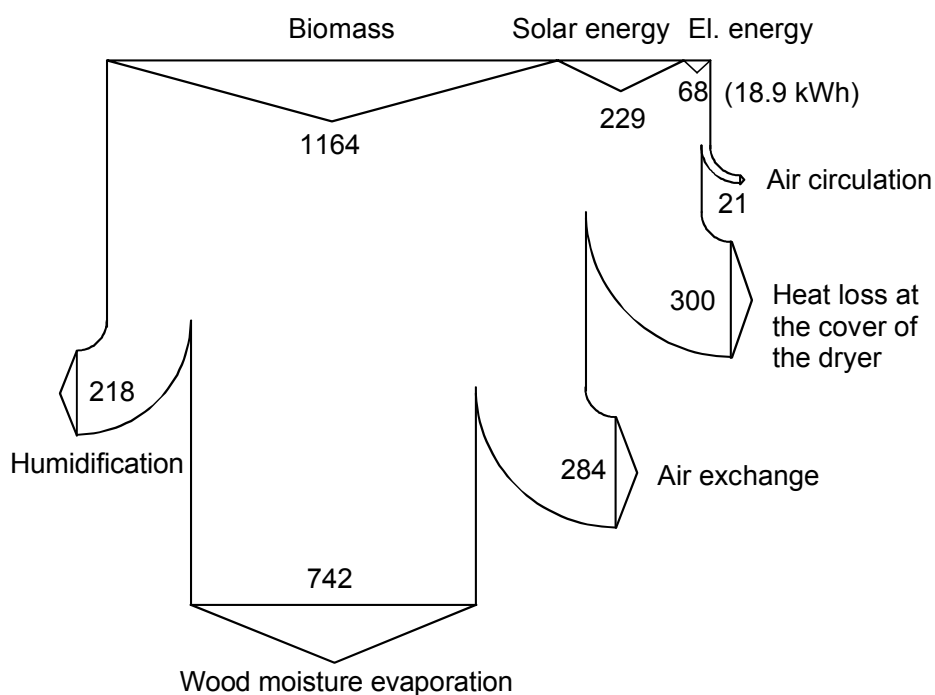


Figure 69: Energy balance for the drying of 27 mm thick boards from *Eucalyptus grandis* in the analysed solar dryer from 60 to 12 % wood moisture content, in MJ per m³ of dried timber.

The energy balance of the drying process changed slightly when 42 mm thick eucalypt boards were dried, **Figure 70**. The proportion of the added thermal energy decreased to less than 70 % while the part of solar energy was higher than 30 %. This was due to the prolonged drying times at a lower temperature level. The total thermal energy demand was significantly higher with about 2.0 GJ. This corresponds to a thermal energy demand for the evaporation of one kg of wood water of about 6.8 MJ. This was slightly higher than the cited energy demand of 6.2 MJ for hardwood [84; 146]. The energy used for the vaporization of the wood moisture decreased to a share of about 35 % while the part for the evaporation of the sprayed water by the humidifier increased to 25 %. This was due to the longer drying times with a higher number of re-humidifying cycles. The thermal energy losses by convection and heat radiation summarised to about 22 % and the losses due to air exchange totalised to 15 %. The electrical energy demand for the drying of 1 m³ of eucalypt timber was about 151 MJ, whereby 49 MJ were used for forced ventilation.

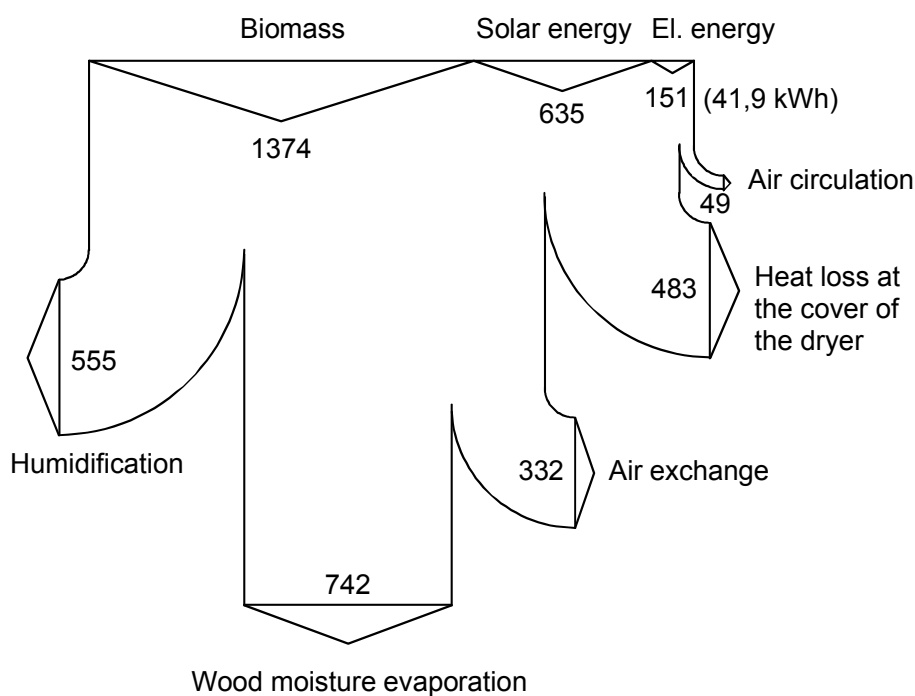


Figure 70: Energy balance for the drying of 42 mm thick boards of *Eucalyptus grandis* in the solar dryer from 60 to 12 % wood moisture content, in MJ per m³ of dried timber.

The energy demand for the drying of 27 mm thick eucalypt boards in the solar dryer was compared with that in a high temperature dryer. While information about the thermal and electrical energy demand for the drying of eucalypt timber could not be found in literature, reliable data was received from two Brazilian sawmills that use high temperature dryers for the drying of the investigated eucalypt species [251; 252]. Besides this, extensive information was available for the drying of beech which is quite similar to the analysed eucalypts in terms of drying demands due to comparable biological wood characteristics [32; 253-255].

Both the thermal and the electrical energy demand for the drying of 1 m³ eucalypt timber in the solar dryer was significantly lower than in a high temperature dryer, **Table 9**. The thermal energy demand in the solar dryer was only about 40 % of that required in the high temperature dryer. This was due to the utilisation of solar energy, the application of a low temperature schedule, the reduction of the heat losses at the dryer cover by adjusting the drying air temperature to the ambient air temperature and by an optimised air exchange. The low thermal energy demand in the solar dryer allowed the use of a supplemental biomass furnace with a 70 % smaller heating output than that required for a high temperature dryer. The electrical energy demand and therefore the installed electrical power was re-

duced by almost 80 %. This was mainly due to the application of highly efficient axial flow fans that were constructed for low air flow velocities at low pressure drops. Besides this, missing air flow reversion allowed a higher fan efficiency.

However, the significantly lower specific energy demand in the solar dryer was also due to its specific construction characteristics. Especially the 14 m long timber stack allowed a better utilisation of the electrical and thermal energy compared to high temperature dryers with usually much shorter stacks of 4 to 8 m.

Table 9: Comparison of the electrical and thermal energy demand for the drying of 27 mm thick *E.grandis* boards in the solar-assisted and a high temperature dryer from 60 to 12 % wood moisture content.

	High temperature*	Solar**
Installed electrical output, W/m ³	180.2	30.8
Installed thermal output, kW/m ³	1.85	0.56
Electric energy demand, kWh/m ³	98	20
Thermal energy demand, GJ/m ³	2.95	1.16

* [32; 251; 251-255]; ** CAF Sta. Bárbara Ltda, Brazil 2000.

5.3 Evaluation of the Results

Up to 250 m³ of sensitive eucalypt timber could be dried simultaneously in one chamber of the solar dryer. Drying schedules for 18, 27, 32 and 42 mm thick boards from *Eucalyptus grandis* with daily temperature oscillations and re-humidifying intervals were elaborated. Green boards were loaded immediately after sawing into the solar dryer to prevent drying defects and were dried to the desired low wood moisture contents of 8 and 12 %. The moisture distribution of the timber load, casehardening and discolorations were extremely low after the drying process. Cell collapse was never found. However, drying defects like deformations and fissures existed already before drying, respectively developed inevitably during drying due to the low quality of the processed young eucalypt trees. A quality evaluation of conventionally dried timber was not available for the investigated eucalypt variety. However, observations in other sawmills did not show a better quality of eucalypt

sawnwood that was dried in high temperature dryers in spite of better raw material. Timber that was dried under controlled conditions in ambient air had a significantly lower final wood quality whereby the required low wood moisture contents for the furniture industry could not be reached. Besides this, the drying times were much longer in ambient air drying than in solar drying. Compared to high temperature dryers, the thermal and electrical energy demand for the drying of sensitive eucalypt hardwood could be reduced significantly in the solar dryer.

Altogether, it was shown that the newly developed low temperature drying schedules for the solar-assisted timber dryer were suitable to dry sensitive eucalypt hardwood at high timber quality and significantly reduced electrical and thermal energy demand compared to conventional high temperature dryers. The microprocessor control of the solar dryer guaranteed a reliable application of the elaborated drying programs. Further modifications respectively adaptations of the pre-programmed drying schedules to specific requirements of other wood species and sawnwood dimensions will be easy to realise.

6 ECONOMIC EVALUATION OF THE SOLAR DRYER

Until now, the Brazilian furniture industry processes mainly timber from natural tropical rain forests. Increasing distance between the forests and the manufacturing industries and legal restrictions for deforestation caused a significant rise in the timber price. On the other side, extensive plantations of fast growing eucalypt species exist in Brazil for the production of charcoal and cellulose. Provided that an adapted drying process is available for these sensitive wood species, eucalypt sawnwood presents an economic alternative to the tropical woods. Time intensive ambient air drying does not allow an adequate control of the drying conditions and the required low wood moisture contents of about 10 to 14 % cannot be reached. Therefore, eucalypt timber for the furniture industry is almost exclusively dried in energy intensive high temperature dryers. Since national dryers are reported to be of low quality in terms of mechanical reliability and control of the drying air conditions, most Brazilian sawmills and wood companies are using imported high temperature dryers from Europe and North America. This means that the economic feasibility of the solar-assisted timber dryer had to be compared with that of a sophisticated high temperature dryer. Thereby, the investment costs for both types of dryer, the drying costs per m³ eucalypt timber under subtropical climate conditions, the influence of important expense factors on the drying costs and the resulting payback period for the dryers were analysed.

6.1 Material and Methods

6.1.1 Investment Costs

The installation of two solar drying plants with 13 drying chambers and a total annual drying capacity of 35 000 m³ of timber in Brazil allowed a reliable calculation of the required investment costs for this type of timber dryer. On the other hand, the average investment costs for a high temperature dryer were derived from the literature and from quotations of German manufacturers [32; 253-257]. Country specific cost factors like construction material and manpower were adapted to the Brazilian standards. Same costs for both types of dryer could be used for the control chamber, the local water and electricity supply, the transport of the dryer from the German manufacturer to the Brazilian purchaser and the installation. Besides this, same percentages for taxes and fees like import tax, industry tax, value added tax, insurance for the container and port fee were added to the respective pur-

chase price of the dryer [258]. Since only steam boilers but not suitable heaters for hot water were available on the Brazilian market, the investment costs for the supplementary heating system for both dryer types were derived from average purchase prices for common steam boilers.

6.1.2 Drying Costs

To compare the drying costs in the solar dryer to that in a high temperature dryer, a cost analysis was done for the drying of 27 mm thick eucalypt boards from 60 to 12 % wood moisture content. Drying more than 20 000 m³ eucalypt sawnwood during this research work supplied extensive data for the calculation of the drying costs in the solar dryer. Average drying costs for hardwood in a high temperature dryer were derived from 1 200 drying cycles for beech sawnwood – a wood species that is quite comparable to eucalypt in terms of wood density and drying sensitivity [32; 129; 208; 254; 255]. Additional information about the costs for conventional drying of eucalypt hardwood was provided by two Brazilian sawmills which dry about 25 000 m³ of eucalypt timber per year in high temperature dryers [251; 252].

6.1.3 Methods of Calculation

The “cost comparison method” allows the comparison of two or more alternatives of investment in terms of their economic feasibility. The lower the costs for a time period or a processed unit, the higher is the profitability of this method [259; 260]. Therefore, the drying costs per m³ of eucalypt timber in the solar-assisted dryer were compared to those in a high temperature dryer. The drying costs were separated in variable and fixed costs. Variable costs resulted mainly from the thermal and electrical energy demand while fixed costs were caused primarily by the costs of investments. The fixed drying costs were calculated from the annuity AN of the total investment costs for the timber dryers A_0 to consider the compounded interest. A depreciation period n of 15 years for a high temperature dryer is common in the timber industry [129; 208; 254]. The same time period was assumed for the solar-assisted dryer while its air bubble foil cover was depreciated in 10 years due to a lower life span. Annual cost of repairs of 5 % of the total investments seemed to be realistic for both dryers. Since the salvage value S is sufficient to cover the expenses for demo-

lition, this value was neglected. Inflation was not especially considered due to a low Brazilian inflation rate of 1.7 % in 1998 [261]. The annuity of the total investment costs was then:

$$AN = (A_0 - S \cdot q^{-n}) \cdot \frac{q^n \cdot (q - 1)}{q^n - 1} \quad (60),$$

whereby the interest coefficient q was derived from the interest rate i by:

$$q = 1 + \frac{i}{100} \quad (61).$$

The payback period respectively the time of amortisation TA was also analysed as parameter of an economic comparison. It was calculated from the annual return flow RF , the investment costs A_0 and the interest coefficient q by [262; 263]:

$$TA = \frac{\ln\left(\frac{RF}{A_0}\right) - \ln\left(1 + \frac{RF}{A_0} - q\right)}{\ln q} \quad (62).$$

6.2 Results

6.2.1 Investment Costs

The total investment costs for a solar-assisted timber dryer with a timber capacity of 220 m³ were 95 040.- € and therefore about 35 % lower than that for a high temperature dryer with a capacity of 130 m³, **Table 10**. This was primarily due to a 40 % lower purchase price of the solar dryer which reduced also the costs for taxes and fees. Since one 40' container is sufficient for the transport of both dryers, the transport costs from Germany to Brazil were the same. Also the installation costs for the control chamber and the water and electricity supply were similar. Construction costs were higher for the solar dryer due to the required sidewall and a bigger base plate. The expenses for installation of the high temperature dryer were superior due to a more complex structure and design. An extra charge of 30 % had to be added to the purchase price of the heater for the high temperature dryer

dryer due to the required higher thermal output of about 70 %. A more detailed list of the investment costs is given in **Table A 3** in the appendix.

Table 10: Investment costs for the solar-assisted and a high temperature timber dryer in € (exchange rate from January 1999, 1.00 € = 1.17 US\$ = 1.69 R\$) [254; 257; 264].

Cost group	Solar dryer	High temp. dryer
Purchase price	43 970.-	75 670.-
Taxes	21 250.-	35 970.-
Fees and insurance	2 310.-	2 470.-
Transport (1 container)	3 290.-	3 290.-
Construction work (base and walls)	1 240.-	180.-
Control chamber	580.-	580.-
Water and electricity supply	490.-	450.-
Manpower	1 640.-	2 260.-
Heater (proportional)	11 810.-	15 350.-
Surcharge for inaccuracy of 10 %	8 640.-	13 630.-
Total	95 040.-	150 170.-

6.2.2 Drying Costs

6.2.2.1 Fixed Costs

Table 11 shows the fixed drying costs for one m³ of 27 mm thick eucalypt timber. About 3.50 € respectively 44 % of the total drying costs were required for the investments of the solar dryer. These expenses were more than twice as high for the high temperature dryer with 7.70 € respectively 42 % of the total drying costs. Approximately 15 % of the total drying costs were needed for repairs for both dryers. This corresponded to 1.20 €/m³ for the solar dryer and 2.60 €/m³ for the high temperature dryer. Labour costs were assigned to the fixed drying costs since more time was needed for supervision of the dryer than for timber loading and unloading due to long drying times. This means that the labour costs

were relatively independent from the annual production. However, costs for labour had a relatively low share of about 5 % of the total drying costs due to the low Brazilian wages. Higher interest costs for the timber due to longer drying times and additional costs for the plastic cover were found for the solar dryer.

Table 11: Fixed drying costs for 27 mm thick timber of *E.grandis* for the solar-assisted dryer and the high temperature dryer in €/m³ (exchange rate from January 1999, 1.00 € = 1.17 US\$ = 1.69 R\$) [254].

Cost groups	Solar dryer		High temperature dryer	
	€/m ³	%	€/m ³	%
Investments	3.50	44.3	7.70	42.3
Air bubble foil	0.10	1.3	0	0
Maintenance and repairs	1.20	15.2	2.60	14.3
Labour	0.50	6.3	0.70	3.8
Interest for timber	1.00	12.7	0.90	4.9
Total	6.30	79.8	11.90	65.3

6.2.2.2 Variable Costs

The share of the variable costs in the total drying costs is given in **Table 12**. The costs for thermal energy were relatively low for both drying systems since the required wood chips were produced as a by-product in the sawmill. Only about 5 % of the total drying costs respectively 0.30 € for the solar dryer and 0.90 € for the high temperature dryer were required for additional heating. However, whenever cost-efficient biomass is not available, other fuels like oil or electricity would increase the thermal energy costs significantly which would privilege the solar dryer. The costs for electrical energy were noticeably higher in the high temperature dryer than in the solar dryer due to a higher velocity of the drying air and a corresponding high pressure drop. About 1.20 € respectively 15 % of the total drying costs were needed for electrical energy in the solar dryer. However, 5.40 € respectively almost 30 % of the total drying costs were required by the electrical energy demand in the high temperature dryer. The costs for the water needed for the daily tem-

perature oscillations and for the re-humidifying cycles were only about 0.10 € for the solar dryer. In contrast, no remarkable water consumption existed in the high temperature dryer.

Table 12: Variable drying costs for 27 mm thick timber of *E. grandis* in the solar-assisted dryer and a high temperature dryer for sawnwood in €/m³ (exchange rate from January 1999, 1.00 € = 1.17 US\$ = 1.69 R\$) [254].

Cost group	Solar dryer		High temperature dryer	
	€/m ³	%	€/m ³	%
Wood chips	0.30	3.8	0.90	4.9
Electricity*	1.20	15.1	5.40	29.8
Water**	0.10	1.3	0	0
Total	1.60	20.2	6.30	34.7

* Electricity prices in Brazil [265]; ** Water prices in Brazil [266].

6.2.3 General Cost Comparison

A general comparison between the solar dryer and a high temperature dryer indicates that the timber loading capacity of the solar dryer was about 40 % higher than that in a high temperature dryer, **Table 13**.

Table 13: General comparison for the drying of 27 mm thick boards of *Eucalyptus grandis* from 60 to 12 % wood moisture content in the solar-assisted dryer and in a high temperature dryer.

Cost factor	Solar dryer	High temperature dryer
Chamber capacity, m ³	220	130
Drying time, d	27	22
Annual production, m ³	2 970	2 140
Investment costs*, €/m ³	430.-	1 160.-
Total drying costs**, €/m³	7.90	18.20

* Dryer with heater, foundation and installation; ** Costs for capital, energy and depreciation.

The drying time for the sensitive sawnwood of *E.grandis* in the solar dryer was only about 20 % longer than in the high temperature dryer. These two parameters resulted in a 30 % higher annual timber production for the solar dryer. Due to the low purchase price of the solar dryer, the investment costs per m³ timber capacity were only about 40 % of that of the high temperature dryer. Altogether, the low investment costs, the low energy demand and the high drying capacity reduced the total drying costs for sensitive hardwood in the solar dryer by more than 50 % compared to those in a high temperature dryer. Thereby, total drying costs of about 8.- € were calculated for the solar dryer and about 18.- € for the high temperature dryer.

6.2.4 Sensitivity Analysis for Important Cost Factors

A sensitivity analysis was made for important cost factors like the investment costs, the interest rate and the energy costs with regard to the specific economical situation in Brazil.

6.2.4.1 Investment Costs

The investment costs for the investigated timber dryers are primarily influenced by their purchase price. Since both dryers would have to be imported, the purchase price depended significantly on the exchange rate of the Brazilian currency. High value fluctuations of the Brazilian Real between 1.40 and 3.90 R\$ for one European € were described in the last few years. The exchange rate for the preceded cost calculation was 1.70 R\$ per €. A rate of 3.00 R\$ per € would cause 80 % higher investment costs for both dryers whereby the influence on the total drying costs would be significantly higher for the high temperature dryer than for the solar dryer due to the higher purchase price, **Figure 71**.

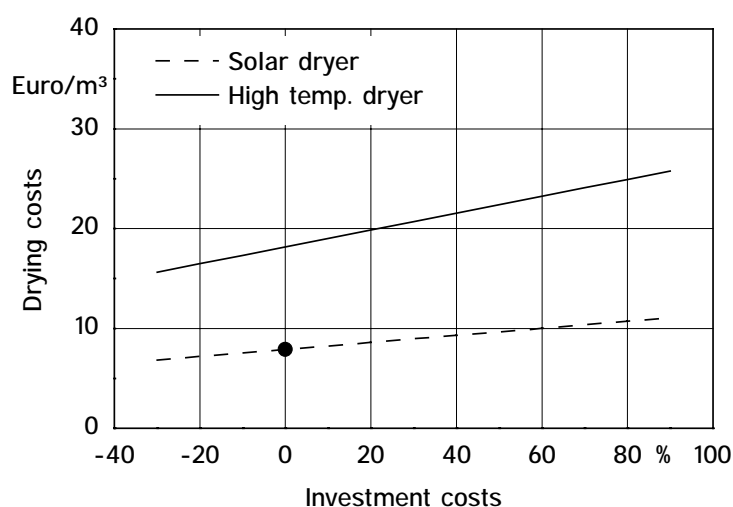


Figure 71: Influence of the investment costs on the specific drying costs in the solar and high temperature dryer.

6.2.4.2 Interest Rate

Due to the instable Brazilian currency, the Brazilian central bank has changed the prime rate various times reaching maximum rates of up to 48 %. This has a direct influence on the interest rates for bank credits. The prime rate during this research was 19 % on average

which caused an interest rate for capital of up to 30 %. Special credits of 12 % from the Brazilian bank of development (BNDES) were acquired by the Brazilian partner which is why this rate was used for the preceding calculation [267]. Since this type of credit is not available for all investors, the influence of the interest rate on the total drying cost for investment credits between 10 and 40 % was analysed, **Figure 72**. Notice that a rising interest rate has a higher influence on the absolute drying costs in the case of the high temperature dryer compared to that of the solar dryer.

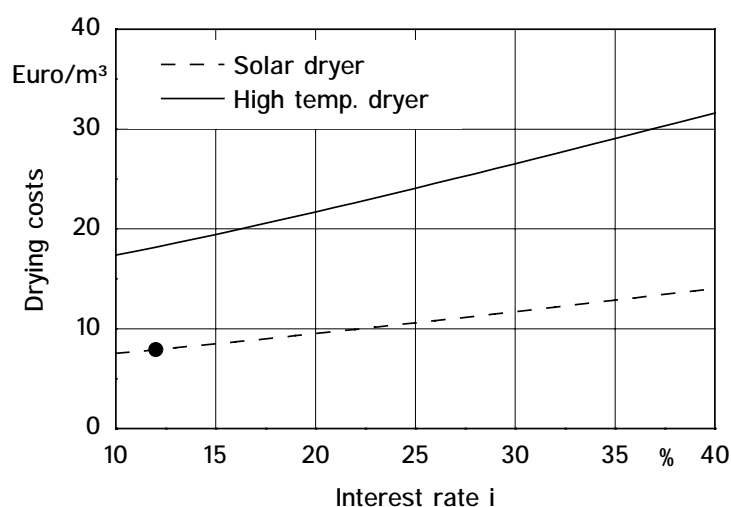


Figure 72: Influence of the interest rate for Brazilian bank credits on the specific drying costs in the solar and in the high temperature dryer.

6.2.4.3 Energy Costs

The electrical energy in Brazil is presently supplied to 95 % by hydroelectric energy sources [268]. Due to low rainfalls in the last years, the Brazilian government decreed a rationalisation of the electricity consumption by 20 % for all industries. This energy crisis showed that Brazil will need a future diversification of the electricity production. Therefore, a further increase of the electricity costs can be expected why its influence on the drying costs was analysed. The electricity price for the preceding calculation of the drying costs was 0.08 € per kWh. An increase of the electricity costs would have a bigger influence on the high temperature dryer than on the solar dryer due to a significantly higher electrical energy consumption, **Figure 73**.

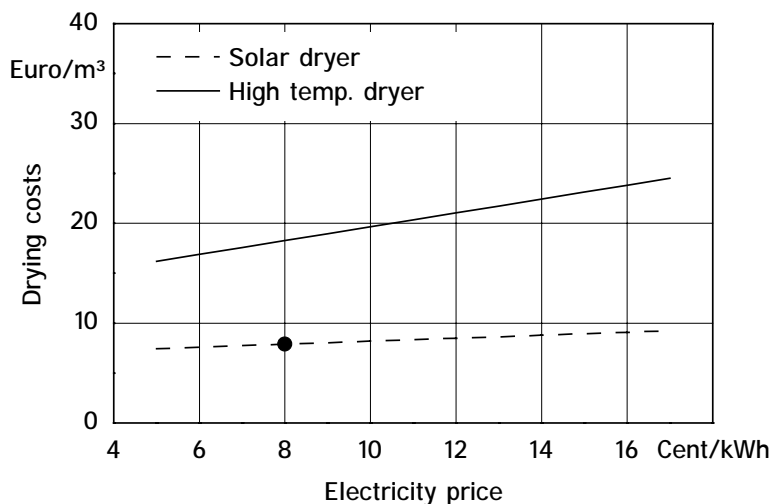


Figure 73: Drying costs per m³ eucalypt timber in the solar and high temperature dryer in dependence on the electricity price.

6.2.5 Payback Period

The payback period for the analysed sawnwood dryers depends on the surcharge to the dried eucalypt timber in comparison to ambient air dried respectively not dried timber,

Figure 74.

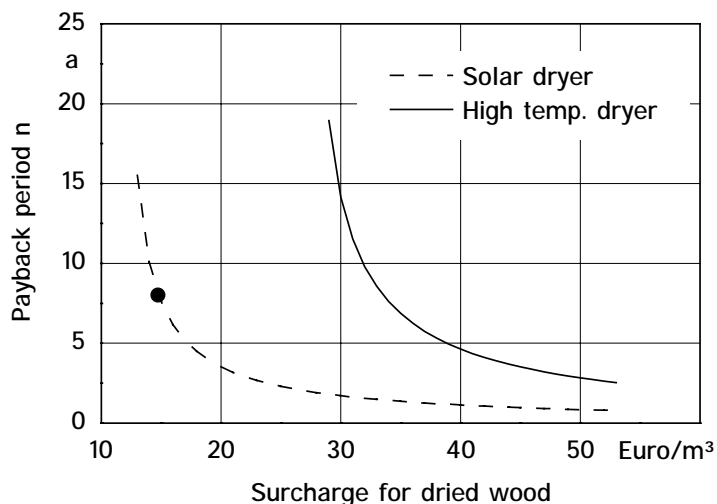


Figure 74: Payback period for the solar and the high temperature dryer depending on the surcharge to the sales price for dry eucalypt sawnwood.

During this research work, the Brazilian sawmill added a surcharge of about 15.- € per m³ to the solar dried timber which resulted in a payback period of about 8 years [269]. Due to the difficult situation of the Brazilian furniture industry, only this relatively low surcharge could be added to the sales price. On the other side, eucalypt timber had to be introduced

as a new product into the furniture market. A payback period of less than 3 years would have required a surcharge of about 22.- €/m³ for the solar dryer and of 49.- €/m³ for the high temperature dryer. However, adding almost 50.- € to the sales price of 110.- € for one m³ of ambient air respectively not dried eucalypt timber seems to be impossible. This showed that an installation of a high temperature dryer for the drying of eucalypt timber would have been inefficient at the economic situation in Brazil during this study.

6.3 Evaluation of the Results

It was shown that the drying costs for timber of *Eucalyptus grandis* in the investigated solar dryer are with 8.- €/m³ about 50 % lower than those in a conventional high temperature dryer with approximately 18.- €/m³. This cost reduction is primarily due to significantly lower expenses for investments and energy. The investment costs were reduced primarily by the low purchase price due to the simple dryer design and by the smaller supplemental heating system. The costs for energy were rather reduced by the lower electrical than by the reduced thermal energy demand. Cost reductions from thermal energy savings through the utilisation of solar energy were relatively low due to the available cheap woodchips. The influence of the investment costs, the interest rate and the electrical energy prices on the total drying costs were significantly higher for the high temperature dryer than for the solar dryer due to a higher purchase price and an increased energy demand. A payback period of less than 3 years could be reached for the solar dryer with a surcharge of about 22.- €/m³ to the sales price for ambient air dried timber while almost 50.- €/m³ were required for the high temperature dryer. At a present sales price of 125.- € for solar dried eucalypt timber, an extra charge of 30.- €/m³ could be decisive for a successful launch of eucalypt timber in the Brazilian furniture market. The economic analysis could prove that timber from sensitive hardwood species could be dried much more economically in a solar dryer than in a high temperature dryer which confirmed similar observations from the literature [34; 36; 155; 182].

7 SUMMARY

The Brazilian furniture industry consumes about 45 million m³ of sawnwood per year which is mainly supplied by deforestation of the tropical rainforest. At the same time, fast growing eucalypt species are produced on almost 3 million ha for the production of wood pulp and charcoal. Meanwhile, several Brazilian companies try to substitute the expensive natural woods by hardwood from eucalypt trees for the production of high quality sawnwood. However, eucalypt wood has to be dried very carefully under controlled conditions to prevent drying defects. Ambient air drying is not suitable since missing control causes high losses and long drying times. Besides this, the low wood moisture content required in the furniture industry cannot be achieved. Artificial drying technologies reduce the drying time, the timber can be dried to a low wood moisture content and the quality can be improved. However, sophisticated high temperature dryers cause high investments. Locally manufactured timber dryers do not allow an adequate control of the drying process. Furthermore, the required slow drying process increases the thermal and electrical energy consumption causing high drying costs.

To overcome the existing problems, Bux developed in the framework of a close cooperation with the Institute of Agricultural Engineering in the Tropics and Subtropics of the University of Hohenheim (ATS), the German company THERMO-SYSTEM Industrie- & Trocknungstechnik Ltd (THS), Alfdorf and the Brazilian forest company CAF Santa Barbara Ltda (CAF) a patented solar-assisted dryer for sawnwood with integrated solar collector and biomass backup heating system [37-39].

Aim of this research work was to analyse the newly developed solar dryer and to develop a suitable drying schedule which allows the economical production of high quality sawnwood for the furniture industry. Therefore, a prototype of the greenhouse type dryer was installed under subtropical climate in Brazil. Due to the low thermal insulation of the solar dryer and missing experience with the extremely sensitive Brazilian varieties of *Eucalyptus grandis*, a new type of drying schedule had to be developed. The new schedule considers not only the general drying demands of eucalypt sawnwood but also the system immanent characteristics of the solar dryer and the ambient air conditions. An oscillation of the drying air temperature according to the ambient air allowed the acceleration of the drying process and reduces the condensation of water on the cover without a negative impact on

the timber quality. In more than 80 drying tests with 16 000 m³ of eucalypt sawnwood the schedule was tested and improved. Based on experiments and information from literature, the course of the temperature, relative humidity and velocity of the drying air and the mode of remoistening was systematically optimised. Thereby, the influence of the changing drying conditions on the drying time, the timber quality, the energy consumption and the drying costs were analysed.

Within the research program, suitable drying schedules for 18, 27, 32 and 42 mm thick eucalypt sawnwood were elaborated. At the beginning of all drying schedules, the temperature of the drying air was limited to a maximum of 40 °C and the relative humidity was kept over 70 %. These conditions were found to avoid cells collapse, known as a main drying defect for most eucalypt species. The maximum temperature was then increased to 55 °C and the relative humidity was decreased to a minimum of 25 % at the end of the drying process. During the entire drying schedule, the drying air temperature in the solar dryer followed the ambient air temperature and was only limited by quality related maximum temperatures. Thereby, the temperature difference between ambient and drying air was increased from 10 K at the beginning to 30 K at the end of the drying process. Higher temperature differences increased the drying rate but also the energy consumption significantly. During remoistening intervals of 1 to 4 hours, the relative humidity of the drying air was increased to over 90 %. The adaptation of the remoistening cycles to the board thickness allowed an acceleration of the drying process without an increase of the drying defects. The velocity of the drying air was kept between 1.5 and 2.5 m/s since no acceleration of the drying process was measured with increasing air velocity. Since international standards for the quality evaluation of sawnwood were not available, an evaluation method and a classification system for the criteria “average moisture content”, “wood moisture distribution” and “casehardening” was adapted and standardised for eucalypt sawnwood from an European pre-norm. Other quality parameters like deformations, fissuring and cell collapse were described quantitatively.

With the final version of the drying schedule, 27 mm thick boards could be dried in the solar dryer from a average wood moisture content of 60 to 12 % d.b. in 27 days. This drying time was about 20 % higher than in a high temperature dryer. However, a drying time of at least 60 days was required to reduce the moisture content to about 20 % d.b. at ambient air drying. The electric energy consumption in the solar dryer was reduced to about

20 kWh per m³ dried eucalypt sawnwood. This is only 20 % of the energy usually consumed in a high temperature dryer. The thermal energy consumption was 1.2 GJ per m³ of dried timber which is about 60 % less than the energy required in conventional high temperature dryers. The low thermal and electrical energy consumption combined with the considerably lower investment costs for the solar-assisted timber resulted in average drying costs of 7.90 Euro per m³. This is only half of the costs caused by drying 27 mm thick eucalypt hardwood in a high temperature dryer. For an economic evaluation, a sensitivity analysis was done for the most important cost parameters. The electrical energy costs, the currency exchange rate and the interest rate for credits were found to be the main influencing parameters under the Brazilian market conditions. However, solar drying was generally more cost efficient than conventional high temperature drying.

In the framework of this research work, it was proven that Brazilian eucalypt timber can be dried economically to a low moisture content of 10 to 12 % at a high quality level by applying the developed drying schedule in the optimised patented solar-assisted dryer. Meanwhile, approximately 35 000 m³ of eucalypt hardwood is dried annually in two solar-assisted drying plants contributing significantly to the protection of the natural rain forests.

8 ZUSAMMENFASSUNG

Die brasilianische Holz- und Möbelindustrie verarbeitet gegenwärtig rund 45 Millionen m³ Schnittholz pro Jahr, das in erster Linie durch die Abholzung von tropischem Regenwald gewonnen wird. Gleichzeitig stehen fast 3 Millionen ha schnellwachsender Eukalyptusplantagen für die Produktion von Zellulose und Holzkohle zur Verfügung. Mittlerweile versuchen mehrere brasilianische Holzfirmen das kostenintensive Schnittholz aus Naturwäldern durch günstigeres Eukalyptusholz zu ersetzen. Allerdings muss das harte Eukalyptusholz sehr vorsichtig getrocknet werden, um Trocknungsschäden zu vermeiden. Freilandtrocknung ist dafür nicht geeignet, da durch fehlende Kontrollmöglichkeiten hohe Verluste und lange Trocknungszeiten entstehen. Daneben kann die für die Möbelindustrie notwendige geringe Holzfeuchte nicht erreicht werden. Künstliche Trocknungsverfahren ermöglichen eine kontrollierte Trocknung auf geringe Holzfeuchten bei Beibehaltung einer hohen Holzqualität und kurzen Trocknungszeiten. Jedoch verursachen technisch ausgereifte Hochtemperaturtrockner hohe Investitionskosten. Kostengünstigere lokal hergestellte Holz Trockner besitzen keine ausreichenden Kontrolleinrichtungen zur Überwachung des Trocknungsprozesses. Außerdem erhöht eine langsame Trocknung des empfindlichen Holzes in Hochtemperaturtrocknern den thermischen und elektrischen Energiebedarf, was wiederum die Trocknungskosten erhöht.

Aufgrund dieser Problematik hat Bux im Rahmen einer engen Zusammenarbeit mit dem Institut für Agrartechnik in den Tropen und Subtropen der Universität Hohenheim (ATS), dem deutschen Unternehmen THERMO-SYSTEM Industrie- & Trocknungstechnik GmbH (THS), Alfdorf und dem brasilianischen Forstbetrieb CAF Santa Barbara Ltda (CAF) einen solargestützten Trockner für Schnittholz mit integriertem Solarkollektor und zusätzlicher Biomasseheizung entwickelt [37-39].

Ziel der vorliegenden Forschungsarbeit war es, ein Trocknungsprogramm zu entwickeln, das es erlaubt, mit Hilfe des Solartrockners kostengünstig hochwertiges Schnittholz für die Möbelindustrie zu produzieren. Dazu wurde ein Prototyp des neuentwickelten Gewächshaus Trockners unter subtropischen Klimabedingungen in Brasilien aufgebaut und untersucht. Aufgrund der geringen Wärmedämmung des Trockners und fehlender Trocknungserfahrung mit der brasilianischen Varietät von *Eucalyptus grandis*, musste eine vollkommen neue Art der Trocknungsführung entwickelt werden. Das neuentwickelte Trock-

nungsprogramm berücksichtigt nicht nur die Ansprüche des extrem empfindlichen Eukalyptusschnittholzes, sondern auch die systemimmanenten Anforderungen des Solartrockners, die eine Berücksichtigung der täglichen Schwankungen des Umgebungsklimas erforderlich machen. Die bewusste Anpassung der Trocknungstemperatur an die Umgebungsluft ermöglicht dabei die Beschleunigung des Trocknungsprozesses ohne eine Betauung der Trocknerhülle und einen negativen Einfluss auf die Holzqualität in Kauf nehmen zu müssen. In mehr als 80 Trocknungsversuchen mit über 16 000 m³ Eukalyptusschnittholz wurde das Trocknungsprogramm untersucht und weiterentwickelt. Auf Grundlage der durchgeführten Versuche und von Literaturangaben wurde der Verlauf der Temperatur, der relativen Feuchte und der Strömungsgeschwindigkeit der Trocknungsluft, neben Häufigkeit und Dauer von Wiederbefeuchtungsintervallen, systematisch verbessert. Maßgeblich war hierbei der Einfluss der sich ändernden Trocknungsbedingungen auf die Trocknungsdauer, die Holzqualität, den Energiebedarf und die Trocknungskosten.

Während des Forschungsvorhabens wurden geeignete Trocknungsprogramme für 18, 27, 32 and 42 mm dickes Eukalyptusschnittholz ausgearbeitet. Zu Beginn jeder Trocknung wurde dabei die Temperatur der Trocknungsluft auf maximale 40 °C begrenzt und die relative Feuchte auf über 70 % gehalten. Diese Einstellungen waren geeignet, um den bei den meisten Eukalyptusarten gefürchteten Kollaps der Holzzellen zu vermeiden. Die Maximaltemperatur wurde zum Ende des Trocknungsprozesses auf 55 °C erhöht und die relative Feuchte auf 25 % verringert. Während des ganzen Trocknungsvorganges folgte dabei die Temperatur der Trocknungsluft im Solartrockner der Temperatur der Umgebungsluft. Nach oben wurde der Temperaturbereich durch qualitätsbedingte Maximaltemperaturen und nach unten aus Gründen der Trocknungsdauer sowie aus regelungstechnischen Erfordernissen notwendigen Minimaltemperaturen begrenzt. Dabei wurde die Temperaturdifferenz zwischen der Umgebung und der Trocknungsluft von 10 K zu Beginn auf 30 K zum Ende des Trocknungsprozesses erhöht. Eine Erhöhung der Temperaturdifferenz hatte neben der Beschleunigung der Trocknung auch einen signifikant höheren Energiebedarf zur Folge. Während den 1 bis 4 stündigen Wiederbefeuchtungsintervallen wurde die relative Feuchte der Trocknungsluft auf über 90 % erhöht. Eine Anpassung der Wiederbefeuchtungszyklen an die Brettstärke ermöglichte eine Beschleunigung des Trocknungsprozesses ohne eine Zunahme von Trocknungsschäden. Die Geschwindigkeit der Trocknungsluft wurde bei 1.5 bis 2.5 m/s gehalten, da mit höherer Luftgeschwindigkeit unter den gegebenen Verhältnissen keine Erhöhung der Trocknungsrate gemessen werden konnte. Da Qua-

litätsstandards für Eukalyptusschnittholz nicht zur Verfügung standen, wurde ein Bewertungs- und Klassifizierungssystem für die Kriterien “mittlere Holzfeuchte”, “Holzfeuchtestreuung” und “Verschalung” auf Basis einer europäischen Vornorm an die spezifischen Erfordernissen von Eukalyptusholz angepasst. Qualitätsparameter wie Verformungen, Risse und Zellkollaps wurden quantitativ bestimmt.

Mit dem entwickelten Trocknungsprogramm konnten 27 mm dicke Eukalyptusbretter im Solartrockner von einer durchschnittlichen Anfangsfeuchte von 60 % in 27 Tagen auf 12 % getrocknet werden. Dabei war die Trocknungsdauer etwa 20 % länger als bei Hochtemperaturtrocknern. Vergleichend dazu konnte im Freiland die Holzfeuchte in 60 Tagen nur auf ungefähr 20 % verringert werden. Der Bedarf an elektrischer Energie betrug im Solartrockner etwa 20 kWh pro m³ getrocknetem Eukalyptusholz, was nur 20 % der in einem Hochtemperaturtrockner erforderlichen Energie entsprach. Der thermische Energiebedarf war mit 1.2 GJ pro m³ etwa 60 % geringer als bei konventionellen Hochtemperaturtrocknern. Der geringe thermische und elektrische Energiebedarf, zusammen mit den erheblich geringeren Investitionskosten für den solargestützten Schnittholztrockner, ergab durchschnittliche Trocknungskosten von 7.90 Euro pro m³. Dies entsprach einer Halbierung der Kosten im Vergleich zu Hochtemperaturtrocknern. Zur weiteren ökonomischen Bewertung des Solartrockners wurde eine Sensitivitätsanalyse der wichtigsten Kostenfaktoren durchgeführt. Dabei wurden die elektrischen Energiekosten, der Wechselkurs der Landeswährung und der Zinssatz für Bankkredite als die wichtigsten Einflussfaktoren unter den brasilianischen Marktgegebenheiten ermittelt. Generell war die Solartrocknung immer deutlich kostengünstiger als die konventionelle Hochtemperaturtrocknung.

Im Rahmen der vorliegenden Forschungsarbeit konnte gezeigt werden, dass brasilianisches Eukalyptusschnittholz, unter Beibehaltung einer hohen Qualität, mit Hilfe der solaren Trocknungsanlage sowie der neuentwickelten Trocknungsprogramme kostengünstig auf eine geringe Holzfeuchte von 10 bis 12 % getrocknet werden kann. Diese Aussage hat sich in der Praxis insofern bestätigt, als zwischenzeitlich etwa 35 000 m³ Eukalyptushartholz in zwei solargestützten Trocknungsanlagen pro Jahr erfolgreich getrocknet werden. Es liegt auf der Hand, dass dies einen maßgeblichen Beitrag zum Schutz der natürlichen Regenwälder leistet.

9 REFERENCES

- [1] VERMAAS, H.F.: Drying eucalypts for quality: material characteristics, pre-drying treatments, drying methods, schedules and optimisation of drying quality. *South African Forestry Journal* (1995) No. 174, pp. 41-49.
- [2] LANGENDORF, G., E. SCHUSTER, and L. WAGNER: *Rohholz*. VEB Fachbuchverlag Leipzig, Leipzig (Germany), 1990.
- [3] ZIMMER, B. and G. WEGENER: Stoff- und Energieflüsse vom Forst zum Sägewerk. *Holz als Roh- und Werkstoff* 54 (1996), pp. 217-223.
- [4] WEGENER, G.: Perspektiven der Holznutzung. *Forstwirtschaftliches Zentralblatt* 114 (1995) No. 2, pp. 97-106.
- [5] GRESHAM, G.E.: Mercado de madeira de florestas plantadas. *Seminário Internacional de Utilização da madeira de Eucalipto para Serraria, Anais, Instituto de Pesquisas e Estudos Florestais IPEF, Piracicaba (Brazil), 1995, pp. 147-153.*
- [6] JANKOWSKY, I.P.: A indústria madeireira no Brasil: devastação ou conservação da floresta tropical. *Revista de Madeira* 1 (1992) No. 4, pp. 20-21.
- [7] ANON.: *Marktdaten zur FEMADE 2000*. Hannover Messe International GmbH, Hannover (Germany), 2000, pp. 1-2.
- [8] TOMASELLI, I. and J.D. GARCIA: Ameaças a indústria de madeiras do Brasil. *Informativos STCP* (1998) No. 2, pp. 13-16.
- [9] ANON.: Eucalipto - pesquisas criam a madeira para todos os usos. *Revista Madeira & Tecnologia* 1 (1997) No. 5, pp. 29-31.
- [10] FLYNN, B.: Brazilian mill benefits from "dream" growing conditions. *Wood Technology* (1999) No. 7, pp. 18-21.
- [11] JANKOWSKY, I.P.: Possibilidade e limites para uso da madeira reflorestada. *Revista de Madeira* 3 (1994) No. 13, pp. 30-31.
- [12] ANON.: Porque devo plantar eucalipto? Porque não devo plantar eucalipto? *Informativo Sementes* No. 1, Instituto de Pesquisas e Estudos Florestais IPEF, Piracicaba, Sao Paulo (Brazil), 1997, pp. 1-2.
- [13] KAUMAN, W.G., J. GERARD, J.Q. HU, and H.J. WANG: Processing of eucalypts. *Commonwealth Forestry Review* 74 (1995) No. 2, pp. 147-154.
- [14] SERRANO, O., G. BULL, and D. LEE: Global wood resources, production and international trade of forest products. *First International Seminar on Solid Wood Products of High Technology - First Meeting on Adapted Technologies of Sawing, Drying and Use of the Wood of Eucalyptus, Sociedade de Investigações Florestais, Universidade de Viçosa, Departamento de Engenharia Florestal, Viçosa, Minas Gerais (Brazil), 1998, pp. 1-19.*

- [15] MONTAGNA, R.G., R.H. PONCE, P.D.S. FERNANDES, and C. RIBAS: Desdobro de *Eucalyptus grandis* Hill ex Maiden visando a diminuir o efeito das tensões de crescimento. *Revista do Instituto Florestal* 3 (1991) No. 2, pp. 181-190.
- [16] JANKOWSKY, I.P.: Secagem de madeira de reflorestamento, técnica e equipamentos. Seminário sobre processamento e utilização de madeira para reflorestamento, Associação Brasileira de Preservadores de Madeireira ABPM, Curitiba (Brazil), 1996, pp. 107-117.
- [17] SHIVA, V. and J. BANDYOPADHYAY: Inventário ecológico sobre o cultivo de eucalipto. Comissão Pastoral da Terra de Minas Gerais, Belo Horizonte (Brazil), 1991.
- [18] WAUGH, G.: Sawing of young, fast-grown eucalypts. First international Seminar on Solid Wood Products of High Technology, First Meeting on Adapted Technologies of Sawing, Drying and Use of the Wood of Eucalypts, Sociedade de Investigações Florestais, Universidade de Viçosa, Departamento de Engenharia Florestal, Viçosa, Minas Gerais (Brazil), 1998, pp. 69-81.
- [19] SILVA, J.R.M.: Air drying of *Eucalyptus grandis* wood for furniture making. *CERNE* 3 (1997) No. 1, pp. 170-186.
- [20] VERMAAS, H.F.: Drying of *Eucalyptus* with special reference to young, fast-grown plantation material. First International Seminar on Solid Wood Products of High Technology, First Meeting on Adapted Technologies of Sawing, Drying and Use of the Wood of Eucalypts, Sociedade de Investigações Florestais, Universidade de Viçosa, Departamento de Engenharia Florestal, Viçosa, Minas Gerais (Brazil), 1998, pp. 107-118.
- [21] HILLIS, W.E. and A.G. BROWN: *Eucalypts for wood production*. CSIRO, Griffin Press Limited, Adelaide, South Australia (Australia), 1978.
- [22] LELLES, J.G.D. and J.D.C. SILVA: Problemas e soluções sobre rachaduras de topo de madeira de *Eucalyptus* spp. nas fases de desdobro e secagem. *Informação Agropecuária* 18 (1997) No. 186, pp. 62-69.
- [23] MARDER, R.C., A.P. ROBINSON, and H.C. COOTE: The performance of a timber drying kiln fuelled by sawdust and a solar kiln. *Tropical Science* 34 (1994) No. 3, pp. 321-334.
- [24] VERMAAS, H.F.: Case for the low temperature kiln drying of *Eucalyptus grandis*. *South African Forestry Journal* (1987) No. 140, pp. 72-77.
- [25] VERMAAS, H.F. and C.J. NEVILLE: Low temperature drying of *Eucalyptus grandis*. A preliminary laboratory evaluation. *Holzforschung* 42 (1988) No. 4, pp. 265-271.
- [26] VERMAAS, H.F. and C.J. NEVILLE: Evaluation of low temperature and accelerated low temperature drying schedules for *Eucalyptus grandis*. *Holzforschung* 43 (1989) No. 3, pp. 207-212.

- [27] STÖHR, H.P.: Progress towards the efficient kiln drying of *Eucalyptus grandis*. Symposium on Forest Products Research, International Achievements and the future, National Timber Research Institute of the South American Council for Scientific and Industrial Research, Pretoria (South Africa), 1985, pp. (8-6)1-(8-6)18.
- [28] SANTOS, J.A.D.: Secagem da madeira de eucalipto. *Revista Florestal* 11 (1998) No. 2, pp. 37-45.
- [29] BRUNNER, R.: *Die Schnittholztrocknung*. Brunner-Hildebrand, Hannover (Germany), 1988.
- [30] KRÖLL, K. and W. KAST: *Trocknungstechnik 3. Band: Trocknen und Trockner in der Produktion*. Springer Verlag, Heidelberg (Germany), 1989.
- [31] ANON.: *Wirtschaftliche Holztrocknung, Technischer Stand und Trocknungsverfahren*. *Der deutsche Schreiner* (1992) No. 2, pp. 46-51.
- [32] BRUNNER, R.: *Vakuumtrocknung im Wirtschaftlichkeitsvergleich. Teil 2: Vergleich der Trockenkosten für Buche und Fichte bei Frisch-/ Ablufttrocknung und Vakuumtrocknung*. *Holz Zentralblatt* 125 (1999) No. 56, pp. 858-859.
- [33] STEINMANN, D.E. and H.F. VERMAAS: Control of equilibrium moisture content in a solar kiln. *Holz als Roh- und Werkstoff* 48 (1990) No. 4, pp. 147-152.
- [34] SATTAR, M.A.: Solar drying of timber - a review. *Holz als Roh- und Werkstoff* 51 (1993), pp. 409-416.
- [35] LITTLE, R.L.: Industrial use of solar heat in lumber drying: a long-term performance report. *Forests Products Journal* 34 (1984) No. 9, pp. 22-26.
- [36] SATTAR, M.A.: Economics of drying timber in a greenhouse type solar kiln. *Holz als Roh- und Werkstoff* 54 (1994), pp. 157-161.
- [37] BUX, M., W. MÜHLBAUER, K. BAUER, and B. KÖHLER: Solar-assisted drying of timber in industrial scale. International Conference "Rational use of Renewable Energy Sources in Agriculture", Budapest (Hungary), 2000.
- [38] BUX, M.: *Entwicklung eines solargestützten Trocknungsverfahrens für Zigarrentabak*. Dissertation, Institut für Agrartechnik in den Tropen und Subtropen, Universität Hohenheim, Max-Eyth-Gesellschaft im VDI (VDI-MEG), Stuttgart (Germany), 1996.
- [39] BUX, M., M. ARNOLD, P. SERRANO, and W. MÜHLBAUER: Solar greenhouse dryer. FAO-SREN 1st Workshop on Decentralized Rural Energy Sources: Solar, Wind, Geothermal Energy, Landtechnik Weihenstephan, Freising (Germany), 1996.

- [40] EDG-Richtlinie "Trocknungsqualität" zur Bestimmung und Bewertung der Trocknungsqualität von technisch getrocknetem Schnittholz (Pilot Version). European Committee for Standardization, Brussels (Belgium), 1994.
- [41] WELLING, J.: Zur Ermittlung der Trocknungsqualität von Schnittholz. Holz als Roh- und Werkstoff 54 (1996), pp. 307-311.
- [42] MALAN, F.S.: Eucalyptus improvement for lumber production. Seminário sobre processamento e utilização de madeira para reflorestamento, Anais, Instituto de Pesquisas e Estudos Florestais IPEF, Piracicaba (Brazil), 1995, pp. 1-19.
- [43] ILIC, J. and W.R. HILLIS: The prediction of collapse in dried wood of ash type eucalypts. Symposium on Forest Product Research, International Achievements and the Future, Council of Scientific and Industrial Research CSIR, Pretoria (South Africa), 1985, pp. (8-7)1-(8-7)12.
- [44] RAVEN, P., R. EVERT, and H. CURTIS: Biologie der Pflanzen. Walter de Gruyter, Berlin, New York (Germany), 1988.
- [45] DINWOODIE, J.M.: Timber - Its nature and behaviour. The Trinity Press, Worcester, (Great Britain), 1981.
- [46] KISSELOFF: Die physikalischen Vorgänge bei der Holz Trocknung - Noch längst nicht völlig erforscht. Schweizer Holzzeitung (1990) No. 26, pp. 18-19.
- [47] STÖHR, H.P.: Drying of *E. grandis*: a new approach with HH orientated schedules. North American Wood Drying Symposium, Mississippi Forest Products Utilization Laboratory, Mississippi (USA), 1984, pp. 72-77.
- [48] RIBEIRO, F.D.A. and J.Z. FILHO: Variação da densidade básica da madeira em espécies / procedências de *Eucalyptus* spp. Report No. 46, Instituto de Pesquisas e Estudos Florestais IPEF, Piracicaba (Brazil), 1993, pp. 76-85.
- [49] LOHMANN, U., T. ANNIES, and D. ERMSCHER: Holz-Handbuch. DRW-Verlag, Leinfelden-Echterdingen (Germany), 1991.
- [50] CINIGLIO, G.: Avaliação da secagem de madeira serrada de *E. grandis* e *E. urophylla*. Dissertation, Escola Superior de Agricultura Luiz de Queiroz, Universidade de São Paulo, Piracicaba (Brazil), 1998.
- [51] FERNANDES, P.D.S., S.M. BORGES FLORSHEIM, F.T. ROCHA, R.G. MONTAGNA, and H.T.Z.D. COUTO: Tenções de crescimento em procedências de *Eucalyptus grandis* Hill ex Maiden e suas relações com as características das fibras e densidade básica. Revista do Instituto Florestal 1 (1989) No. 1, pp. 215-234.
- [52] FILHO, M.T.: Variação radial da densidade básica e da estrutura anatômica da madeira do *Eucalyptus saligna* e *Eucalyptus grandis*. Report No. 29, Instituto de Pesquisas e Estudos Florestais, Piracicaba (Brazil), 1985, pp. 37-45.

- [53] REZENDE, M.A. and E.S.B. FERRAZ: Densidade anual da madeira de *Eucalyptus grandis*. Report No. 30, Instituto de Pesquisas e Estudos Florestais IPEF, Piracicaba (Brazil), 1985, pp. 37-41.
- [54] FILHO, M.T.: Estrutura anatômica da madeira de oito espécies de eucalipto cultivadas no Brasil. Report No. 29, Instituto de Pesquisas e Estudos Florestais, Piracicaba (Brazil), 1985, pp. 25-36.
- [55] FILHO, M.T.: Variação radial da densidade básica e da estrutura anatômica da madeira do *Eucalyptus globulus*, *E. pellita* e *E. acmenioides*. Report No. 33, Instituto de Pesquisas e Estudos Florestais, Piracicaba (Brazil), 1987, pp. 35-42.
- [56] FILHO, M.T.: Variação radial da densidade básica e da estrutura anatômica da madeira do *Eucalyptus gummifera*, *E. microcorys* e *E. pilularis*. Report No. 30, Instituto de Pesquisas e Estudos Florestais, Piracicaba (Brazil), 1985, pp. 45-54.
- [57] KOLLMANN, F. and W.A. COTE: Principles of wood science and technology - Solid wood. Springer Verlag, Berlin, Heidelberg, New York (Germany), 1968.
- [58] EICHLER, H.: Praxis der Holz Trocknung. VEB Fachbuchverlag Leipzig, Leipzig (Germany), 1978.
- [59] ILIC, J. and W.R. HILLIS: Variation in collapse in the dried wood of re-growth ash-type eucalypts. Symposium on Forest Product Research, International Achievements and the Future, Council of Scientific and Industrial Research CSIR, Pretoria (South Africa), 1985, pp. (8-4)1-(8-4)10.
- [60] MELLADO, E.C.E.R.: Contribuição ao desenvolvimento tecnológico para a utilização de madeira serrada de *E. grandis* (Hill Ex Maiden) na geração de produtos com maior valor agregado. Diploma, Ciências Agrárias, Universidade Federal do Paraná, Curitiba (Brazil), 1983.
- [61] LISBOA, C.D.J.: Estudo das tensões de crescimento em toras de *E. grandis* Hill ex Maiden. Dissertation, Ciências Agrárias, Universidade Federal do Paraná, Curitiba (Brazil), 1993.
- [62] VORREITER, L.: Holztechnologisches Handbuch, Band II: System Holz-Wasser-Wärme. Holz Trocknung. Dämpfen und Kochen. Spanlose Holzverformung. Verlag Georg Fromme & Co., Munich (Germany), 1958.
- [63] BERTHOLD, K.: Einführung in die Holztechnik. VEB Fachbuchverlag, Leipzig (Germany), 1965.
- [64] BÖHNER, G.: Überlegungen und Ergänzungen zum "Keylwerth-Diagramm". Holz als Roh- und Werkstoff 54 (1996) No. 2, pp. 73-79.
- [65] SIMPSON, W.T.: Equilibrium moisture content prediction of wood. Forests Products Journal 21 (1971) No. 5, pp. 48-49.

- [66] CHAFE, S.C. and J. ILIC: Shrinkage and collapse in thin sections and blocks of Tasmanian mountain ash regrowth. 1. Shrinkage, specific gravity and the fibre saturation point. *Wood Science and Technology* 26 (1992) No. 2, pp. 115-129.
- [67] CHAFE, S.C.: Relationships between shrinkage and specific gravity in the wood of *Eucalyptus*. *Australien Forestry* 57 (1994), pp. 59-61.
- [68] CHAFE, S.C.: The effect of resaturation on the shrinkage specific gravity relationship in *Eucalyptus regnans* F. Muell. *Holzforschung* 46 (1992) No. 5, pp. 379-384.
- [69] CHAFE, S.C. and J. ILIC: Shrinkage and collapse in thin sections and blocks of Tasmanian mountain ash regrowth. 2. The R-ratio and changes in cell lumen volume. *Wood Science and Technology* 26 (1992) No. 3, pp. 181-187.
- [70] CHAFE, S.C. and J. ILIC: Shrinkage and collapse in thin sections and blocks of Tasmanian mountain ash regrowth. 3. Collapse. *Wood Science and Technology* 26 (1992) No. 5, pp. 343-351.
- [71] SANDLAND, K.M.: Stress and strain in drying wood - a literature survey. Report No. 34, Norwegian Institute of Wood Technology, Oslo (Norway), 1996, pp. 1-33.
- [72] UTERHARCK, F.: *Handbuch für die künstliche Holztrocknung*. Dr. Sändig Verlag, Wiesbaden (Germany), 1952.
- [73] KEEY, R.B., T.A.G. LANGRISH, and J.C.F. WALKER: *Kiln-Drying of Lumber*. Springer Verlag 1997, Berlin, Heidelberg, New York (USA), 1999.
- [74] AGUIAR, O.J.R. and I.P. JANKOWSKY: Prevenção e controle das rachaduras de topo em tora de *eucalyptus grandis* Hill ex Maiden. Report No. 2640, Escola Superior de Agricultura "Luiz de Queiroz", Departamento de Ciências Florestais, Universidade de São Paulo, Piracicaba, São Paulo (Brazil), 1986, pp. 1-26.
- [75] CHAFE, S.C.: Growth stress in trees. *Australien Forest Research* 9 (1979) No. 3, pp. 203-223.
- [76] BOYD, J.D.: The key factor in growth stress regeneration: lignification or crystallisation? *International Association Wood Anatomy Bulletin* 6 (1985) No. 2, pp. 139-150.
- [77] MALAN, F.S.: The wood properties and qualities of three South African grown eucalypt hybrids. *South African Forestry Journal* (1993) No. 167, pp. 35-44.
- [78] FERNANDES, P.D.S.: Densidade da madeira e suas relações com as tensões de crescimento. Instituto Florestal, São Paulo (Brazil), 1986, pp. 1-22.

- [79] BARNACLE, K.E.: Rapid effect of drying on development of heart cracks (*Eucalyptus camaldulensis*, logs). *Australian Forestry* 35 (1971) No. 4, pp. 251-257.
- [80] GARCIA, J.N.: Técnicas de desdobro de eucalipto. Seminário Internacional de Utilização da madeira de Eucalipto para Serraria, Anais, Instituto de Pesquisas e Estudos Florestais IPEF, Piracicaba (Brazil), 1995, pp. 59-67.
- [81] JANKOWSKY, I.P.: Fundamentos de secagem de madeiras. Documentos Florestais No. 10, Escola Superior de Agricultura Luiz de Queiroz, Departamento de Ciências Florestais, Universidade de São Paulo, Piracicaba (Brazil), 1990, pp. 1-13.
- [82] TOMASELLI, I.: Secagem de madeira. Fundação de Pesquisas Florestais do Paraná FUPF, Curitiba (Brazil), 1979, pp. 1-26.
- [83] LANGRISH, T.A.G. and N. BOHM: An experimental assessment of driving forces for drying in hardwoods. *Wood Science and Technology* 31 (1997) No. 6, pp. 415-422.
- [84] HUSTEDE, K.: *Schnittholztrocknung*. Deutsche Verlags Anstalt, Stuttgart (Germany), 1979.
- [85] TUOMOLA, T.: *Über die Holztrocknung*. Dissertation, Technische Hochschule Finnlands, Finnish Literature Society, Helsinki (Finland), 1943.
- [86] STEPHAN, K.: Thermodynamik. In: *Dubbel-Taschenbuch für den Maschinenbau* No. D. Ed.: BEITZ, W. and K.H. KÜTTNER, Springer Verlag, Berlin (Germany), 1990, pp. 1-45.
- [87] INNES, T.C.: Pre-drying of collapse prone wood free of surface and internal checking. *Holz als Roh- und Werkstoff* 54 (1995), pp. 195-199.
- [88] KARABAGLI, A., E. MOUGEL, L. CHRUSCIEL, and A. ZOULALIAN: Study on a low temperature convective wood drier. Influence of some operating parameters on drier modelling and on the quality of dried wood. *Holz als Roh- und Werkstoff* 55 (1997) No. 4, pp. 221-226.
- [89] BOHL, W.: *Technische Strömungslehre*. Vogel Buchverlag, Würzburg (Germany), 1991.
- [90] BRUNNER, R.: Die Turbotrocknung - eine neue Dimension in der Holztrocknungstechnik Teil 2: Beschreibung des Verfahrens und der technischen Einrichtungen. *Holz Zentralblatt* 115 (1989) No. 50, pp. 6-8.
- [91] DREESSEN, V.: Aspects of latest kiln drying technology. Symposium on Forest Product Research, International Achievements and the Future, Council of Scientific and Industrial Research CSIR, Pretoria (South Africa), 1985, pp. (8-11)1-(8-11)17.
- [92] HERRMANN, G.: Trends in der technischen Schnittholztrocknung. *HOB Die Holzbearbeitung* 35 (1988) No. 6, pp. 18-20.

- [93] BRUNNER, R.: Die Turbotrocknung - eine neue Dimension in der Holz-trocknungstechnik Teil 1: Grundsätzliches zur Frage der Luftgeschwindigkeit und der Luftführung in der Trockenkammer. Holz Zentralblatt 115 (1989) No. 50, pp. 1-5.
- [94] TORGESON, O.W.: The drying rate of sugar maple as affected by relative humidity and air velocity. Research Reports FPL No. 1274, Forest Products Laboratory, Forest Service, US Department of Agriculture, Madison (USA), 1940, p. 1.
- [95] BRUNNER, R. and K.P. HEINE: Computer controlled drying. Symposium on Forest Products Research, International Achievements and the Future, National Timber Research Institute of the South American Council for Scientific and Industrial Research CSIR, Pretoria (South Africa), 1985, pp. (8-12)1-(8-12)9.
- [96] KISSELOFF: Qualitätsminderung nicht immer vermeidbar. Schweizer Holzzeitung (1990) No. 26, pp. 22-23.
- [97] ANON.: Tabela de umidades de equilíbrio para algumas cidades do Brasil. Departamento de Ciências Florestais, Universidade Federal de Lavras, Lavras, Minas Gerais (Brazil), 1996, p. 1.
- [98] JANKOWSKY, I.P., A.T.D.O. BRANDAO, H.D. OLIVEIRA, J.D.C. LIMA, and S. MILANO: Estimativas de umidade de equilíbrio para cidades da região sul do Brasil. Report No. 32, Instituto de Pesquisas e Estudos Florestais IPEF, Piracicaba (Brazil), 1986, pp. 61-64.
- [99] MARTINS, A.V.: Secagem de madeira serrada. Laboratório de Produtos Florestais, Departamento de Pesquisa, Instituto Brasileiro de Desenvolvimento Florestal, Ministério da Agricultura, Brasilia (Brazil), 1988, pp. 1-56.
- [100] FRANZOI, L.C.: Konventionelle Trocknungsprogramme für Eukalyptus-schnittholz. Centro Tecnológico do Mobiliário, Serviço Nacional de Aprendizagem Industrial SENAI (Brazil), 1997, pp. 1-15.
- [101] WI 175.091. Schnittholz - Verfahren zur Ermittlung der Verschalung. European Committee for Standardization, Brussels (Belgium), 2001.
- [102] BEKELE, T.: Degradation of boards of Eucalyptus globulus Labill. and Eucalyptus camaldulenses Dehnh. during air drying. Holz als Roh- und Werkstoff 53 (1995) No. 6, pp. 407-412.
- [103] Gesetzliche Handelsklassensortierung für Rohholz (Forst-HKS). Ministerium für ländlichen Raum, Ernährung und Forsten Baden-Württemberg, Stuttgart (Germany), 1983.
- [104] SIMPSON, W.T.: Warp reduction in kiln drying hardwood dimension. Forests Products Journal 32 (1982) No. 5, pp. 29-32.
- [105] VERMAAS, H.F.: Interaction of wood, water and stresses during drying: a review. South African Forestry Journal (1998) No. 181, pp. 25-32.

- [106] CHAFE, S.C.: Preheating green boards of mountain ash (*Eucalyptus regnans* F. Muell.) 2: Relationships amongst properties. *Holzforschung* 48 (1994) No. 2, pp. 163-167.
- [107] KAUMAN, W.G.: Zellkollaps im Holz. Erste Mitteilung: Einflussgrößen bei der Entstehung des Zellkollaps und seine Rückbildung. *Holz als Roh- und Werkstoff* 22 (1964), pp. 183-196.
- [108] BARISKA, M.: Collapse phenomena in eucalypts. *Wood Science and Technology* 26 (1992) No. 3, pp. 165-179.
- [109] INNES, T.C.: Collapse and internal checking in the latewood of *Eucalyptus regnans* F. M. *Wood Science and Technology* 30 (1996) No. 6, pp. 373-383.
- [110] CAVALCANTE, A.D.A.: Ocorrência do colapso na secagem da madeira de *Eucalyptus grandis* e *Eucalyptus saligna*. Diploma, Universidade de São Paulo, Escola Superior de Agricultura Luiz de Queiroz, Piracicaba, São Paulo (Brazil), 1991.
- [111] INNES, T.C.: Collapse free pre-drying of *Eucalyptus regnans* F. M. *Holz als Roh- und Werkstoff* 53 (1995), pp. 403-406.
- [112] CAVALCANTE, A.D.A.: Alterações na estrutura anatômica da madeira de Cedro (*Cedrela* sp.) e Eucalipto (*Eucalyptus grandis* Hill ex - Maiden) durante o processo de secagem. Escola Superior de Agricultura Luiz de Queiroz, Universidade de São Paulo, Piracicaba (Brazil), 1988, pp. 1-10.
- [113] CHAFE, S.C.: The effect of boiling on shrinkage, collapse and other wood-water properties in core segments of *Eucalyptus regnans* F. Muell. *Wood Science and Technology* 27 (1993) No. 3, pp. 205-217.
- [114] BEKELE, T.: Kiln drying of sawn boards of young *Eucalyptus globulus* Labill. and *Eucalyptus camaldulensis* Dehnh. grown on the Ethiopian Highlands. *Holz als Roh- und Werkstoff* 52 (1994), pp. 377-382.
- [115] ALEXIOU, P.N.: Optimisation of an accelerated drying schedule for re-growth *Eucalyptus pilularis* Sm. *Holz als Roh- und Werkstoff* 49 (1991) No. 4, pp. 153-159.
- [116] NEUMANN, R.J. and A. SAAVEDRA: Check formation during the drying of *Eucalyptus globulus*. *Holz als Roh- und Werkstoff* 50 (1992) No. 3, pp. 106-110.
- [117] NASSIF, N.M.: Continuously varying schedule (CVS): a new technique in wood drying. *Wood Science and Technology* 17 (1983), pp. 139-141.
- [118] JANKOWSKY, I.P.: Equipamentos e processos para secagem de madeiras. Seminário Internacional de Utilização da madeira de Eucalipto para Serraria, Anais, Instituto de Pesquisas e Estudos Florestais IPEF, Piracicaba (Brazil), 1995, pp. 109-118.

- [119] EMMANUEL, C.E., C. ROZAS, and I. TOMASELLI: Secagem de madeira serrada de *Eucalyptus viminalis*. *Ciência Florestal* 3 (1993) No. 1, pp. 147-159.
- [120] ALEXIOU, P.N., J.F. MARCHANT, and K.W. GROVES: Effect of pre-steaming on moisture gradients, drying stresses and sets, and fuse checking in regrowth *Eucalyptus pilularis* Sm. *Wood Science and Technology* 24 (1990) No. 2, pp. 201-209.
- [121] BREESE, M.C., S. ZHAO, and G. MCLEOD: The use of acoustic emissions to reduce checking during drying of European oak. *Holz als Roh- und Werkstoff* 53 (1995) No. 6, pp. 393-396.
- [122] GLOSSOP, B.R.: Effect of hot water soaking or freezing pre treatments on drying rates of two eucalypts. *Forests Products Journal* 44 (1994) No. 10, pp. 29-32.
- [123] ILIC, J.: Advantages of pre-freezing for reducing shrinkage related degrade in eucalypts: general considerations and review of the literature. *Wood Science and Technology* 29 (1995) No. 4, pp. 277-285.
- [124] CHAFE, S.C. and J.M. CARR: Effect of preheating on internal checking in boards of different dimension and grain orientation in *Eucalyptus regnans*. *Holz als Roh- und Werkstoff* 56 (1998) No. 1, pp. 15-23.
- [125] CHAFE, S.C.: Preheating green boards of mountain ash (*Eucalyptus regnans* F. Muell.) 1: Effects of external shrinkage, internal checking and surface checking. *Holzforschung* 48 (1994) No. 1, pp. 61-68.
- [126] CHAFE, S.C.: Effect of brief pre-steaming on shrinkage, collapse and other wood-water relationships in *Eucalyptus regnans* F. Muell. *Wood Science and Technology* 24 (1990) No. 4, pp. 311-326.
- [127] CHADWICK, W.B. and T.A.G. LANGRISH: A comparison of drying time and timber quality in the continuous and cyclic drying of Australian turpentine timber. *Drying Technology* 14 (1996) No. 3/4, pp. 895-906.
- [128] MÜLLER.W.: Holzlagerung - Natürliche Holz Trocknung: Ohne Holz Trocknung keine Qualitätsarbeit. *Schweizerische Schreinerzeitung* 101 (1990) No. 51, pp. 1262-1265.
- [129] HUSTEDE, K.: Welche Kosten entstehen bei der Schnittholztrocknung. *Der deutsche Schreiner* (1979) No. 8, pp. 32-34.
- [130] ANON.: Energiesparen durch Nutzung der Sonnenenergie. *Holzrundschaue* 38 (1982) No. 855/856, pp. 266-267.
- [131] WENGERT, E.M. and L.C. OLIVEIRA: Solar heated, lumber dry kiln designs. Virginia Polytechnic Institute and State University, Blacksburg, Virginia (USA), <http://www.woodweb.com>, 06.02.2001.

- [132] CHMIELEWSKI, W., M. MATEJAK, and U.E. POPOWSKA: Untersuchungen über die Solartrocknung von Holz. *Holzindustrie* (1982) No. 2, pp. 40-42.
- [133] KOUKAL, J.: Trocknen von Schnittholz mittels Sonnenenergie. *Holztechnologie* 25 (1984) No. 2, pp. 71-73.
- [134] ANON.: Solarbeheizung für Schnittholztrockner -Hildebrand. *Holz im Handwerk* 5 (1981), pp. 25-252.
- [135] TSCHERNITZ, J.L. and W.T. SIMPSON: FPL Design for Lumber Dry Kiln Using Solar/Wood Energy in Tropical Latitudes. Forest Products Laboratory Research Paper No. 44, Forests Service, United States Department of Agriculture, Madison, Wisconsin (USA), 1985, pp. 1-18.
- [136] KAVVOURAS, P.K. and M.A. SKARVELIS: Performance of a solar heated, forced-air, fully automated lumber dryer. *Holz als Roh- und Werkstoff* 54 (1996) No. 1, pp. 11-18.
- [137] ARK, D.: Schnittholztrocknung, beheizt mit Sonnenenergie. *Holz im Handwerk* (1980) No. 6, pp. 2-3.
- [138] TSCHERNITZ, J.L.: Solar energy for wood drying using direct or indirect collection with supplemental heating: a computer analysis. Forest Products Laboratory Research Paper No. 477, Forest Service, United States Department of Agriculture, Madison, Wisconsin (USA), 1986, pp. 1-81.
- [139] SIMPSON, W.T. and J.L. TSCHERNITZ: Performance of a solar / wood energy kiln in tropical latitudes. *Forests Products Journal* 39 (1989) No. 1, pp. 23-30.
- [140] SHARMA, S.N., N. PREM, and S.P. BADONI: A direct method for determination of energy savings by thermal insulation in a glasshouse type solar kiln. *Journal of the Timber Development Association* 28 (1982) No. 1, pp. 25-30.
- [141] SATTAR, M.A.: Thermal performance of a solar heated wood seasoning kiln. *Holz als Roh- und Werkstoff* 53 (1995) No. 1, pp. 43-47.
- [142] GLOSSOP, B.R.: Estimated fuel savings for a passive solar timber drying kiln in Australia. *CALM-Science* 1 (1993) No. 1, pp. 19-34.
- [143] KRAMES, U.: Ein kombinierter Solar- und Kondensationstrockner für Schnittholz. *Holzrundscha* 39 (1983) No. 867/868, pp. 79-80.
- [144] KRAMES, U.: Ein solarer Schnittholztrockner mit Außenkollektoren. *Internationaler Holzmarkt* 72 (1981) No. 22, pp. 15-18.
- [145] KRAMES, U.: Holztrocknung mit Solarenergie - Aussichten in Mitteleuropa. *Holz im Handwerk* (1980) No. 10, pp. 18-20.

- [146] KOBERLE, M.: Trocknen von Schnittholz mittels kombinierter Heizung unter Verwendung von Sonnenenergie. *Holzindustrie* 35 (1982) No. 2, pp. 42-43.
- [147] SIMPSON, W.T. and J.L. TSCHERNITZ: Design and performance of a solar lumber dryer for tropical latitudes. IUFRO Division V Conference, Wood drying papers, IUFRO, Oxford (Great Britain), 1980, pp. 59-70.
- [148] TSCHERNITZ, J.L. and W.T. SIMPSON: Solar heated forced air, lumber dryer for tropical latitudes. *Solar Energy* 22 (1979), pp. 563-566.
- [149] COULIBALY, B., D.C. LAFOND, M. FOURNIER, D. PALLET, and A. THEMELIN: A new timber solar dryer for tropical countries. IUFRO Division 5 Meeting, Wood drying working party sessions, Instituto de Pesquisas Tecnológicas do Estado de São Paulo, São Paulo (Brazil), 1988, pp. 58-67.
- [150] PALLET, D., B. COULIBALY, M. FOURNIER, and A. THEMELIN: Design, modelling and experimentation of a timber solar dryer in French Guiana. International Conference on Agricultural Engineering, Paris (France), 1988, pp. 1-11.
- [151] THEMELIN, A., D. GRIFFON, and J.P. HEBERT: Utilization of solar energy for drying of tropical products applications and prospects in hot areas. French-Israeli Symposium on Greenhouse Technology, Section III: Utilization of Solar Energy for Agricultura, Tel Aviv (Israel), 1988, pp. 1-20.
- [152] LIMA, L.M.Q. and A.D.A. CAVALCANTE: Módulo para secagem de madeiras - Aplicações tecnológicas da energia solar. *Acta Amazônica* 13 (1983) No. 5-6, pp. 869-873.
- [153] ANON.: Timber dehydration system utilizing solar energy. Sumitomo Metal Industries Ltd., Tokyo (Japan), 1988.
- [154] GUZMAN, J.A., A. LAUTERBACH, and R. JORDAN: Performance of wood solar kilns with box type collector. *Energy in Agriculture* (1985) No. 4, pp. 243-252.
- [155] BLAUBAUM, T.: Drying timber using a solar-assisted kiln. *CADDET Renewable Energy Newsletter* (1998) No. 12, pp. 19-21.
- [156] MARAIS, G.: Solar drying tunnel. *Wood Southern Africa* 7 (1982) No. 11, p. 26.
- [157] GOUGH, D.K.: Timber seasoning in a solar kiln. IUFRO Division V Conference, Wood drying papers, IUFRO, Oxford (Great Britain), 1980, pp. 97-105.
- [158] PALMER, G. and S.D. KLEINSCHMIDT: Timber seasoning in a solar kiln. Technical Paper No. 50, Queensland Forest Service, Queensland (Australia), 1992, pp. 1-10.

- [159] CHUDNOFF, M., E.D. MALDONADO, and E. GOYTIA: Solar drying of tropical hardwoods. ITF Research Paper No. 2, USDA Forest Service, Washington D.C. (USA), 1966, pp. 1-26.
- [160] PAL, P.C.: Solar timber seasoning plant for round-the-clock operation for small entrepreneur. National Solar Energy Convention, Solar Energy Society of India, New Delhi (India), 1982.
- [161] CHEN, P.Y.S. and C.E. HELTON: Design and evaluation of a low-cost solar kiln. *Forests Products Journal* 39 (1989) No. 1, pp. 19-22.
- [162] ANON.: Versuche für kostengünstige solare Holz Trocknung. *Schweizer Ingenieur und Architekt* (1989) No. 45, p. 1238.
- [163] RICHTER, K.: Holz Trocknung in kostengünstigen Solartrocknern. *Schweizerische Schreinerzeitung* (1989) No. 23, p. 546.
- [164] RICHTER, K.: Holz Trocknung in Solaranlagen? Möglichkeiten neuer Technologien in der Schweiz. *Schweizer Holzbau* 55 (1989) No. 8, p. 43.
- [165] OLIVEIRA, L.C., C. SKAAR, and E.M. WENGERT: Solar and air lumber drying during winter in Virginia. *Forests Products Journal* 32 (1982) No. 1, pp. 37-44.
- [166] NOVES, H.A. and J.I.F.G. SECO: Solar drying of sawn lumber in Spain. *Holz als Roh- und Werkstoff* 48 (1990) No. 5, pp. 173-178.
- [167] BENITEZ, F., A. SAMELA, F. IBARRA, and R. SPOTORNO: Secadero solar de maderas complementado con gasogeno de residuos de aserrado: escala semiindustrial. *Revista de Ciencia y Tecnologia de la Universidad Tecnologica Nacional* 2 (1997) No. 4, pp. 35-42.
- [168] KAVVOURAS, P.K. and M.A. SKARVELIS: Computerised control system for an experimental solar lumber dryer. *Holz als Roh- und Werkstoff* 51 (1993), pp. 267-271.
- [169] DURAND, P.Y.: Experimentations de sechoirs solaires a bois de type rustiques en Cote-d'Ivoire. *Bois et Forets des Tropiques* 208 (1985), pp. 49-56.
- [170] DURAND, P.Y.: Experimentations with low-cost solar timber drying kiln in Ivory Coast. *North American Wood Drying Symposium*, Mississippi Forest Products Utilization Laboratory, Mississippi (USA), 1985, pp. 223-231.
- [171] STEINMANN, D.E.: Temperature control in a solar kiln. *Holz als Roh- und Werkstoff* 48 (1990) No. 7/8, pp. 287-291.
- [172] STEINMANN, D.E.: The control of a solar kiln for wood drying. *Medeling Communications* 98 (1982) No. 2, pp. 672-685.
- [173] STEINMANN, D.E., H.F. VERMAAS, and J.B. FORRER: Microprocessor control of a solar kiln. *IUFRO Division V Conference, Wood drying papers*, IUFRO, Oxford (Great Britain), 1980, pp. 71-96.

- [174] AWASTHI, A.P.: Solar seasoning kiln. *Journal of the Timber Development Association* 26 (1980) No. 4, pp. 27-30.
- [175] FUWAPE, J.A. and J.A. FUWAPE: Construction and evaluation of a timber drying solar kiln. *Bioresource Technology* 52 (1995) No. 3, pp. 283-285.
- [176] DAS, A.K.: Solar drying of timber in Nepal. *Symposium on Forest Product Research, International Achievements and the Future, Council of Scientific and Industrial Research CSIR, Pretoria (South Africa), 1985*, pp. (8-8)1-(8-8)14.
- [177] SATTAR, M.A.: Comparative studies of wood seasoning with a special reference of solar drying. *Bangladesh Journal of Forest Science* 16 (1987) No. 1-2, pp. 30-42.
- [178] SHARMA, S.N.: Feasibility of solar timber drying in tropical locations. *IUFRO Division V Conference, Wood drying papers, IUFRO, Oxford (Great Britain), 1980*, pp. 107-127.
- [179] KLAMECKI, B.E.: Utilizing solar energy in the forest products industry. *Forests Products Journal* 28 (1978) No. 1, pp. 14-20.
- [180] VITAL, B.R.: Utilização de energia solar para secagem de madeira. *Revista Ceres* 23 (1976) No. 125, pp. 1-10.
- [181] SATTAR, M.A.: Drying characteristics of a greenhouse type solar kiln in Bangladesh. *Bangladesh Journal of Forest Science* 21 (1992) No. 1/2, pp. 20-31.
- [182] SATTAR, M.A.: Rural application of solar energy - timber drying. *First World Renewable Energy Congress on Energy and the Environment into the 1990s, Oxford (Great Britain), 1990*, pp. 599-605.
- [183] YANG, K.C.: Solar kiln performance at a high latitude, 48 degree North. *Forests Products Journal* 30 (1980) No. 3, pp. 37-40.
- [184] KRAMES, U.: Leistungsdaten eines mit Sonnenenergie beheizten Holz Trockners auf dem 48. nördlichen Breitengrad. *Internationaler Holzmarkt* 71 (1980) No. 15, pp. 13-14.
- [185] SCHNEIDER, A., F. ENGELHARDT, and L. WAGNER: Vergleichende Untersuchungen über die Freilufttrocknung und Solartrocknung von Schnittholz unter mitteleuropäischen Wetterverhältnissen. Teil 1: Versuchsanlage und Ergebnisse der ersten Trocknungsversuche. *Holz als Roh- und Werkstoff* 37 (1979), pp. 427-433.
- [186] SCHNEIDER, A. and L. WAGNER: Vergleichende Untersuchungen über die Freilufttrocknung und Solartrocknung von Schnittholz unter mitteleuropäischen Wetterverhältnissen. Teil 2: Ergebnisse im zweiten Versuchsjahr; Erkenntnisse und Folgerungen für die Solartrocknung in der Praxis. *Holz als Roh- und Werkstoff* 38 (1980), pp. 313-320.

- [187] BURKE, R.: Solar kiln. Rose Gum Timbers Pty Ltd., Bellingen (Australia), 1998.
- [188] ANON.: The Nomad solar kiln. Cambridge Glasshouse Company Ltd., Cambridge (Great Britain), 1999.
- [189] ANON.: CALM Solar assisted drying kiln. GCD International Pty Ltd., Knoxfield, Victoria (Australia), <http://www.gcd.com.au>, 12.06.1998.
- [190] ANON.: Solar assisted kilns. Australian Design Hardwoods Pty Ltd., Cloucester (Australia), <http://www.hartingdale.com.au>, 20.01.1998.
- [191] GORDON, J.: Processing apparatus. Australia, Patent No. WO8907742, 1989.
- [192] ANON.: Large pre-drying slip-kiln units. Australian Choice Timber, Bayswater, Victoria (Australia), www.choicetimber.com.au, 06.02.2001.
- [193] ANON.: The solardry kiln systems. Solardry Kilns, Wood Village, Oregon (USA), 1998.
- [194] BRENNAN, L.J., K.W. FRICKE, W.G. KAUMAN, and G.W. WRIGHT: Predrying in Australia. The Australian Timber Journal - Congress Issue (1966) No. 12, pp. 360-369.
- [195] ANON.: Kondensationsgeräte in der Praxis. Sonderdruck aus BM Bau- und Möbelschreiner No. 12, Konradin Verlag, Leinfelden-Echterdingen (Germany), 1988, pp. 1-4.
- [196] HUSTEDE, K.: Technische Holz Trocknung: Stand und technische Möglichkeiten. Bau und Möbelschreiner (1983) No. 4, pp. 63-66.
- [197] ANON.: Energiesparsysteme und Computersteuerungen optimieren Schnittholz trockner. HOB Die Holzbearbeitung (1988) No. 7/8, pp. 21-31.
- [198] LEMPELIUS, J.: Neues Vakuum-Trocknungssystem für Schnittholz hat Erfolg. Holz Zentralblatt 116 (1990) No. 30, pp. 430-432.
- [199] ANON.: Trends. Der deutsche Schreiner und Tischler (1993) No. 9, pp. 48-52.
- [200] BRUNNER, R.: Die Schnittholztrocknung im Vakuum - eine echte Alternative bietet sich an. Teil 1: Grundlagen der Vakuumtrocknung, Stand der bisherigen Verfahrenstechnik. Holz Zentralblatt 117 (1991) No. 54, pp. 1-5.
- [201] BRUNNER, R.: Die Schnittholztrocknung im Vakuum - eine echte Alternative bietet sich an. Teil 2: Technische Beschreibung des neuen High-Vac-Trockners. Holz Zentralblatt 117 (1991) No. 54, pp. 6-9.
- [202] HELMER, W.A.: A general collector sizing method for solar kilns. Forests Products Journal 36 (1986) No. 6, pp. 11-18.

- [203] HUSTEDE, K.: Entwicklungstendenzen auf dem Gebiet der Regelanlagen für die Schnittholztrocknung. HOB Die Holzbearbeitung (1990) No. 6, pp. 52-54.
- [204] HUSTEDE, K.: Mess- und Regeltechnik bestimmt die Trocknungsqualität. HOB Die Holzbearbeitung (1996) No. 6, pp. 56-58.
- [205] HUSTEDE, K.: Richtige Trockner-Automatisierung im Holzhandwerk - genauso wichtig wie im Großbetrieb. HOB Die Holzbearbeitung (1984) No. 3, pp. 67-71.
- [206] HERMA, W.: Moisture measurement - essential for kiln drying. Symposium on Forest Product Research, International Achievements and the Future, Council of Scientific and Industrial Research CSIR, Pretoria (South Africa), 1985, pp. (8-13)1-(8-13)11.
- [207] FORRER, J.B.: Modification of dry kiln electronics for greater flexibility. Symposium on Forest Product Research, International Achievements and the Future, Council of Scientific and Industrial Research CSIR, Pretoria (South Africa), 1985, pp. (8-14)1-(8-14)23.
- [208] HUSTEDE, K.: Trocknungszeiten und -kosten in modernen Schnittholztrocknern. HOB Die Holzbearbeitung (1973) No. 3, pp. 39-40.
- [209] GALVÃO, A.P.M. and I.P. JANKOWSKY: Secagem racional de madeira. Livraria Nobel S.A., Sao Paulo (Brazil), 1985.
- [210] SIMPSON, W.T.: Grouping tropical wood species for kiln drying using mathematical models. Drying Technology 12 (1994) No. 8, pp. 1877-1896.
- [211] LITTLE, R.L.: Microcomputer monitoring and control of a lumber dry kiln. Symposium on Forest Product Research, International Achievements and the Future, Council of Scientific and Industrial Research CSIR, Pretoria (South Africa), 1985, pp. (8-10)1-(8-10)12.
- [212] KININMONTH, J.A., W. MILLER, and S. RILEY: Energy consumption in wood drying. IUFRO Division V Conference, Wood drying papers, IUFRO, Oxford (Great Britain), 1980, pp. 1-18.
- [213] BREINER, T.A., D.G. ARGANBRIGHT, and D. HUBER: On-line monitoring of heat and power consumption in a commercial scale lumber dry kiln. North American Wood Drying Symposium, Mississippi Forest Products Utilization Laboratory, Starkville, Mississippi State (USA), 1984, pp. 119-129.
- [214] HELMER, W.A. and P.Y.S. CHEN: Computer simulation of a new method to dry lumber using solar energy and absorption refrigeration. Wood and Fiber Science 17 (1985) No. 4, pp. 464-476.
- [215] WELLING, J. and J. RESSEL: Computergesteuertes Datenerfassungssystem für die Schnittholztrocknung. Holz als Roh- und Werkstoff 43 (1985), pp. 131-134.

- [216] HUSTEDE, K.: Trends bei der Holzfeuchtemessung und bei der technischen Holz Trocknung. *Bau und Möbelschreiner* (1991) No. 12, pp. 81-82.
- [217] ANON.: Intelligente Umluftsteuerung spart Energie beim Schnittholztrocknen. *Holz Zentralblatt* (1999) No. 55, p. 829.
- [218] SIMON, V.: Optimierung einer solargestützten Trocknungsanlage für Schnittholz in Brasilien. Diploma, Institut für Agrartechnik in den Tropen und Subtropen, Universität Hohenheim, im Selbstverlag, Stuttgart (Germany), 1997.
- [219] REISINGER, G., W. MÜHLBAUER, and V. WITTEWERT: Noppenfolie im Langzeittest. Bisherige Erfahrungen im praktischen Einsatz. *Deutscher Gartenbau* 42 (1988) No. 33, pp. 2009-2016.
- [220] REISINGER, G. and W. MÜHLBAUER: Air bubble foil with weather-strip fastening system - an energy saving greenhouse cover. *Acta Horticulturae* (1990) No. 281, pp. 67-73.
- [221] LINCKH, G.: Thermodynamische Optimierung von Luftkollektoren für solare Trocknungsanlagen. Dissertation, Institut für Agrartechnik in den Tropen und Subtropen, Universität Hohenheim, Max-Eyth-Gesellschaft im VDI (VDI-MEG), Stuttgart (Germany), 1993.
- [222] OSCHMANN, J.: Druckerhöhung bei Axialventilatoren. Ziehl-Abegg, Künzelsau (Germany), 1998.
- [223] DIN EN ISO 6946. Wärmedurchlasswiderstand und Wärmedurchgangskoeffizient, Berechnungsverfahren. Beuth-Verlag, Berlin (Germany), 1996.
- [224] WAGNER, W.: Konvektion. In: *Wärmeübertragung* No. 3. Vogel Buchverlag, Würzburg (Germany), 1993, pp. 53-100.
- [225] MCADAMS, W.H.: Heat transmission. McGraw-Hill Book Company, New York (USA), 1954.
- [226] DIN 4108-3. Wärmeschutz und Energie-Einsparung in Gebäuden, Teil 3: Klimabedingter Feuchteschutz, Anforderungen, Berechnungsverfahren und Hinweise für Planung und Ausführung. Beuth-Verlag, Berlin (Germany), 2001.
- [227] FISCHER.M.: Untersuchung der Eignung verschiedener Feuchtemessgeräte bei unterschiedlicher Temperatur und relativer Feuchte der Luft. Diploma, Institut für Agrartechnik in den Tropen und Subtropen, Universität Hohenheim, im Selbstverlag, Stuttgart-Hohenheim (Germany), 1994.
- [228] DUFFIE, J.A. and W.A. BECKMAN: Solar engineering of the thermal process. John Wiley and Sons, New York (USA), 1980.
- [229] MÜLLER.J.: Trocknung von Arzneipflanzen mit Solarenergie. Dissertation, Institut für Agrartechnik in den Tropen und Subtropen, Universität Hohenheim, Ulmer Verlag, Stuttgart (Germany), 1991.

- [230] SPRINGER, G.: Fachkunde Elektrotechnik. Verlag Europa-Lehrmittel, Haan-Gruiten (Germany), 1996.
- [231] BOHL, W.: Ventilatoren. Vogel Buchverlag, Würzburg (Germany), 1983.
- [232] ZIMMER, A.: Strömungstechnik Formelsammlung. Fachhochschule Köln, Fachbereich Versorgungstechnik, Cologne (Germany), <http://www.skript.vt.fh-koeln.de>, 12.10.2002.
- [233] ANON.: CAF madeira de eucalipto. CAF Santa Bárbara, Martinho Campos (Brazil), www.caf.ind.br, 01.03.2001.
- [234] ANON.: NASA Surface meteorology and solar energy - Data set. NASA, Washington, D.C. (USA), <http://eoswb.larc.nasa.gov>, 05.04.2001.
- [235] ANON.: NASA Surface meteorology and solar energy - Methodology. NASA, Washington, D.C. (USA), <http://eoswb.larc.nasa.gov>, 05.04.2001.
- [236] ANON.: NASA Surface meteorology and solar energy - Accuracy. NASA, Washington, D.C. (USA), <http://eoswb.larc.nasa.gov>, 05.04.2001.
- [237] ANON.: NASA Surface meteorology and solar energy - Parameters. NASA, Washington, D.C. (USA), <http://eoswb.larc.nasa.gov>, 05.04.2001.
- [238] ANON.: Observações meteorológicas. Departamento Meio Ambiente, CAF Santa Bárbara, Bom Despacho (Brazil), 1996, pp. 1-25.
- [239] ANON.: NASA Surface meteorology and solar energy - Data set Martinho Campos. NASA, Washington, D.C. (USA), <http://eoswb.larc.nasa.gov>, 05.04.2001.
- [240] prEN 175.092. Schnittholz - Ermittlung der Trocknungsqualität. European Committee for Standardization, Brussels (Belgium), 2001.
- [241] UNGERER: Messgeräte und Messverfahren für Baustofffeuchte. Lauth u. Partner (Germany), 1995, pp. 1-16.
- [242] HUSTEDE, K.: Elektrisches Messen der Holzfeuchte - ein Vergleich. Boden-Wand-Decke (1994) No. 10, pp. 100-101.
- [243] HUSTEDE, K.: Elektronische Messgeräte erfassen Holz- und Baustofffeuchte. HOB Die Holzbearbeitung (1990) No. 3, pp. 53-54.
- [244] prEN 13183-2. Round and sawn timber - Method of measurement of moisture content - Part 2: Method for determining moisture content of a piece of sawn timber - Electrical resistance method. European Committee for Standardization, Brussels (Belgium), 2000.
- [245] prEN 13183-1. Round and sawn timber - Method of measurement of moisture content - Part 1: Method for determining moisture content of a piece of sawn timber - Oven dry method. European Committee for Standardization, Brussels (Belgium), 2000.

- [246] ANON.: Der Holzfeuchte auf der Spur. HOB Die Holzbearbeitung (1987) No. 9, pp. 63-65.
- [247] WELLING, J.: Spezifikation und Überprüfung der Trocknungsqualität von Schnittholz. HOB Die Holzbearbeitung (1993) No. 11, pp. 56-62.
- [248] ANON.: VDI-Wärmeatlas. Berechnungsblätter für den Wärmeübergang. VDI-Gesellschaft Verfahrenstechnik und Chemieingenieurwesen, VDI-Verlag GmbH, Düsseldorf (Germany), 1991.
- [249] LORENZ, R.J.: Grundbegriffe der Biometrie. Gustav-Fischer-Verlag, Stuttgart (Germany), 1996.
- [250] TOWNSEND, I.K.: Moisture content variability in an industrial dry kiln. North American Wood Drying Symposium, Mississippi Forest Products Utilization Laboratory, Mississippi (USA), 1984, pp. 46-48.
- [251] BOFF, V.S.H.: Personal Communication, Aracruz S.A., Posta de Mata, Bahia (Brazil), 2000.
- [252] SINVAL, J.: Personal Communication, Fábrica de Móveis Sinfas Ltda., Bom Despacho (Brazil), 2000.
- [253] BRUNNER, R.: Vakuumtrocknung im Wirtschaftlichkeitsvergleich. Teil 1: Rechteckgehäuse in Modulbauweise unter Verwendung von versteifenden Alu-Strangprofilen senkt die Kosten. Holz Zentralblatt 125 (1999) No. 55, p. 823.
- [254] BRUNNER, R.: Wann müssen Sie sich heute für Vakuumtrocknen entscheiden? Fachinformation zum Thema Schnittholztrocknung im Vakuum Hildebrand Holztechnik GmbH, Oberboihingen (Germany), 1999, pp. 1-20.
- [255] BRUNNER, R.: Vakuumtrocknung im Wirtschaftlichkeitsvergleich. Teil 3: Vergleich der Trockenkosten von Eiche - Entwicklung der Anlagenpreise - Ausblick. Holz Zentralblatt 125 (1999) No. 57/58, pp. 874-875.
- [256] MAGNI, R.: Oferta para 5 secadores para madeira de eucalipto. Brunner Hildebrand, Oehningen (Germany), 1997.
- [257] SCHADE, Y.: Angebot für einen konventionellen Schnittholztrockner. Mahild Drying Technologies, Nürtingen (Germany), 2002.
- [258] ANON.: So geht's: Export nach Brasilien. Deutsch Brasilianische Industrie- und Handelskammer, Sao Paulo (Brazil), 2000.
- [259] VAHS, D. and J. SCHÄFER-KUNZ: Einführung in die Betriebswirtschaftslehre. Schäffer-Poeschel Verlag, Stuttgart (Germany), 2000.
- [260] FINCK, H. and G. OELERT: Leitfaden zur Berechnung der Wirtschaftlichkeit von Investitionskosten zur Energieversorgung. Gesellschaft für technische Zusammenarbeit GTZ, Eschborn (Germany), 1982.

- [261] ANON.: Brasilien auf stabilem Wachstumskurs. Brasilianische Botschaft in Deutschland, Munich (Germany), www.brasilianische-botschaft.de, 10.03.2002.
- [262] MILDE, T., C. MENKE, R. SCHULZ, R. ZAWALLICH, and W. OLDEKOP: Technisch-Wirtschaftlicher Leitfaden zur solaren Tabaktrocknung am Beispiel Thailands. Gesellschaft für technische Zusammenarbeit GTZ, Eschborn (Germany), 1986.
- [263] ANON.: Über die Wirtschaftlichkeit eines Vorschaltgerätewechsels in beleuchteten Aussenwerbeanlagen. Opt-Immo, Langenfeld (Germany), www.opt-immo.de, 13.03.2003.
- [264] MOTTA, C.: Investitionskosten für einen Solartrockner mit 2 Trocknungskammern. CAF Santa Bárbara, Belo Horizonte (Brazil), 1999.
- [265] ANON.: Allgemeine Stromtarife. CEMIG, Martinho Campos, Minas Gerais (Brazil), 1999, p. 1.
- [266] ANON.: Allgemeine Wassertarife. COPASA, Martinho Campos, Minas Gerais (Brazil), 1999, p. 1.
- [267] ANON.: Allgemeine Bankzinsen. Banco do Brasil, Martinho Campos, Minas Gerais (Brazil), 1999, pp. 1-4.
- [268] ANON.: Brazil - enough wind for everyone. REFOCUS (2001) No. 1, pp. 20-22.
- [269] ANON.: Tabela de preços de madeira serrada e resíduos. CAF Santa Bárbara, Martinho Campos, Minas Gerais (Brazil), 1999, p. 1.

10 APPENDIX

Table A1: Measuring range and accuracy of the used instruments.

Measurand	Instrument	Measuring range	Accuracy
Temperature	NiCr-Ni-Thermocouple (Heraeus, type K)	-40 - 350 °C	+/- 0.2 %
	Pt-100-Sensor (Greisinger GHTU)	-20 - 80 °C	+/- 0.3 °C
	NTC Thermistor (RS Com- ponents)	-20 - 50 °C	+/- 0.5 °C
Relative humid- ity	Capacitive thin-film sensor (Greisinger GHTU)	0 - 100 %	+/- 2 %
	Capacitive thin-film sensor (RS Components)	10 - 90 %	+/- 3 %
Wood moisture content	Capacitive resistance mois- ture meter (Greisinger GHH 91 and HF 91)	3 - 100 %	3-25 % +/- 0.2 % 25-60 % +/- 0.5 % 60-100 % +/- 2.5 %
Isolation	Pyranometer (Kipp & Zo- nen CM 11/121)	0 - 1000 W/m ²	+/- 0,5 %
Pressure	Manometer (Halstrup GmbH, EMA 150)	0 - 199.9 Pa	+/- 1 %
Mass	Laboratory scale (Mettler)	0 - 4 kg	0.1 g
Water mass flux	Flow transmitter (Bürkert 8035)	0.3 - 10 m/s	+/- 0.5 %

Table A2: Description of the measuring points at the solar dryer.

Number	Measurand	Description
TIR 1	Temperature	Ambient air
TIR 2 - 5		Drying air below the absorber
TIR 6		Absorber
TIR 7 - 11		Drying air above the absorber
TIR 12 - 14		Timber stack
TIR 15 - 16		Surface of the air bubble foil
TIR 17 - 18		Heating water
TIR 19		Dryer floor
MIR 1	Humidity	Relative humidity of the ambient air
MIR 2 - 4		Relative humidity of the drying air
MIR 5 - 11		Wood moisture content
RIR 1	Radiation	Global radiation
FIR 1	Flow	Heating water
FIR 2		Drying air
PDI 1	Pressure	Pressure drop

Table A3: List of the investment costs for the solar-assisted and the high temperature dryer in € (exchange rate from January 1999, 1.00 € = 1.17 US\$ = 1.69 R\$).

Group	Material	Price	Solar dryer	High temp. dryer
Transport	Stuttgart – Hamburg	1 360.00	1 360.00	1 360.00
	Hamburg – Vitória	1 790.00	1 790.00	1 790.00
	Vitória – Bahia	142.00	142.00	142.00
Fees and taxes	Harbour dues	719.00	719.00	719.00
	Building permission	1 358.00	1 358.00	1 358.00
	Import tax	18 %	8 278.00	14 013.00
	Industry tax	5 %	2 713.00	4 593.00
	Value added tax	18 %	10 256.00	17 361.00
	Insurance	0.5 %	229.00	387.00

Group	Material	Price/Unit	Units	Total	Units	Total
Construction works	Concrete	25.00	27 m ³	675.00	5 m ³	125.00
	Steel 5 mm	0.05	260 m	13.00	50 m	2.50
	Steel 10 mm	0.20	80 m	16.00	15 m	3.00
	Steel grids	1.50	180 m ²	270.00	30 m ²	45.00
	Blocks	0.20	900 pc.	180.00	-	-
	Finery	24.00	3.5 m ³	84.00	-	-
Water and electricity supply	Cable duct	3.90	30 m	117.00	20 m	78.00
	Hot water pipe	3.50	8 m	28.00	8 m	28.00
	Cold water pipe	1.20	8 m	9.60	8 m	9.60
	Heater pump	305.00	1 pc.	305.00	1 unit	305.00
	Humidifier pump	30.00	1 pc.	30.00	1 unit	30.00
Manpower	Headman	4.50	80 h	360.00	160 h	720.00
	Assembler	1.50	480 h	720.00	800 h	1 200.00
	Bricklayer	2.80	120 h	336.00	40 h	112.00
	Plumber	2.80	8 h	22.40	8 h	22.40
	Electrician	2.80	8 h	22.40	8 h	22.40
	Engineer	23.00	8 h	184.00	8 h	184.00